Technologies d'assistance pour personnes handicapées utilisant les potentiels d'action d'unités motrices des muscles du visage

Carlos Galvao Pinheiro Júnior

Université de Lorraine

Co-mentorship thesis with the Universidade Federal de Uberlândia - BR

A Thesis submitted for the degree of Doctor of the Université de Lorraine

Carlos Galvão PINHEIRO Júnior

Assistive technology for the severely motor impaired by using online processing of motor unit action potentials of facial muscles

Laboratoire de Conception, Optimisation, Modélisation des Systèmes

École Doctorale IAEM

Supervisor: Guy BOURHIS

Co-Supervisor: Adriano de OLIVEIRA ANDRADE

Metz - Lorraine
2013

Université de Lorraine

THESE DE DOCTORAT

En Cotutelle avec l'Universidade Federal de Uberlândia - BR

Pour obtenir le grade de

Docteur de L'Université de Lorraine

Carlos Galvão PINHEIRO Júnior

Technologies d'assistance pour personnes handicapées utilisant les potentiels d'action d'unités motrices des muscles du visage

Préparée au Laboratoire de Conception, Optimisation, Modélisation des Systèmes

Dans le cadre de l'École Doctorale IAEM

Directeur de thèse: Guy BOURHIS

Co-Directeur de thèse: Adriano de OLIVEIRA ANDRADE

Metz - Lorraine
2013

UNIVERSITÉ DE LORRAINE

Université de Lorraine

THESE DE DOCTORAT

En Cotutelle avec l'Universidade Federal de Uberlândia - BR

Pour obtenir le grade de

Docteur de L'Université de Lorraine

Carlos Galvão PINHEIRO Júnior

Technologies d'assistance pour personnes handicapées utilisant les potentiels d'action d'unités motrices des muscles du visage

Soutenue le 12/07/2013 devant la commission d'examen:

Dr. Guy BOURHIS	Directeur de thèse
Dr. Adriano de OLIVEIRA ANDRADE	Co-Directeur de thèse
Dr. Alcimar BORBOSA SOARES	Président
Dr. Teodiano Freire BASTOS FILHO	Rapporteur
Dr. François CEBESTAING	Rapporteur
Dr. Eduardo LAZARO MARTINS NAVES	Examinateur
Dr. Rui LOUREIRO	Examinateur
Dr. Yann MORERE	Examinateur

Metz - Lorraine
2013

To Fabrinne, our child and Jule.

Acknowledgment

At this point sitting in front of the computer I believe it is much harder to write this text than it was to write the thesis conclusion. More than methods, algorithms, equations I start to think about the people I met in the last years. And people are more important than any equation. By far!

I start thanking my supervisors Adriano de Oliveira Andrade and Guy Bourhis. They have showed me a new meaning for excellence and hard work. Their support were not restricted to technical matters and were of great importance during my stay at Metz and Uberlândia.

It is impossible to forget Prof. Adriano Alves helping me out to identify and eliminate the background noise that haunted me for months. Thank you, wizard!

To all friends at BioLab in Brazil, thank you for the healthy and pleasent work environment. Something quite unique indeed.

Life in a foreign country is not always easy. Fortunately, I've found amazing and helpful people at the LASC with patience and ready to help me out. I need to thank specially my fellows Fred and Amine for the interchange of knowledge and the funny talks at the end of the day.

Finally, I feel privileged to have met Pierre Pino and his family. They exercise generosity like no one I have ever met before.

Abstract

In some circumstances, a person may be deprived of natural abilities, such as walking and speaking, perhaps due to limb amputation, spinal cord injuries (SCI), or degenerative diseases. Assistive technology devices allows motor-impaired people to overcome their limitations promoting greater independence. Particularly suitable in the case of people with severe motor impairment, electrical biosignals have been successfully utilised to operate alternative communication devices. For over half a century, information extracted from the electromyographic signal for the purpose of operating a given device has not considered the information provided by the basic unit of the muscle: the motor unit. The objective of this study is to investigate how accessing information at motor unit level would improve the operator's performance during a given task. The hypothesis is that the proposed methodology would allow generating more precise control commands, when compared to traditional approaches relying on global information obtained by conventional electromyographic signal acquisition and processing. A system to detect motor unit action potentials from the electromyographic signal was devised, including the electrode design, and the performance evaluated by measuring the time taken to perform several cursor control tasks. The specifications of the cursor control task were extracted from a different study, which used the traditional electromyographic signal-processing approach. Comparing the results from both studies proved that the novel approach provides better control than the traditional one, being 27% faster in the most difficult task.

Keywords: *Electromyography, Assistive technology, Human-computer interaction, Facial electromyography.*

Contents

List of Figures

List of Tables

List of Abbreviations

AAC Augmentative and Alternative Communication

ACh AcetylCholine

ALS Amyotrophic Lateral Sclerosis

ANN Artificial Neural Network

AP Action Potential

ASR Automatic Speech Recognition

AutoCorrAbs Non-normalized Autocorrelation

BCI Brain Computer Interface

CNS Central Nervous System

DWT Discrete Wavelet Transform

EEG Electroencephalographic

EFSM Extended Finite State Machine

EMG Electromyographic

EOG Electrooculographic

FSM Finite State Machine

HMM Hidden Markov Model

IED Inter-Electrode Distance

ID Index of Difficulty

IP Index of Performance

MAV Mean Absolute Value

MDF Median Frequency

MFAP Muscle Fiber Action Potential

MFCC Mel-Frequency Cepstral Coefficients

MNF Mean Frequency

MS Multiple Sclerosis

MU Motor Unit

MUAP Motor Unit Action Potential

MUAPT Motor Unit Action Potential Train

MVC Maximum Voluntary Contraction

NMAV Normalized Mean Absolute Value

OS Operating System

PC Principal Component

PCA Principal Component Analysis

PSD Power Spectral Density

RMS Root-Mean Square

sEMG Surface EMG

SBC Switch-based control

SCI Spinal Cord Injury

SENIAM Surface EMG for Non-Invasive Assessment of Muscles

SNR Signal to Noise Ratio

SR Sampling Rate

StdAbs Standard deviation of the Absolute value

TP Throughput

Chapter 1

The use of electromyography in assistive technology

Muscle activity is the main biological pathway for the human being to act upon the environment around him. At first, one may argue that speech is more relevant, but even this essential communication tool depends on the movements of facial muscles and the diaphragm. Beyond communication, a person must move around the environment and handle objects, obviously, using the skeletal muscle system[1]. Actually, besides brain activity, it is hard to imagine another form of self-expression without involving muscle activity.

In some circumstances, a person may be deprived of those abilities in various degrees, perhaps due to limb amputation, spinal cord injuries (SCI), or degenerative diseases. In these cases, assistive devices are relevant tools to aid individuals to improve their functional capacities.

The idea of using muscle activity in assistive technology devices consists in decoding such activity in order to execute specific actions, which differ from the original purpose

[1]The human body has three types of muscle tissue: cardiac, smooth and skeletal. The first two are under control of the autonomous nervous system, and their activities are involuntary. The somatic nervous system, in the other hand controls skeletal muscles, i.e. their contraction are voluntary.

of a given muscle. For instance, the contraction of the *Frontalis* muscle is related to facial expressions, although it could be employed to control a device, such as a switch. Before muscle activity may be used in this manner, it must be detected by means of specific sensors (electrodes and circuit for signal conditioning). The detected signal, named electromyographic (sEMG) signal, is then interpreted, generating commands to be applied to assistive devices. If surface electrodes are used in the process, the signal is named surface EMG (sEMG).

Muscle activity is not the only source of information available for assistive devices. Brain activity, represented by electroencephalographic (EEG) signals are used in brain computer interfaces (BCIs) [1] providing a channel of communication for subjects with severe motor impairments. A suitable scenario for using EEG is the case of total locked-in syndrome, in which the patient is aware and awake but cannot move or communicate verbally due to complete paralysis. Other possible channel of communication is using eye movements, registered by electrooculographic (EOG) signals [2] or cameras, as in gaze based devices. Finally, in some circumstances, elaborated systems involving bioelectrical activity and signal processing tools are not needed at all and low-tech solutions, such as a push button may be employed to provide the subject with the desired channel of interaction with the surrounding world.

This chapter presents a review on assistive devices operated by sEMG signals, focusing on augmentative and alternative communication (AAC) devices. This review focuses mostly upon the use of these devices for controlling the movement of a cursor on a computer screen, being this the task used in the verification of the hypothesis of this thesis. Furthermore, the objectives of the study are summarized.

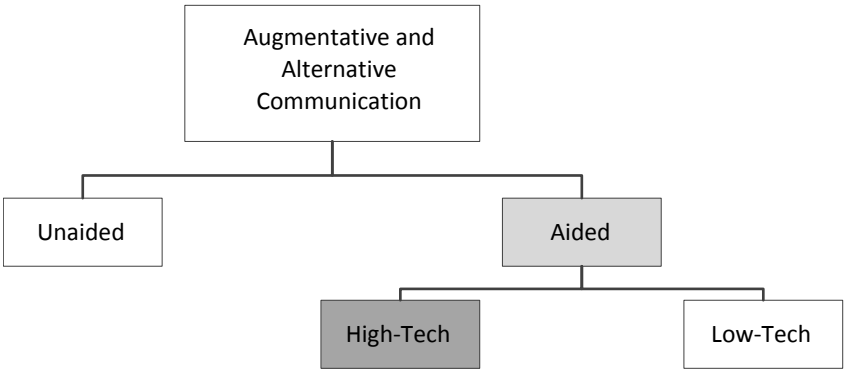

Figure 1.1: Forms of Augmentative and Alternative Communication.

1.1 Assistive devices based on sEMG signals

One of the most well-known applications of the sEMG signal on assistive devices is the control of prosthetic limbs. Pioneering work goes back in the 1950s [3] achieving simple but reliable control for open and close actions of artificial hands. The necessary information is extracted from the remaining muscles to operate the artificial limb. Prosthesis control has grown in complexity to include targeted muscle reinnervation [4] and has expanded in capacity to include finger control [5].

Beyond prosthetics limbs, sEMG signal processing is also present in AAC. The AAC term covers any methods used to supplement or replace speech or writing for those with impairments in the production or comprehension of spoken or written language [6][7]. Primary classification divides AAC into unaided and aided devices 1.1. Unaided systems do not require an external tool, and include facial expression, vocalizations, gestures and sign languages. An AAC aid system is any device, either electronic (high-tech) or non-electronic (low-tech), that is used to compose and transmit or to receive messages. Therefore, AAC systems relying on sEMG signal processing are classified as high-tech AAC devices.

AAC systems are designed for several conditions such as locked-in syndrom, Amyotrophic lateral sclerosis (ALS), Multiple sclerosis (MS) and Aphasia in various degrees,

so the ideal AAC device for a given subject depends on several factors, among them the subject dexterity over muscle control. sEMG based devices can be subdivided into three major groups:

- Switch-based control (SBC) device;
- mouse emulation;
- speech recognition.

An SBC device transmits binary signals to the assistive device, utilizing the technology that has been applied for its conception. Such systems work only as a tool to scan various possibilities and make a selection, with the major difficulty being then to decide the scanning delay value [8]. Any muscle still under control are eligible candidates for this kind of application.

Computer interfaces have been operated mainly by mouse and keyboard since the 1980s; therefore, mouse emulation is a natural task when it comes to communication devices. Muscles used in rotation movement, as seen in a joystick, e.g., the neck muscles used to rotate the head [9, 10, 11] and the arm muscles used to rotate the hand, provide an intuitive way of controlling the cursor direction of displacement, since this movement is omnidirectional. Facial muscles are also explored, though the trend is that the cursor movement will be orthogonal as subjects find difficulty in giving two directions, e.g., UP and LEFT, at the same time.

Speech recognition uses the activity of the facial muscles involved in the task. Denby *et al.* [12] conducted an analysis of seven technologies for silent speech interfaces, i.e. without acoustic signal. This group concluded that the sEMG-based system's overall rating was superior to the six other alternatives (electromagnetic articulography markers, ultrasound and optical imaging, non-audible murmur microphone, electromagnetic or vibration sensors, electroencephalography sensors and BCI cortical), considering the following criteria:

- Works in silence: Can the device be operated silently?
- Works in noise: Is the operation of the device affected by background noise?
- Works for laryngectomy: Can the device be used by post-laryngectomy patients? It may be useful for other pathologies as well, but laryngectomy is used as a baseline.
- Non-invasive: Can the device be used in a natural fashion, without uncomfortable or unsightly wires, electrodes, etc.?
- Ready for market: Is the device close to being marketed commercially? This also takes into account in a natural way the current technological advancement of the technique, responding, in essence, to the question,"How well is this technology working as of today?".
- Low cost: is the final product economical?

This axis also takes into account the current technological advancement of the technique, responding, in essence, to the question: how well is this technology working, as of today? The answer will depend, among other factors, on whether any exotic technologies or procedures are required to make the device function, as well as cost, performance in noisy environments, and invasiveness.

1.1.1 Switched-based control devices

Patients with conditions such as locked-in syndrome retain control of their eyes and cognitive tasks. Therefore, an easy way to communicate is by answering yes/no questions. This approach provides an output channel of communication with a low information-transfer rate and low interactivity, demanding the care provider to have the necessary skills to formulate the right questions.

A subject able to carry out residual movements with his or her head, or at least one limb, may use a pressure device. The same principle can be applied to sEMG signals where the pressure action can be replaced by muscle contraction. Electromyography has been considered previously as an assessment tool for patients with disorders of consciousness, indicating its use as a channel of communication [13]. Using computational solutions, one can generate binary signals, with '1' being associated with muscle activity and '0' assigned otherwise.

One approach consists of composing messages with some kind of code, e.g., the Morse code. Although this seems to be an unnatural mode of communication, the procedure may be extremely valuable for subjects with severe motor impairments. Any biosignal that can be interpreted as a two-state information source is a potential candidate for the use of this code. From the Morse-based code, the subject can control devices and communicate in several ways, depending upon the strategy adopted. Studies using sources other than the sEMG signal have shown that applying the Morse code [14, 15] can be a good option for AAC. Since maintaining a steady typing rate is difficult for disabled subjects, modified forms of the code may be adopted [15].

Park *et al.* [16] developed a system utilizing movements of the *Massetter* muscle of the chin. The signal acquired from these movements is transformed into dot or dash symbols, depending upon the duration of the contraction, and the sequence is decoded into characters that are fed into a voice synthesizer. This study includes a method for fatigue adaptation, an important concern when using sEMG. The major caveat to this system is that humans are not capable of chewing and pausing quickly; therefore, the transfer information rate is low, although not reported in numbers.

The binary signal can also be used to operate a scanning device, e.g., a virtual keyboard and some more complex interfaces. The Impulse® [17] system, one of the few AAC commercial solutions based on the sEMG signal, uses this approach in a wireless solution to offer computer access with a specific scanning interface. This system is not

available for purchase since April 2011.

When comparing the scanning and the code-based approaches, we can observe that both are based in simple signal-processing techniques. The difference lies in the cognitive effort required from the subject: the scanning approach transfers the complexity of the message-generation process to the system interface; whereas, with code-based devices, the subject has to learn the sequence of symbols necessary to compose each character or command.

1.1.2 Cursor control

Since the 1980s, the mouse and keyboard have been the standard input devices for computer operation. Then, the number of studies to develop devices replacing physical keyboards with virtual ones to provide point-and-click functions is understandable. For some studies, though the goal is to provide a hands-free alternative to healthy subjects, the solution could be adapted for a subject with a disability.

Using muscles in the pointing task can be described as a three-step process:

1. Identification of the suitable muscles to be explored;
2. definition of types of control that can be obtained;
3. choice and processing of sEMG signals to generate the command.

In the case of subjects with severe motor disabilities, facial muscles are a common option, as these muscles can be activated. This is true even in the case of subjects suffering from a severe SCI.

Once the number of muscles available has been established, researchers can start to set up the strategy to achieve proper cursor control. One simple strategy is to use each muscle to define the cursor displacement in one direction. There are at least two aspects that will define the system's final capacity to control a cursor: the device type

and the subject's ability to control the muscles. If an analogical device is used, and the subject has the dexterity necessary to control all four muscles at once, the cursor control will be omnidirectional. If an SBC device is employed with the same subject, the cursor can move in eight different directions. Finally, if the SBC device is operated by someone with poor muscle control, it is likely that the cursor will move to only four different directions. The most commonly used facial muscles in the pointing task are the *Corrugator*, the left and right *Frontalis*, the left and right *Temporalis* and the left and right *Zygomaticus* major. Traditional approaches use pairs of muscles to control displacement over the XY axis. Others strategies for exploring the sEMG signal are possible, such as 2-dimensional (2D) control from only one muscle [18]. In fact, in this thesis the task proposed is to control the cursor using only the *Frontalis* muscle.

In addition to all the actions a mouse can perform, it is also capable of right- and left-clicks. In [19] the left-click action and cursor movement (2D) were controlled by sEMG signals from the *Temporalis* and *Frontalis* muscles. Additionally, the system is provided with an ON/OFF switch that is controlled by the EEG signal. The mouse functions were identified by applying a threshold to the amplitude signal, and later, by performing spectral analysis over several frequency bands. The system was implemented over a digital processing signal board, which was identified by the host as an ordinary mouse. At first, only three channels for sEMG signals were necessary, but in [20] a fourth electrode was used, improving the average of correct muscle movements classification from 78.43% to 98.42%. Despite these good results for muscle movements classification, the system took 16.3 s on average to move a cursor from the middle to the corner of the screen, compared to 1-2s with a standard mouse. So, in [21, 22, 23] the same approach was combined with a gaze-based system to create a hybrid system. While the gaze offered the absolute position of the cursor, the sEMG signal provided incremental displacement. As a consequence, the time to move a cursor from the middle to the corner of the screen dropped from 16.3 s to 6.8 s.

Another detailed study that considered multimodal approaches compared a standard mouse and a hybrid device [24]. The cursor position was controlled by gaze and the object selection (left-click) was activated by frowning. The two solutions were compared using Fitts' Law [25]: for small distances a standard mouse showed superior performance, although there was no statistical difference among the devices over large distances.

In [26] the goal was also to provide a pointing device controlled by facial muscles. A continuous wavelet transform measured the activation level of each muscle, providing four direction displacements - associated with both sides of the *Orbicular*, *Massetter* and *Mentalis* muscles. Left and right-click operations were associated with opposite directions executed at the same time (up+down = right click and left+right = left click). The use of the wavelet transform was justified by the shape similarity between the wavelet mother and the motor unit action potentials (MUAPs, to be discussed in Chapter 2). However, this strategy can be questioned, as the system performance was not compared with traditional signal features, e.g. the Root-Mean Square (RMS) value. The study also lacks information about electrodes dimensions and geometry, thus, it is impossible to estimate the electrodes selectivity and therefore if MUAPs could be extracted from the sEMG signal.

Using four muscles to control horizontal and vertical displacement seems a very straightforward idea. Nevertheless, in a novel approach [18] the authors employed the sEMG signal recorded from only one muscle, the *Auricularis Superior*, to control the cursor position in the X and Y axis. The power levels of two different frequency bands extracted from this signal were utilized. The strategy adopted is quite different from the others described earlier, as the absence of muscle activity sets the cursor position to coordinates (0,0) while the contraction moves the cursor. User training is mandatory, because the subject should learn how the contractions affect the cursor position, and also because different subjects present different bands of interest.

For subjects unable to control their upper limbs, using muscles located in the head

may be the only option. However, a subject with a condition such as tetraplegia may a manifest residual control of his or her neck, shoulders, and even arms.

Additionally, using facial muscles seems an unnatural way of controlling a cursor, when compared to using standard mouse. As an example, diagonal movements tend to be accomplished through horizontal and vertical movements [11] when using sEMG signals as source of control. Head motion [27], on the other hand, could be compared to a joystick operation.

In [28, 29], five different motions of the neck and shoulder could be recognized with 95% mean recognition rate and response time of about 0.17s. Two pairs of electrodes were placed over the *Sternocleidomastoid* and the *Trapezius* muscles, on each side of the body.

In [11] three methods offering pointing device control were compared: a standard mouse, head-orientation using an accelerometer and the sEMG-based approach. The *Platysma*, left *Trapezius* and the *Frontalis* muscles were utilized. Cursor speed was a continuous variable, with a maximum value attributed to 70% of Maximum Voluntary Contraction (MVC). As expected, the mouse was superior and the sEMG approach was generally inferior to the head-orientation method, especially due to the difficulty of performing diagonal movements.

In [30] the angle of the head was estimated through linear interpolation of the sEMG signal extracted from the *Sternocleidomastoid* muscle. For small angle rotations, the sEMG signal was too weak to offer any useful information. For this reason a camera was used in its place and the angle was estimated by the relative position of the pupils. In fact, if a subject presents good head and neck control, the camera-based solution seems to be more appropriate, as the software is already available for download and only requires an ordinary webcam.

Finally, the possibility exists of using arm movements to operate a virtual keyboard and mouse. In [31], an omnidirectional pointing device is controlled by the sEMG

signals recorded from the forearm. An artificial neural network (ANN) was used to orient the cursor, while the muscular contraction level controlled the cursor velocity. A recent study involving the Microsoft Corporation [32] presents a similar approach using the sEMG signal in game interfaces and in busy-hands situations, which could also be utilized for subjects presenting some level of disability. The implication of this research by a company highly bound with the field of computing indicates the potential for use of the sEMG signal in computing interfaces. However, solutions for subjects presenting with good arm control are outside the scope of this thesis and, even in the case of adopting an assistive device, an adapted mouse or joystick would be more appropriate for this subject type.

An interesting method is found in [33], as three muscles in the forearm control a 2D cursor with variable speed. The first two muscles rotate the cursor, while the third moves the cursor forward. This approach is similar to the one adopted in the protocol described in Chapter 4.

One final observation concerns the system dimensionality. The above studies cover only 2D cursor operation, qualifying these systems to work on traditional Operating Systems (OS), which may not be suitable for motor impaired users. Scanning based interfaces could be adapted to use 1D cursor control, sliding forward and backwards to select options instead of scanning. The 1D approach is common for BCIs as referred by Wolpaw [34].

Fitts' Law

It was noticed that some studies lack a method to measure performance, therefore impeding the comparison of different approaches. Fitts' Law has been used to compare different pointing devices [35] and has been used in several studies. Measurements of precision while drawing over templates is also suggested [31].

Fitts' law was proposed in 1954 [25] and it is named after his creator, Paul Fitts. It

is a model of human movement that predicts the time to move to a target, depending on the target distance and dimension, as seen in the following equations.

$$T = a + b \cdot ID \tag{1.1}$$

$$ID = log_2(1 + \frac{D}{W}) \tag{1.2}$$

with D representing the distance, W representing the target dimension and ID representing the index of difficulty of the proposed task. The values of a and b are estimated after testing different values of W and D. The original approach by Fitts is shown in Figure 1.2 where the subjects move a stylus alternately back and forth between two separate target regions, tapping targets at the end of each movement.

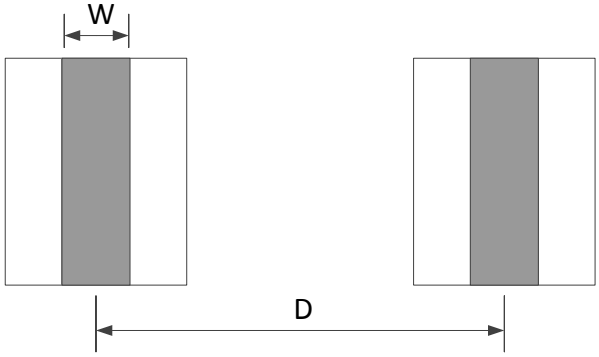

Figure 1.2: Original approach by Fitts where the subject should tap a target (Width=W) distant D units from the other target.

Based on information theory concepts Fitts evaluated the human motor system using tasks such as pin and discs transfers. It was only in the seventies that Card, English and Burr [36] first used Fitts' law to compare different pointing devices. Currently, the ISO 9241-9 standard on the evaluation of pointing device uses the fundamentals of Fitts' law.

An Index of Performance (IP) given in bits/time, can be defined to characterize how

quickly pointing can be done. This is defined in two ways:

$$IP = \frac{1}{b} \tag{1.3}$$

or

$$IP = \frac{ID_{avg}}{MT_{avg}} \tag{1.4}$$

where ID_{avg} is the ID mean for all tasks proposed and MT_{avg} is the mean time measured during movements. In this case, IP is also called throughput (TP).

Speed control

Efficient, natural cursor control depends on speed variability. When far from the target, the cursor moves at higher speed than when the target is nearby. In studies aiming to increase cursor motion efficiency, movement speeds were controlled voluntarily by modulating muscle contractions [33]. Using the following non-linear formula, stronger contractions move the cursor much more quickly than weak ones:

$$Speed = Speed_{max} \cdot \frac{tanh((NMAV - 0.5) * 5) + 1}{2} \tag{1.5}$$

where NMAV is the normalized mean absolute value and Speed_{max} is the maximum speed, set to 1000 pixels per second. Both able-bodied and SCI subjects were capable of using the devised system. However, the improved efficiency brought by modulated speed values is still a matter of discussion, as the experiment results were not compared with the static-speed option.

An alternative to estimating speed by the signal amplitude is presented in [19], in which the system incorporates a three-level graded speed-control scheme. The speed was increased after five consecutive commands indicating the same direction were detected. As soon as the sequence of commands in the same direction was broken, the step-size

for subsequent movements was reduced to a minimum. As in the previous study, no comparisons were made between static and variable cursor speed.

Still, many studies adopt static values for cursor control velocity. This strategy is supported by two factors: fatigue and cognitive effort. Muscle fatigue is an inevitable factor when working with sEMG-based assistive devices, although it varies from subject to subject and between sessions. However, muscle fatigue affects amplitude values found in the sEMG signal. If the speed is modulated by the signal amplitude, then different values are produced, even though the subject is exerting the same level of force.

The use of static values also minimizes the cognitive effort necessary for the subject to perform the task. This is especially true if the dynamics of the original task performed by the muscles involved do not resemble those for cursor control, as in the case of facial muscles. The subjects effort is focused on controlling muscles in a fashion that is completely different than the original.

1.1.3 Automatic speech recognition (ASR)

Since the late 1960s, efforts have been made to achieve a system for speech recognition [34]. Several pieces of software are available in the market and modern OSs for personal computers now offer built-in speech recognition. There are, however, a few drawbacks to the use of typical ASR systems:

- the audible speech prohibits confidential conversation;
- it is not advised to use such systems during meetings or inside a library;
- the performance decays severely in adverse environments such as crowded places;
- some clinical conditions hinder voice communication.

There is a relation among the words pronounced and movements of articulatory facial muscles. Thus, a feasible approach is to use the activation of those muscles to identify

phonemes, and therefore words. This is not an easy task, as the act of speech employs several facial muscles, such as the *Mentalis*, Depressor anguli oris, *Massetter*, *Digastric*, *Zygomaticus major*, *Levator anguli oris*, *Platysma*, and *Orbicularis oris* muscles.

Studies on silent speech interfaces usually regard subjects with voice impairment, such as total laryngectomy patients[37] or those working in situations where the ambient noise impedes communication (e.g. by fire fighters and pilots). Therefore, whether the level of disability compromises the control over the muscles involved in the speech process must be carefully analyzed. An example of this type of subject is a tetraplegic patient using a ventilator system that is adjusted to accommodate cardiopulmonary requirements but is not optimal for speech. Speech produced with typical ventilator adjustments is often characterized by short phrases, long pauses between phrases, abnormal loudness, and poor voice quality [38]. In a study conducted by Denby *et al.* [12] over silent speech interfaces, seven technologies were compared, and the sEMG-based system had the highest overall evaluation.

In [39], hidden Markov Models (HMM) were used to map muscle activation into phonemes. The features extracted from the sEMG signal were Mel-Frequency Cepstral Coefficients (MFCC), as previous studies showed that discrete wavelet transform (DWT) coefficients were superior but slightly different. Only three channels were used with respect to the muscles *Levator anguli oris*, *Zygomaticus major*, and *Depressor anguli oris*. The muscles used and the electrodes were defined heuristically. To evaluate the system a limited vocabulary of 60 words was used and an accuracy of up to 85% was achieved.

In [40] a multimodal ASR with the acoustic information and the sEMG signal allowed a coupled Hidden Markov Model (CHMM) to recognize speech. This solution is compared with two others: audio-only and sEMG-only. When different levels were added to the signal, the audio-only approach was shown to be highly dependent on the SNR, while the sEMG-only proposal was not affected. Five muscle channels were used:

the *Levator anguli oris*, the *Zygomaticus major*, the *Platysma*, the *Depressor anguli oris*, and the anterior belly of the *Digastric*. No criteria were indicated for choosing muscles or the electrode position. The vocabulary used was extremely restricted, with only 10 words.

In [41] only vowels were used, as the shapes of the lips and the mouth cavity were stationary. Three channels were used, with information recorded from the *Mentalis*, *Depressor anguli oris* and *Massetter* muscles, since those are the most active muscles during vowel pronunciation. An ANN using the back-propagation algorithm was used to associate the RMS of the sEMG signal with the vowels. Other studies provide the recognition of isolated words in a small vocabulary [42, 43, 44]. In [44], the aim was to recognize speech of pilots that could be interpreted as commands, and electrodes were embedded in a pilot oxygen mask. The error rate was very low, ranging from 0% to 10.4%, during a speech-recognition task using the numbers zero to nine.

The probability that electrodes are repositioned in the same place as the previous session is very low. In [42], a normalization method found that among sessions, the accuracy decreases by about 10%, yet, without the method, the accuracy decreased more than 21%. Eight channels of information were extracted from the following muscles: *Levator angulis oris*, the *Zygomaticus major*, the *Platysma*, the *Depressor anguli oris*, the anterior belly of the *Digastric* and the tongue. The vocabulary consisted only of the numbers 09.

Wand *et al.* [45] and Jou *et al.* [46] implemented continuous speech recognition using an HMM algorithm. The vocabulary was phonetically balanced and consisted of 108 words. A total of six channels were used. When compared to features from frequency and time-frequency domains, the Wavelet transform showed a slightly advantage.

In general, ASR systems show good results specially because the vocabulary used during tests was usually extremely restricted. Yet, as with other categories of assistive-technology devices, subjects with severe motor impairments may find even a limited

control extremely useful. If 60 words could be associated to different actions, common sense dictates that even this would be extremely helpful for daily activities.

Another issue is that the data used to test each system were obtained under highly controlled situations, with the subjects being under supervision. During normal operation, the subjects will likely be less focused, the pronunciation might be less clear, and the system may not respond very well.

As the goal is to associate phonemes with the activation of related muscles, it is interesting to define some criteria for determining which muscles should be used, as well the electrode positioning which would minimize crosstalk. Although not applied to ASR, in [47] the assessment was conducted for better positioning of electrodes in the forehead, so both electrodes could gather information from different muscles with minimum interference.

1.2 The research objective

The previous section indicates the myriad of applications that are possible using sEMG signals as the source of information for device control. Yet, those systems are not largely disseminated specifically because off issues with lack of stability on the electrode-skin interface and the need for skin preparation and properly electrode placement.

The typical sEMG signal used in those applications represents the ensemble of the activity of several units in the muscle (see Chapter 2) by using large and non-selective electrodes. Although useful, this sEMG signal hides the essential information present.

The objective of this study is to investigate if accessing information at motor unit level would improve the operator's performance during a given task.

The hypothesis is that the proposed methodology would allow generating more precise control commands, when compared to traditional approaches relying on global information obtained by conventional sEMG signal acquisition and processing.

To test the hypothesis, a cursor-control approach is used, and the results using the traditional and the proposed approach are compared.

1.3 Thesis structure

The chapters of this document are organized as follows:

- Chapter 2: aspects of the sEMG signal generation and acquisition are introduced, including physiological factors.
- Chapter 3: the traditional approaches of the sEMG signal-processing are presented, as well the details on the methods used in this research. It also discusses the possibilities of using motor action potentials to generate command signals.
- Chapter 4: the task proposed to verify the hypothesis is described, covering the protocol and its analysis from the point of view of Fitts' Law. Also, the experimental protocol for sEMG signal acquisition and processing is presented.
- Chapter 5: the results found are compared to the results found using the traditional approach, which corroborates the hypothesis.
- Chapter 6: the conclusions are presented and future works are discussed.

1.4 Publications

The following papers have been published as a result of the present work:

- Pinheiro Jr, C.G., Naves, E.L.M., Pino, P., Losson, E., Andrade, A.O., Bourhis, G. "Alternative Communication Systems for people with severe motor disabilities: a Survey", BioMedical Engineering Online 10 , art. no. 31, 2011

- Pinheiro, C.G., Andrade, A.O."The simulation of click and double-click through EMG signal", Proceedings of the Annual International Conference of the IEEE Engineering in Medicine and Biology Society, EMBS , art. no. 6346345, San Diego - USA, pp. 1984-1987, 2012

- Pinheiro Jr, C.G., Andrade, A.O, Bourhis, G. "Myoelectric control system using information at the motor unit level", Proceedings of the XXIII CBEB, pp. 760-762, Porto de Galinhas - Brazil, 2012

Chapter 2

The electromyographic signal generation and acquisition

The sEMG signal is the representation of muscle activity captured by surface electrodes placed over the activated muscle. A sample of the traditional sEMG signal is shown in Figure 2.1.

For those not familiar with sEMG signals, visual inspection shows no difference from ordinary background noise. Further analysis indicates that the sEMG signal may be modeled as a gaussian process with zero-mean value [48] and standard deviation modulated by muscular force. Essentially, this kind of signal results from muscle contractions and can be used in a series of applications, from biomechanics analysis to activation of devices. The sEMG signal, however contains much more information than that shown in the waveform as Figure 2.1 indicates. In fact, appropriate recording techniques unveil important information on how the central nervous system (CNS) operates during specific motor tasks. The following sections present basic aspects of the sEMG signal composition and recording.

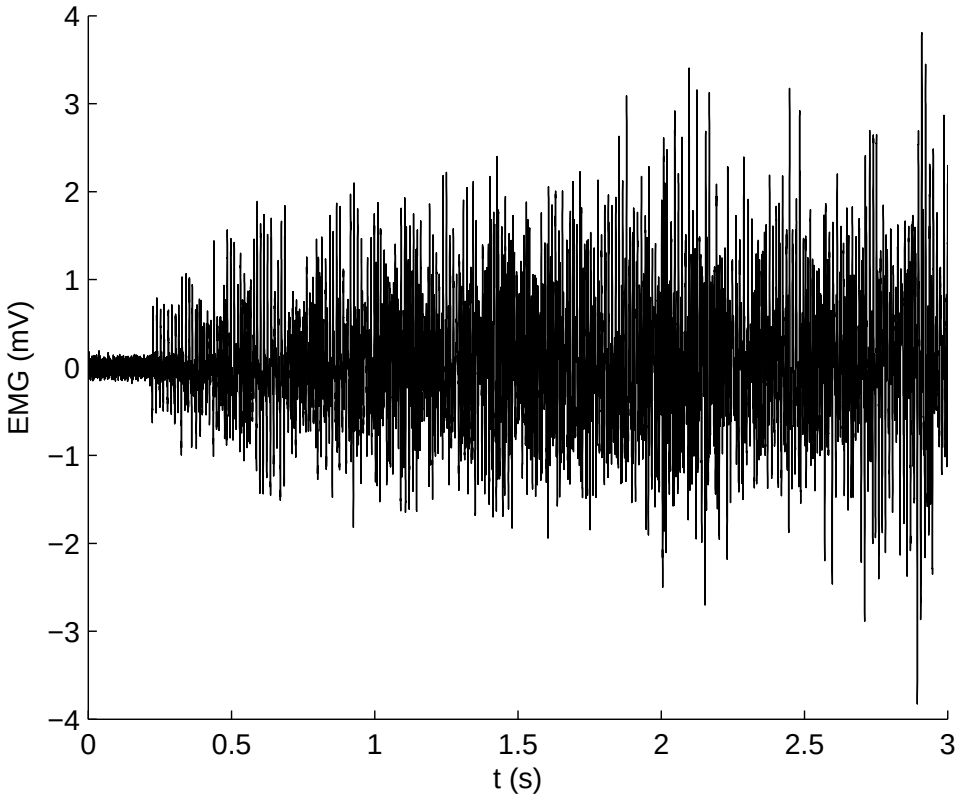

Figure 2.1: sEMG signal recorded at 10 kHz from the *Frontalis* muscle. By visual inspection it was estimated that muscle activity begins at 0.2 s.

2.1 The motor unit

A motor unit (MU) consists of an alpha-motoneuron in the spinal cord and the muscle fibers it innervates (Figure 2.2).

The *alpha*-motoneuron is the final point of summation for all descending and reflex input. The net membrane current induced in this motoneuron by the various synaptic innervation sites determines the discharge (firing) pattern of the MU and, thus, its activity. The number of MUs per muscle in humans may range from about 100 for a small hand muscle to 1000 or more for large limb muscles [49]. It has also been shown

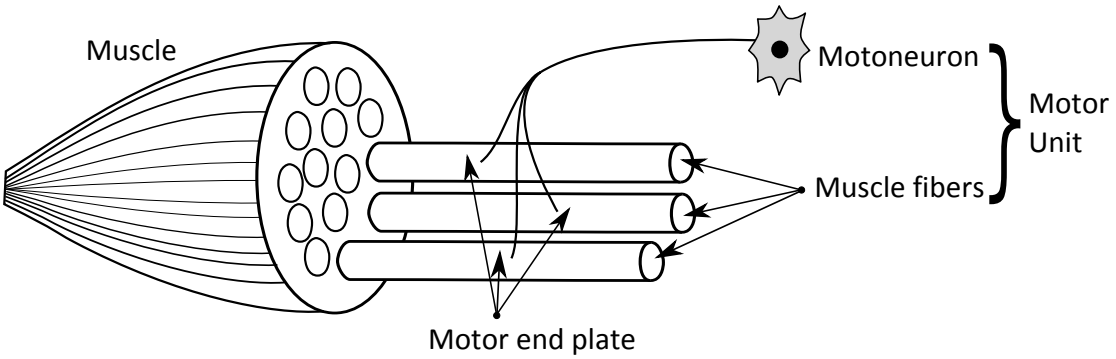

Figure 2.2: The motor unit is composed by the *alpha*-motoneuron and all the fibers innervated by it. The motor end plate is the area where motor nerve fibers and muscle fibers meet.

that different MUs vary greatly in force generating capacity, with a 100-fold or greater difference in twitch force [50].

Muscle fibres vary in size and length between various muscles in the body and between individuals, considering gender, build and age. In a normal adult the mean cross-sectional fibre areas are between 2500 μm^2 (small woman) and 7500 μm^2 (large man), representing a variation in diameter of about 50 to 100 μm [51].

Based on physiological properties such as speed of contraction and sensitivity to fatigue, there are three types of muscle units [52]: fast-twitch, fatigue-resistant (FR or type IIa); fast-twitch, fatigable (FF or type IIb); and slow-twitch (S or type I), which is the type most resistant to fatigue. Muscle fiber composition depends on the muscle function. Antigravity muscles tend to be predominantly type I, while muscles fit to rapid movements have similar proportions of the two fiber types.

In [53] facial muscles were classified based on the muscle fiber type found and three groups emerged:

- phasic muscles comprised of over 80% type II fibers, such as the *Orbicularis oculi*, the *Nasalis* and the *Procerus*;

- tonic muscles with more than 40% of type I fibers, such as the *Frontalis* and the

Corrugator, which are involved in functions requiring sustained facial tonus;

- an intermediate group composed of muscles such as the *Zygomaticus* and *Levator anguli oris*.

2.2 The action potential

The action potential (AP) is a localized event that occurs in excitable cells, notably in neuron and muscle cells. The underlying dynamics of the action potential is described briefly, and its general waveform is shown in Figure 2.3. An actual AP is presented in Figure 2.4.

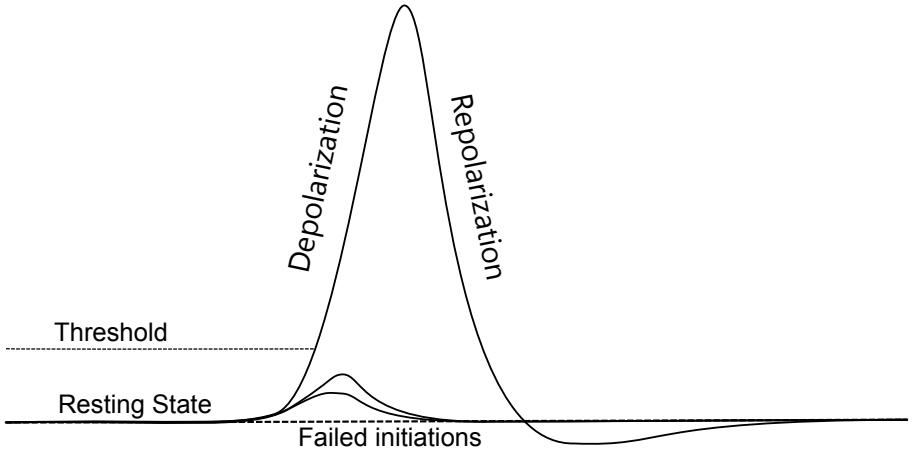

Figure 2.3: Action potential

During the cell membrane resting state, the voltage between the intra and inter-cell medium is about -70 mV and voltage-gated ion channels are closed. Under external stimuli, those gates rapidly open as the membrane potential increases to a precisely defined threshold value. This is the principle known as "all-or-none": a stimulus below the threshold is followed by proportional changes in the membrane voltage change, but not the AP. On the other hand, suprathreshold stimuli will produce APs with similar amplitude and duration.

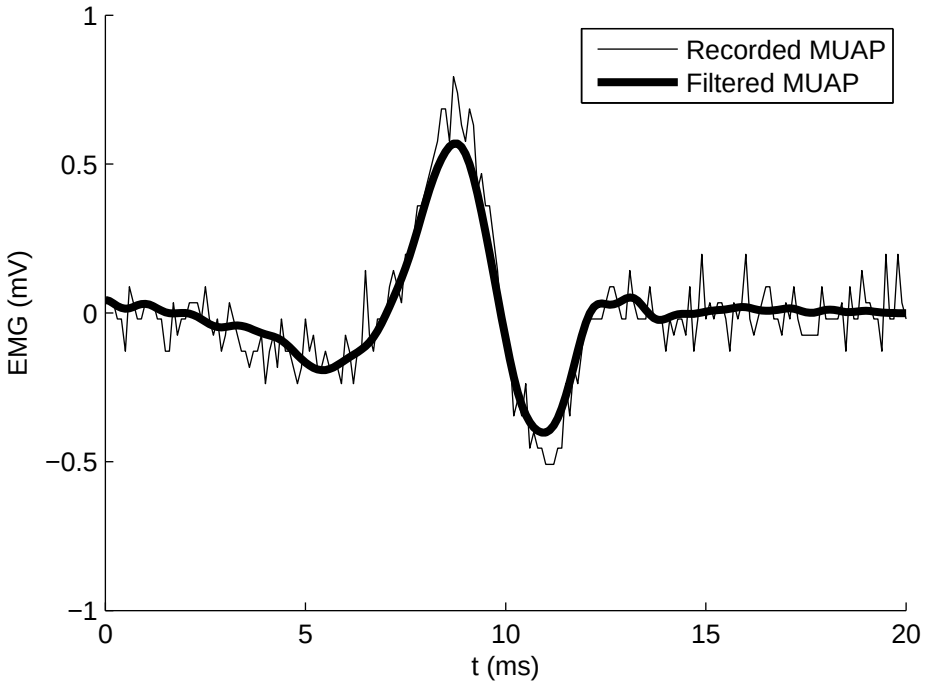

Figure 2.4: Actual motor unit action potential recorded by the equipment used in this study. The signal was acquired from a tetraplegic subject over the *Frontalis* muscle and sampled at 10 kHz.

When the channels open, they allow an inward flow of sodium ions. This current depolarizes the membrane voltage. The process continues until all available ion channels are open, resulting in a large rise in the membrane potential. The rapid influx of sodium ions causes the polarity of the plasma membrane to reverse, and the ion channels then rapidly close. As the sodium channels close, sodium ions can no longer enter the neuron, and they are actively transported out of the plasma membrane. Potassium channels are then activated, and there is an outward current of potassium ions, returning the electrochemical gradient to the resting state. After an AP has occurred, there is a transient negative shift, named the refractory period, which prevents the AP from traveling in the reverse direction. The whole process occurs over a few milliseconds.

As neurons communicate with other cells by means of APs, the AP may be seen

as the most basic bit of information in the human body. Also, APs are responsible for activating internal cell processes. In fact, a neuronal AP is responsible for generating the AP in muscle cells, which in turn stimulates muscle contraction.

The synaptic cleft at the neuromuscular junction separates the motor neuron axon and the motor end plate-membrane. When an AP arrives at the axon terminal, vesicles filled with the neurotransmitter acetylcholine (ACh) are released upon the muscle cell membrane, or sarcolemma. Those neurotransmitters bind with receptors to open the sodium ion gates, causing an AP in the muscle cell membrane, as explained previously. Specifically in a muscle cell, the AP propagates down to the sarcoplasmic reticulum, releasing calcium ions that are ultimately responsible for muscle contraction.

As stated before, the membrane potential rapidly returns to its steady state, but the AP can be seen as a propagating wave along the membrane as described earlier. The region where the AP takes place will be depolarized with respect to distant parts of the cell. This difference in electrical potential is followed by a current flow inside the cell, i.e., positive charges will move out from the region of depolarization, generating the AP in other regions. The velocity at which the AP travels over the muscle fiber is termed muscle fiber conduction velocity, and ranges from 2 to 6 m/s [54]. Several factors affects this velocity, including temperature, muscle length and fiber type.

The size of the action potential, recorded from the surface of the muscle, and the size of the twitch (force) will be proportional to the number of fibres within the contracting motor unit. Within a single muscle there is a range of motor unit size, the number and type of fibres in each depending on the function of the motoneuron. The fast motoneurones support large motor units whereas slow motoneurones support small units.

2.3 sEMG signal

The AP occurring on the muscle fiber is called muscle fiber AP (MFAP), and its properties depend on the physiological aspects of the fiber. Also, in terms of signal detection, the electrode geometry (to be discussed later) and positioning plays an important role on the signal waveform.

A single alpha-motoneuron is capable of innervating several muscle fibers, and this functional unit of cells is called a MU. Therefore, an AP in the muscle fiber is termed a motor unit AP (MUAP). The MUAP waveform is the sum of all MFAPs belonging to the same MU. Then, the MUAP may be represented as

$$MUAP = \sum_{i=1}^{F} MFAP_i(t - \tau) \tag{2.1}$$

where τ represents the temporal offset, which is affected by the conduction velocity and the location of the neuromuscular junction. The variable F is the number of active muscle fibers.

During a muscle contraction, in order for the force to be maintained or increased, the active MU fires a series of sequential MUAPs, called MUAP train (MUAPT).

$$MUAPT_j = \sum_{k=1}^{N} MUAP_k(t - \sigma_k) \tag{2.2}$$

where N is the number of active motor units and σ_k the time of firing of the k-th motor unit.

The tissues separating the muscle cells and the electrode act as a volume-conducting medium. Thus, finally, the sEMG signal can be defined as

$$sEMG = \sum_{j=1}^{M} MUAPT_j + n(t) \tag{2.3}$$

where *n(t)* is the background instrumentation noise and M is the number of MUs in

the electrode range. The value of M is highly dependent on the electrode geometry configuration and its position. Electrodes with a small detection surface area may record the activity of a single MU. This may be appropriate for specific applications, such as medical diagnostics. On the other hand, especially for surface electrodes, as electrode surface area decreases, impedance and recorded background noise increases. Obviously, MUAPs from different MUs are superposed in time. In cases of partially superposed MUAPs, multiphase waveforms may be detected.

Figure 2.5 shows the activity of three motor units and the sum of those MUAPs detected by the same electrode. MUAP superposition can be seen along the combined signal. If the research objective is to discriminate between each MUs activity, which is not true for this study, these superposed signals must be isolated.

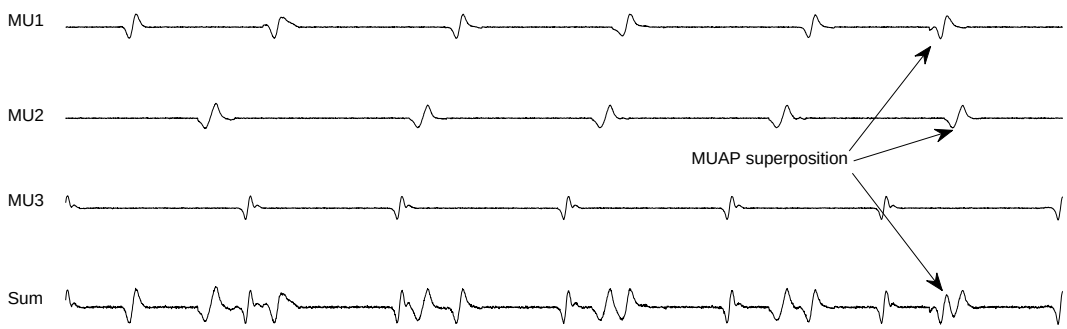

Figure 2.5: Activity of three motor units and the sum of those three signals when registered by the same electrode.

2.4 Force control mechanisms

When a muscle must increase its force exerted, the CNS responds through two mechanisms of action: MU recruitment and rate coding. MU recruitment is regulated by Henneman's size principle [55] which dictates that small MU are recruited before larger ones. Therefore, larger units are recruited according to the increase of force needed. An

important point is that fine motor control is more easily reached with low contraction levels, as the higher the force, larger the size of the next group of MUs recruited.

However, recruitment depends on the type of muscle, and larger muscles tend to recruit all MU at 80% of the MVC [56]. Smaller muscles may use all motor units at about 50% of the MVC and rely more on rate coding - the regulation of the MU firing rate - for force modulation. Minimal and maximal values range from 5-10 impulses/s and above 50 impulses/s, respectively, and are dependent of a series of physiological factors (muscle type, size, age, etc.). As the force required increases, the firing rates of previously recruited MUs also increase. Although the unit impulses/s is appropriate from a physiological point of view, firing rate is commonly indicated using Hertz (Hz), especially in texts from an engineering background. During constant isometric contraction the firing rate is quite regular and presents an approximately Gaussian distribution with σ = 10-20% of the mean [57].

Figure 2.6 [58] presents an EMG signal decomposition in which these aspects of force modulation are observed.

Henneman's size principle is observed in the behaviour of the 34-th MU: this MU has the largest MUAP, is the last to be recruited, and is the first to cease activity. Also, faster firing rates are possible for smaller MUs (recruited first) than larger ones.

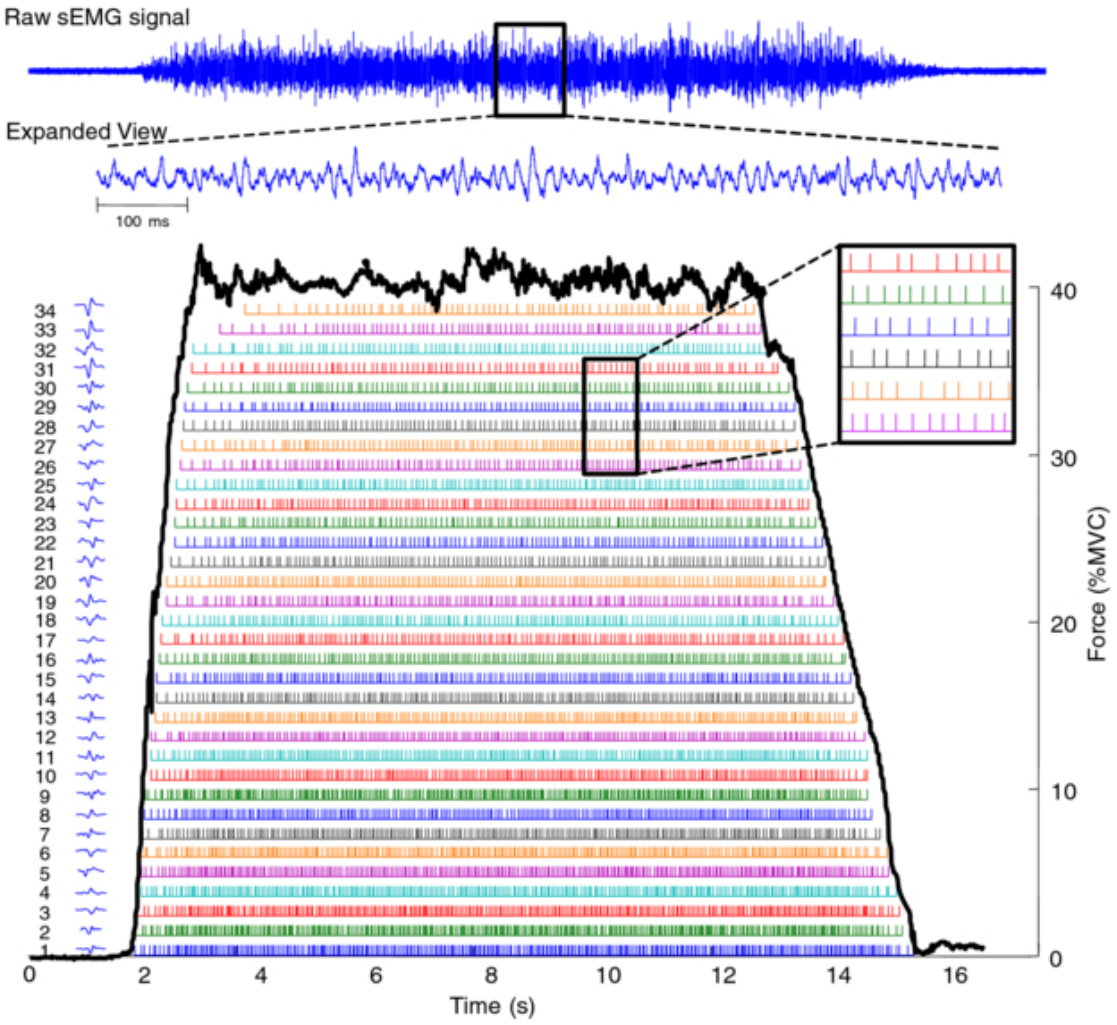

Figure 2.6: EMG decomposition. The level of contraction rises from rest up to 40% of MVC. A total of 34 MUs enumerated in order of appearance and their MUAPs are observed at left. It is possible to see that they are sorted also based on their amplitude, reflecting the Henneman's size principle. It is also possible to visualize the firing rate for each MU (colored bars) and how MUs recruited first have higher firing rate than the ones recruited last. Used with permission from the publisher.

2.5 Signal detection

The EMG signal detection is affected by a series of factors that starts in anatomical and physiological aspects of the muscle observed and ends on technical details of the equipment chosen for the task. As commented previously, the muscle fibers type and

size are determinant in the action potential waveform and amplitude. But there are many other issues of concern that influence the signal characteristics.

- **Signal-to-noise ratio**: this parameter describe the ratio of the wanted signal to the noise, which can be considered as those electrical signals that are not part of the EMG activity.

- **Ambient noise:** this noise originates from sources of electromagnetic radiation (i.e. 60 Hz or 50 Hz). The ambient noise signal may have amplitude that is one to three orders of magnitude greater than the EMG signal. While some equipments allow the use of a notch-filter for noise removal, its use is not recommended as part of the signal information is also removed.

- **Anatomical considerations**: the correct positioning of electrodes on the muscle in analysis is essential. The choice of an incorrect electrode placement site may lead to unexpected results. The SENIAM [59] project offers some recommendations for electrode positioning.

- **Cross-talk**: this refers to the source of EMG signals residing at some distance from the site in analysis, that is, the energy from one muscle group travels over into the recording field of another muscle group.

- **Tissue-filtering**: when the sEMG signal is recorded, the amplitude and frequency are affected by the intervening tissue between the electrodes and the muscle fiber, as this tissue acts as a low-pass filter. This effect is responsible for MUAPs from different motor units presenting similar waveform in the sEMG signal.

The signal collected depends on important factors which are discussed further: the electrode geometry/positioning and the sampling rate.

2.5.1 Electrode geometry

Electromyographic signals may be detected via two possible types of electrodes: indwelling and surface electrodes. Indwelling electrodes may be used for the analysis of deep muscles and they allow for detection of signals from individual motor units. However, they are invasive and needle movements during the examination may cause great discomfort to user. Conversely, surface electrodes provide a safer, easier, and non-invasive method of detecting the signal. However, they are more susceptible to the cross-talk phenomenon, thus, it is more difficult to extract information about the orchestration of the muscle function. Since AAC devices must be operated several hours a day, the following information is restricted to surface electrodes, and more precisely, bipolar ones.

The electrode geometry determines the sEMG signal registered. Therefore two aspects of electrode geometry should be analyzed: electrode surface area and inter-electrode distance (IED). The number of signals from active MUs recorded in the sEMG signal is directly proportional to the electrode area: the tissue between the muscle fibers attenuates the MUAP; therefore, if the distance between the muscle fiber and the electrode is too great, the amplitude of the MUAP will not exceed the background noise and MU activity will not be detected. The electrode can be designed with larger surface area so that the amount of tissue between the electrode and the muscle fiber is no longer an obstacle as seen in Figure 2.7. Conversely, the caveat of decreasing electrode surface area is that impedance increases, resulting in background noise contamination.

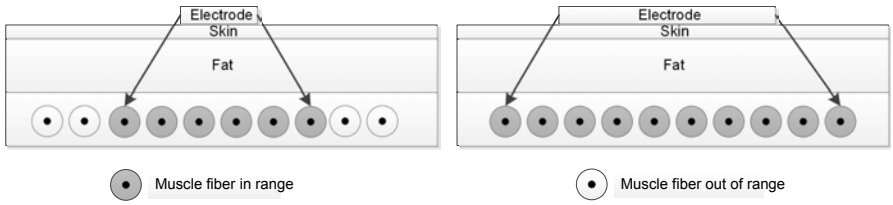

Figure 2.7: Effect of increasing the electrode surface area. If it is increased, further muscle fiber will be in range.

The IED affects the electrode selectivity, which is the ability to record muscle activity from the desired site instead of cross-talk from neighboring muscle fibers. In keeping the IED as short as possible, the amplitude and frequency components from more distant fibers are attenuated [60]. Typical values of IED when detecting MUAPs with surface electrodes are usually within the range of 2-10 mm [61]. The surface EMG for non-invasive assessment of muscles (SENIAM) [62] [59] project recommends IED$\leq$20 mm.

Other features extracted from the sEMG signal are also affected by the IED. In [63], a significant change in sEMG amplitude and in the signal power spectra was observed. The electrode acts as a spatial filter, and short IED results signal of smaller amplitude and higher frequency when compared with the signal resulting from a longer IED.

2.5.2 Sampling Rate

The appropriate choice of the sampling rate (SR) value depends on the Nyquist-Shannon's sampling theorem. This theorem states that in order to preserve the signal information, the SR must be twice the value of the highest frequency found in the signal spectrum.

The energy levels of EMG signals mainly range between 0 and 500 Hz; therefore, SR values around 1 kHz are common in the literature.

In this study, the SR must conform to a more important requirement: the need to properly represent a two-phase wave in the time-domain. The length of the typical AP is not a constant, as different studies present varying values. It is generally accepted that an AP will be longer than 5 ms and shorter than 15 ms.

Although the focus of this project is on using sEMG signals for control purposes, several principles are shared with EMG signal decomposition techniques, since both must detect APs. For the task of EMG signal decomposition, values from 10 kHz to 25 kHz are used. Considering an extremely fast AP with a length of 5 ms, those values of SR would provide 50 and 125 samples respectively.

Figure 2.8 shows the loss of visual information comparing two APs recorded at 10

kHz and subsampled at 2.5 kHz and 625 Hz.

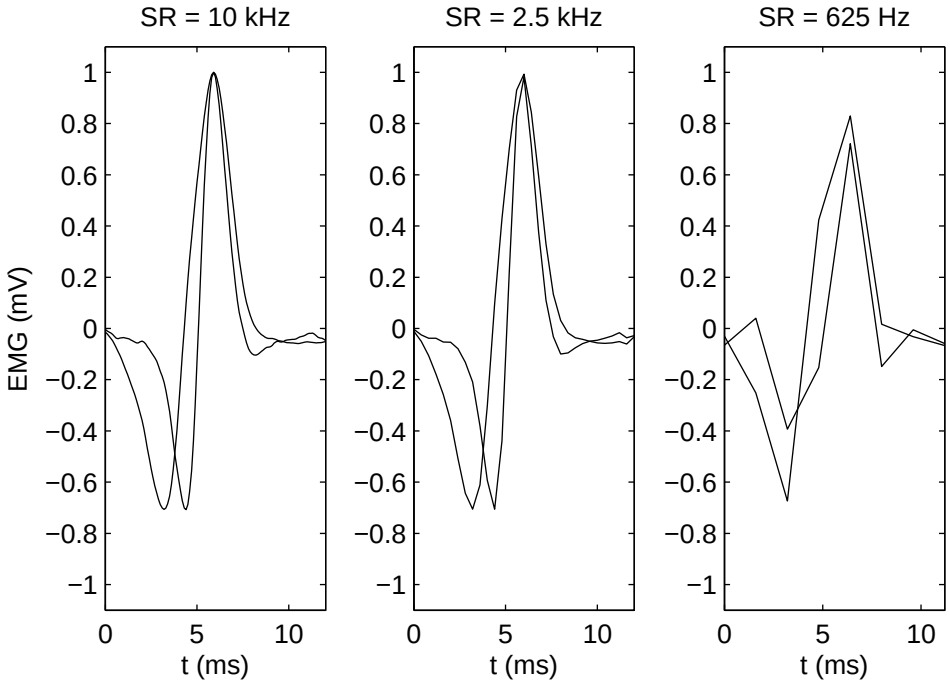

Figure 2.8: Two distinct action potentials recorded at 10 kHz are shown at left. The two following images show the same action potentials subsampled at 2.5 kHz and 625 Hz. The loss of information is clear in the last case.

In the end, the SR must be set with the intended application in mind. For offline clustering analysis to estimate the number of MU present in an EMG signal, an SR of 25 kHz would provide much more information than an SR of only 10 kHz. For systems that must operate in real-time, the amount of data to be processed must comply with signal-processing unit limitations and must be kept as low as possible, without compromising efficiency.

The EMG signal decomposition task is well described in [64], which recommends an SR of 25 kHz as a compromise between oversampling and the minimal rate, the latter being 10 kHz, which may demand interpolation. Studies found in the Journal of Electromyography and Kinesiology between 2008 and 2010, which aimed to detect

muscle activity at the MU level, used signal SR of 25 kHz [65] and 10 kHz [66]. In [67], an SR of 2.048 kHz was used; however the objective was simply to detect the AP occurrence to estimate firing rate and conduction velocity.

For studies not concerned with MU activity, the average SR was 1.484 kHz with the minimum and maximum values being 500 Hz [68] and 3.5 kHz [69] respectively.

For the present study, at first, it was not decided if the MUAPs shape and duration would compose the features to be extracted and the signal was sampled at 10 kHz. Later trials have proved that using on 5 kHz would suffice for correctly detect the MUAPs. Yet, in the end, the 10 kHz value was chosen, as the sEMG signal was stored and may be used in future studies, such as EMG signal decomposition.

Chapter 3

Myoelectric control-based devices

In the few decades, several myoelectrical control-based devices have been developed. Almost all of these are of an assistive nature, such as prostheses [4, 70], wheelchairs [71], basic communication devices [14, 16, 72, 15, 73], cursor-control devices [18, 74] and generic On/Off devices. From all of these possibilities, prostheses are the only devices to available in the consumer market, while the rest have not advanced beyond pilot studies. One of the few AAC commercial solutions based on sEMG signal [17] was a scanning based device and it was available until April 2011.

The steps commonly found in myoelectrical control-based devices are depicted in Figure 3.1 and are explained in the following sections, with consideration of the typical approaches found in the literature.

Later, the methods for MUAP detection are discussed and four methods are evaluated. It was found that the envelope detection method was suitable for this study. Finally, how MUAP information may be explored to generate control signals is discussed.

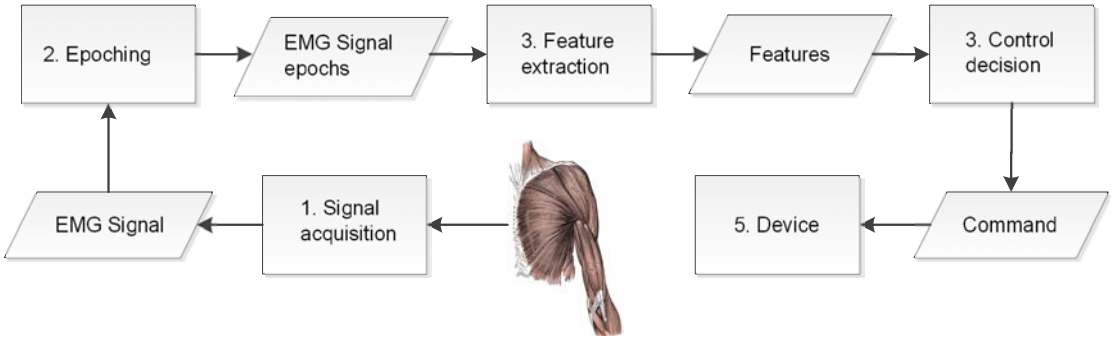

Figure 3.1: sEMG signal is acquired and epochs are extracted. Features are extracted from epochs and feed a control decision system setting the command to the controlled device.

3.1 sEMG acquisition

An assistive device should be designed for daily use, several hours a day; therefore, only surface electrodes are suitable for this application. The SENIAM project [62] [59] found that most studies detailing electrode configuration adopted Ag/AgCl electrodes of 1 cm in diameter. The preferred IED found was 2 cm. As discussed in Chapter 2, the use of this IED provides a sEMG signal composed of the activity of several MUs. The SR does not vary by a large amount, and is commonly found around 1 kHz, as most of the energy signal is assumed to be below 500 Hz.

3.2 Signal pre-processing

In some cases, the signal may be prepared for later processing. Usually this stage involves some kind of noise reduction techniques. But simple operations such as half-wave rectification and envelope estimation for later Mean-average-value extraction is also considered as a pre-processing technique.

The present study consider MUAP detection to generate the commands. One way to minimize MUAP superposition is using the low-pass differential filter (LPD) [75] which has the advantage of being easy to implement both in hardware and software making

LPD eligible for real-time applications. The filter is represented by the equation 3.1.

$$y_k = \sum_{n=1}^{N} x_{k+n} - x_{k-n} \tag{3.1}$$

But as the LPD filter is not an ideal filter, there will exist severe Gibbs phenomenon: the leakage of energy frequency out of the filter pass-band. Under conditions of low signal-to-noise ratio the relatively strong high frequency noise (background activity) may be accentuated. Other possible approaches are based Wavelet de-noising and empiric mode decomposition (EMD) [76]. An example of signal de-noising is shown in Figure 3.2. It is important to remember that the term "signal denoising" is usually devoted to the recovery of a digital signal that has been contaminated by additive white Gaussian noise (AWGN).

A wavelet is a wave-like oscillation with an amplitude that starts out at zero, increases, and then decreases back to zero. Unlike the sines used in Fourier transform for decomposition of a signal, wavelets are generally much more concentrated in time. They usually provide an analysis of the signal which is localized in both time and frequency, whereas Fourier transform is localized only in frequency. As in the Fourier transform, the Wavelet transform describes the signal in terms of coefficients and their functions (version of the original wavelet): detail and approximation coefficients, the latter ones representing 'low-frequency' terms that usually contain important components of the signal, and are less affected by the noise. The de-noise action occurs when detail coefficients are eliminated when smaller than a threshold.

As in the Fourier transform, the EMD method also attempts to represent the signal by a series of functions called Intrinsic Mode Functions (IMFs) which do not have an explicit equation but that must satisfy two criteria: in the whole time-series, the number of extrema and the number of zero crossings must be either equal or differ at most by one and at any point in the time-series, the mean value of the envelopes, one defined by

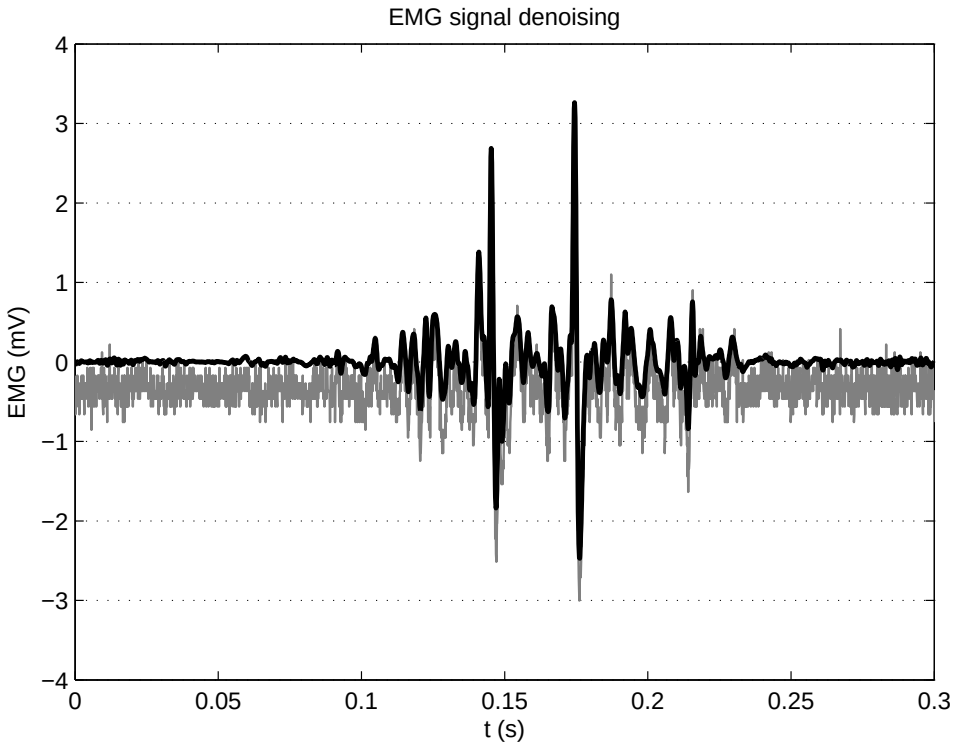

Figure 3.2: Original sEMG signal (gray) and the de-noised signal (black) using the empiric mode decomposition method. acquired and epochs are extracted. Features are extracted from epochs and feed a control decision system setting the command to the controlled device.

the local maxima (upper envelope) and the other by the local minima (lower envelope), is zero. IMFs are thresholded and the signal is then reconstructed.

Beyond signal de-noising, signal whitening is used to decorrelate the signal, improving EMG-based motion classification [77][78]. Whitening orthogonalizes, in time, the EMG samples, thus increasing the statistical bandwidth of the data to compensate for the limited bandwidth of EMG. The whitened EMG have more degrees of freedom, and therefore reduce the variance of the amplitude estimate.

3.3 Data epoching

Out of the continuous flow of data coming from the signal acquisition system, an epoch is extracted and processed to generate a command. At this point, the researcher must make two decisions with respect to epoch length and epoch overlapping.

First, the epoch length should provide adequate available data for the extraction of reliable information. Second, the system must comply with real-time constraints of the required processing time, and the adjacent epoch length should be $\leq$300 ms. Because the muscle activity is composed by the rest-contraction transition and steady intervals, the epoch length is also a key factor when interpreting the EMG signal, specially for devices using pattern-recognition classification, such as prosthesis control. Devices operating by onset intervals will benefit from small-length epochs with higher temporal resolution.

Two approaches for data epoching stands out: adjacent as shown in Figure 3.3 and overlapping epoching, shown in Figure 3.4.

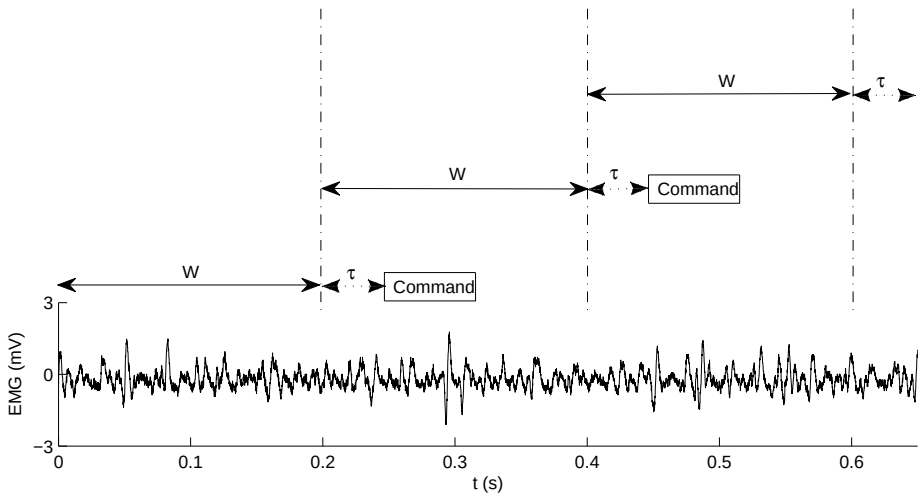

Figure 3.3: EMG signal with 200 ms adjacent epochs. The signal was sampled at 10 kHz which is the rate the signal processing unit must work (10 thousand values per second).

Using adjacent epochs with W length, the system responds with a command every W seconds, assuming the time required for signal-processing and decision-making is

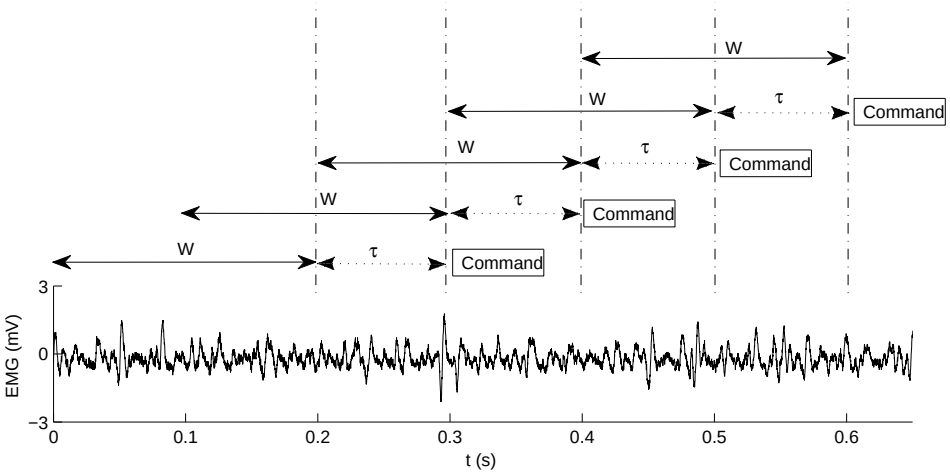

Figure 3.4: EMG signal with 200 ms overlapping epochs and 100 ms increment time (50% overlap). The signal was sampled at 10 kHz, and with 50% overlapping, the signal processing element must compute 20 thousand values per second.

constant. In the overlapping epoch technique, the next epoch overlaps the previous one every (W-τ) seconds, but in this scenario, the system provides a command at every τ seconds assuming the signal-processing and decision-making processes are able to compute the data before the next epoch is available. If this is not the case, then τ must be increased. As superposition increases, so does the commands redundancy and time resolution. The effects of increasing τ is seen in Figure 3.5 in which the variance of each epoch is estimated from an sEMG signal.

In [79], the stream of redundant commands is used in a post-processing method called majority voting. This method utilizes the last and next m-decisions for a given point, to generate a new command. The final decision of each point is based on the greatest number of occurrences in $2m + 1$ decision points. The value of m is determined by signal-processing time and the acceptable delay.

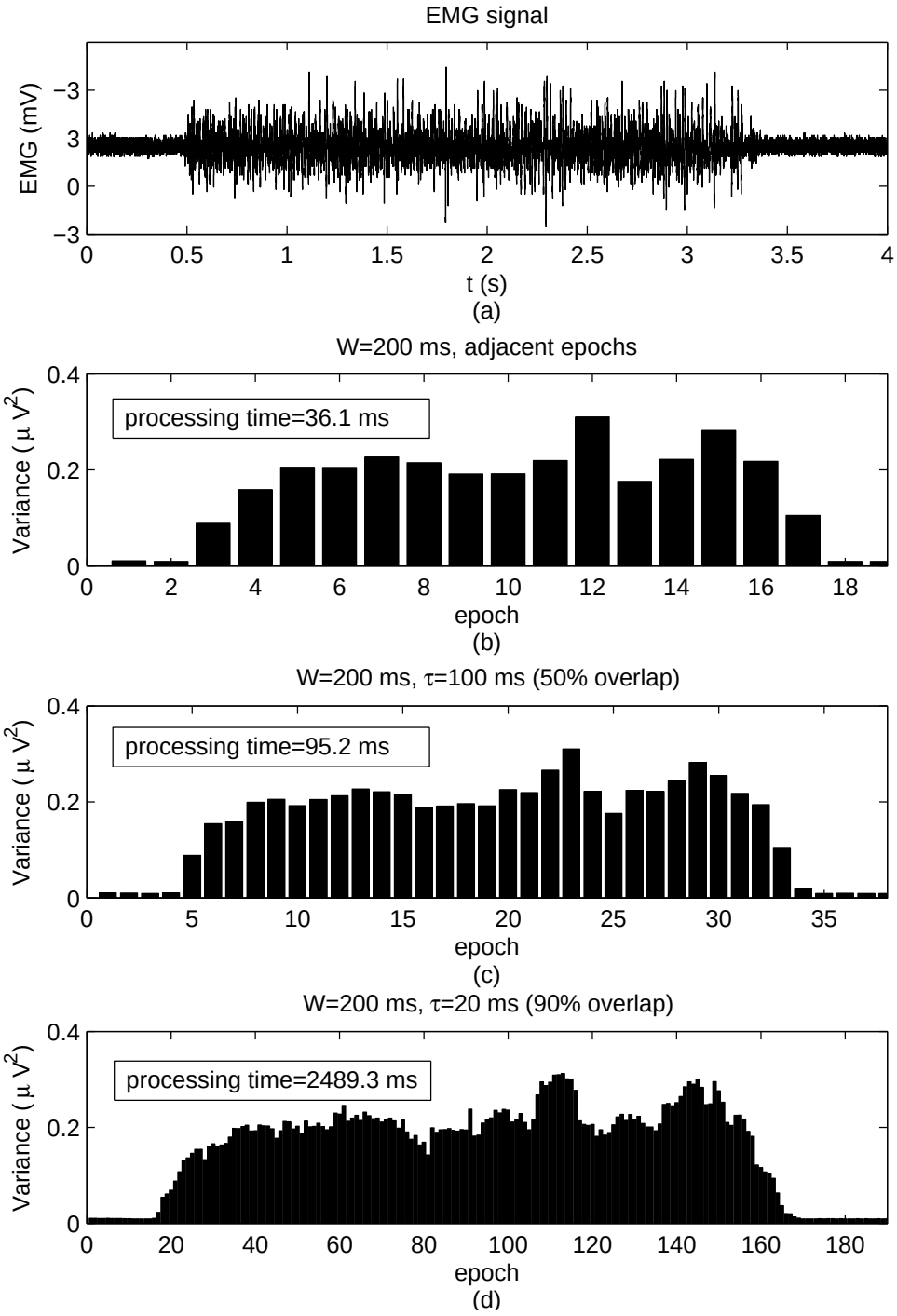

Figure 3.5: sEMG signal (a) with adjacent epochs (b), and overlapping epochs with τ=100 ms (c) and τ=20 ms (d).

3.4 Feature extraction tools

The detected sEMG signal, as presented in Chapter 2, is composed by several MUAPs superposed and contaminated by background noise. It is considered a complex and non-stationary signal. A sample data feature computed over the epoch is a biased approximation of the true value. Amplitude and related features are investigated in time-domain analyses and frequency-domain is related to power spectrums features. Between these are wavelet-extracted features in a time-scale domain.

Several time-domain features are used to estimate of amplitude. Mean absolute value (MAV) and RMS are well-known options. While RMS is suitable for constant force and non-fatiguing contraction, MAV is preferred when the signal is modeled as a Laplacian process, and is usually associated with fatigue and low levels of contraction [80].

Several time-domain features can be combined, as in [81] where the epoch is described as a three-dimensional (3D) vector, composed of the MAV, the non-normalized autocorrelation function of the signal and the absolute value of the standard deviation.

Time-domain features are the straight forward approach to analyze the signal as amplitude increases during a contraction. But frequency-domain features also suffer changes during contraction as the power spectral density (PSD) shifts to the left when compared to the background noise PSD.

The PSD is defined as the Fourier transform of the signal autocorrelation function. Two features extracted from the PSD provide information about the signal changing over time: mean frequency (MNF; shown in Figure 3.6) and median frequency (MDF).

MNF is an average frequency calculated as the sum of product of the EMG power spectrum and the frequency divided by the total sum of the power spectrum. The definition of MNF is given by Eq. 3.2.

$$MNF = \frac{\sum_{i=1}^{M} f_i P_i}{\sum_{i=1}^{M} P_i} \tag{3.2}$$

where f_j is the frequency value of EMG power spectrum at the frequency bin j, P_j is the EMG power spectrum at the frequency bin j, and M is the length of frequency bin.

MDF is a frequency at which the EMG power spectrum is divided into two regions with equal amplitude and its definition is given by Eq. 3.3.

$$\sum_{i=1}^{MDF} P_i = \sum_{i=MDF}^{M} P_i = \frac{1}{2}\sum_{i=1}^{M} P_i \tag{3.3}$$

Fourier transform is based on the assumption that the signal is stationary, but even in a state of constant contraction, this is not the case, as the firing rate of active MUs varies slightly over time. However, during low-level muscle contractions (20-30% MVC) the EMG signal is assumed to be wide-sense stationary. For higher-level contractions, the signal can be assumed stationary for 500-1500 ms intervals [82]. In [83] an epoch length of 250-500 ms for non-stationary conditions is reported as suitable for achieving less variance and bias in estimation; however, epoch lengths shorter than 125 ms lead to high variance and bias and should be avoided.

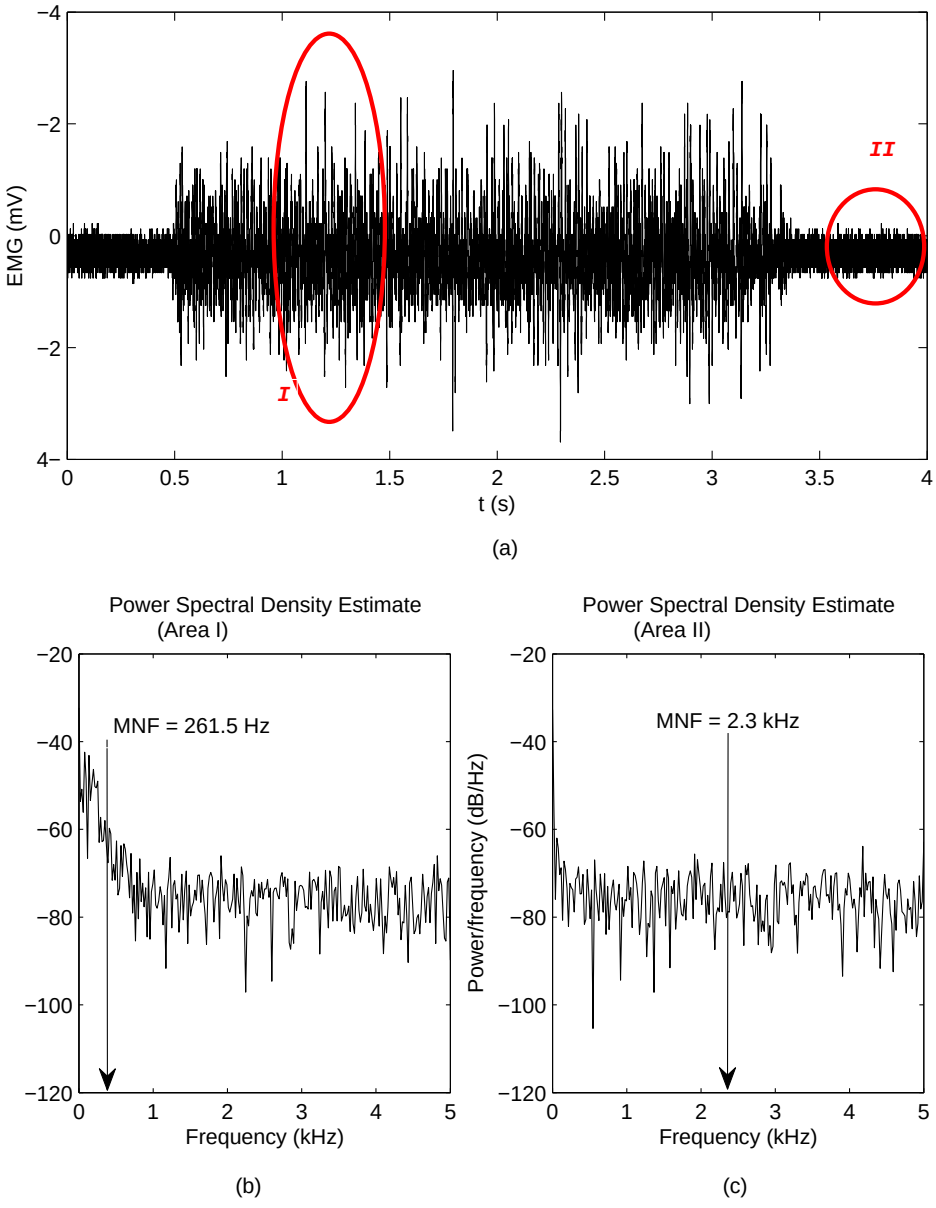

Figure 3.6: The sEMG signal (a) was sampled at 10 kHz and presents areas of muscle contraction (Area I) and rest (Area II). The PSD was estimated and the MNF calculated for each 500 ms epochs representing muscle contraction (b) and muscle resting (c).

3.5 Classification

The myoelectrical control system processes the collection of features extracted from all the muscles involved in the task, to generate the command that is sent to the operating device. The classification task is based in three categories:

- pattern recognition;
- on-set intervals;
- state-machine.

Applications such as prosthesis control may need to classify the feature set as one of many possibilities: grasping, opening the hand, etc. The recorded sEMG signal undergoes alterations over the course of the day caused by several factors, such as changes in electrode position, fatigue, and weakening of the electrode-skin interface by sweat or evaporated conducting gel. A signal classifier should be able to cope with such varying patterns optimally and should prevent over-fitting. It is important to make a clear difference between signal non stationarities caused by technical problems on one side, and by a modification of the user behavior on the other side. A number of factors could be listed as technical: the electrode structure and placement, fiber type composition in the muscle, amount of tissue between surface of the muscle and the electrode and changes in the skin-electrode interface. It is possible to predict and model the change of those parameters [84], but not the level of involvement of the user in the task or his/her fatigue which leads to a series of modifications in the signal: number of active motor units, firing rate of those MUs, etc.

Classification should be adequately fast, in order to meet real-time constraints. A suitable classifier must be efficient in identifying novel patterns; online training can maintain the stability of classification performance throughout long-term operation. Pattern

recognition belongs to the greater scientific field of machine learning, and includes neural networks, fuzzy logic and probabilistic models such as HMMs.

Simpler devices require detection only when the muscle is active. Onset-based systems are substantially more simple than pattern recognition solutions and are, therefore, less prone to error. The performance of an onset-detection method is mainly evaluated by the bias and variance of the estimated onset and offset time, as well as sensitivity to signal-to-noise ratio (SNR).

The single-threshold method is the essential approach. In this method, rectified raw signals are compared with thresholds that are obtained based on the mean power of background noise.

This method is very fast and simple in implementation, but too sensitive for SNR. This method is better suited to ON/OFF detection, rather than detection of slowly increasing muscle activities. An improved single-threshold method is based on a time-enveloped signal, rather than on the instant value. For example, the MAV of a low-pass filtered signal is compared with a threshold that relates to background noise. Due to the time delay in computing, filters cause bias in estimated onset time. An improved single-threshold method is not well-suited to standardization, since its performance depends primarily on signal envelope and threshold estimation methods.

In the double-threshold method proposed in [48] single-threshold detection is applied to a fixed number of consecutive values of an auxiliary variable, and onset is detected when at least a certain number of them cross the threshold. Therefore, the false-alarm probability and detection probability, as well as time resolution, can be adjusted independently. Because a double-threshold method involves more parameters to tune, including the acceptable error, it is superior to a single-threshold method. A double-threshold method also yields a higher detection probability for a fixed value of false-alarm probability than a single-threshold method, and in addition, subjects can adapt the link between the two mentioned probabilities with a higher degree of freedom. Onset-based

methods demand a post-processor cascaded to the detector to reject transitions shorter than an acceptable interval.

Finite-state machines (FSMs) or extended FSMs (EFSMs), output pre-defined commands based on the sequences of input signals. They are composed of a finite number of states, transitions between those states, and commands. States often represent pre-defined actions, and transition roles are associated with raw signal or signal features. This method allows the operation of a device with more commands than the number of muscles involved in the task. In [85] a wheelchair was controlled using the *Frontalis* muscle that provided two commands: single-click and double-click. The devised FSM was enough to issue four different commands: LEFT, RIGHT, STRAIGHT and HALT. The proposed task in this study, which is depicted in the next chapter, also uses an FSM for cursor control.

3.6 MUAP detection

In this study, the source of information explored for system control is the sEMG signal, and more precisely, the MUAPs that compose that signal. This means that onset and offset intervals must be detected to discriminate MUAPs from background noise.

Traditional methods on processing sEMG signal do not detect individual MUAPs, differently from the task known as EMG decomposition. The approach consists of separating the EMG signal into the constituent MUAPTs. Through the EMG decomposition one can detect neuromuscular disorders and investigate the state of muscles and nerves. The more accurate the decomposition is, the more applicability it finds in distinct areas, for instance, such results may be employed in biofeedback applications and muscle fatigue monitoring. The EMG decomposition can be divided into four stages:

- MUAP detection;
- MUAP clustering;

- superposition solving;
- assign each MUAP to the appropriate MU.

The present study can explore the techniques on signal acquisition and MUAP detection but the remaining steps are not necessary to the goal of this study.

Several techniques have been developed throughout the years of research of EMG decomposition. Four MUAP detection methods were selected for comparison, which use the: (i) the envelope amplitude [86]; (ii) the signal amplitude [87][88]; the signal variance [89] and (iv) a combination of both slope and amplitude thresholds [90]. The first one was developed by members of our researching group and presented good potential. The three others were represented their respective group (based on the feature observed). Modifications were made in the original algorithms to suit signal processing for the proposed task.

The method described in [86] uses the signal envelope amplitude to find the regions of activity (RA), which may contain one or more MUAPs. Using the signal envelope, only one threshold must be used as only positive values are found in the signal envelope. An easy approach to obtain the signal envelope is to use low-pass and curve-fitting techniques filtering techniques or by using the Hilbert transform to compute the analytic signal. The latter has the lack of parameters as main advantage but demands higher computational power than using the low-pass filtering approach. Since the test would use a modern laptop, this was not a concern. However, a embedded implementation of this solution may require a digital signal processor instead of simple and inexpensive microcontroller. From the signal envelope, local minima and maxima points are estimated in order to reduce the number of candidate points to be searched by the peak detector. As a consequence, the processing time is also reduced, which may be relevant for the analysis of either long or oversampled time-series. Another benefit is that noise activity may be eliminated.

The role of the peak detector is to identify extrema points which are above or below a threshold. Once a location of a maximum t_o is found, the mean of the samples within a small time window, $h_o = t_o + u$, is estimated, and only if the mean is above the pre-defined threshold, t_o, will be selected as the beginning of an RA. In this system, u is set to 1 ms. Such a procedure may avoid the selection of spurious activities (e.g., noise). The end of an RA is detected when a minimum t_f is found. t_f is considered to be valid only if the mean of the window $h_o = t_o - u$ is below the threshold. The threshold, th, is estimated as $th = k \times Wnoise$, where $Wnoise$ is a window of noise selected from the signal being analyzed and k is a user-defined constant, which controls the threshold level. A typical value for k, justified by Chebyshev's theorem, is 5, which means, in practice, that any sample within the range has 96% chance of really being noise. Therefore, to use this method, one has to set only the value of u which will affect the running time, but not the envelope itself. A segment of the EMG signal and the RAs detected using the signal envelope are shown in Fig. 3.7.

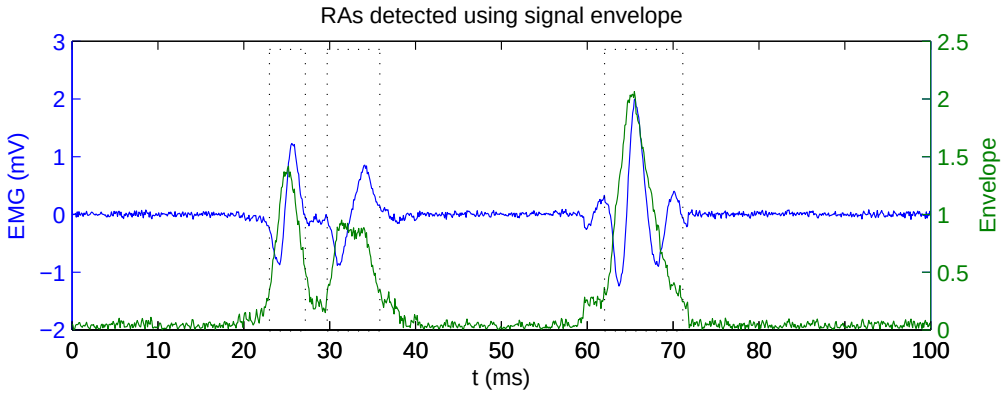

Figure 3.7: Regions of activity detected using the signal envelope.

In [89], the variance of the signal is used to find the RAs. A window with length, N, is passed along the EMG signal. If the variance inside the window exceeds a detection threshold $thrd$, a new segment is detected. By searching backwards and forwards from this index until the variance drops below a delimiting threshold $thrl$, the beginning and

end of the segment is obtained.

Estimation of *thrd* is carried out from the amplitude density function of the normalized variance signal. A local maximum in the density function represents a set of MUAPs with the given variance. From this, *thrd* is defined as the first local minimum searched, when starting from the origin where the smallest MUAPs are assumed to be distinguished from the noise. The segment-delimiting threshold *thrl* is estimated from: $thrl = 0.35 \times thrd + 0.65 \times blmv$, where *blmv* denotes the mean of the baseline variance, which is calculated by pre-segmenting the EMG signal with $thrl = thrd/2$. As in the previous method, one has to set only the value of window length N. As seen in Fig. 3.8 the variance obtained using a sliding window acts as an filter and the response is affected by the window length. Using window of 10 ms in length, the two first MUAPs are seen as one. If the window is 5 ms, those two MUAPs could be detected correctly, depending on the threshold.

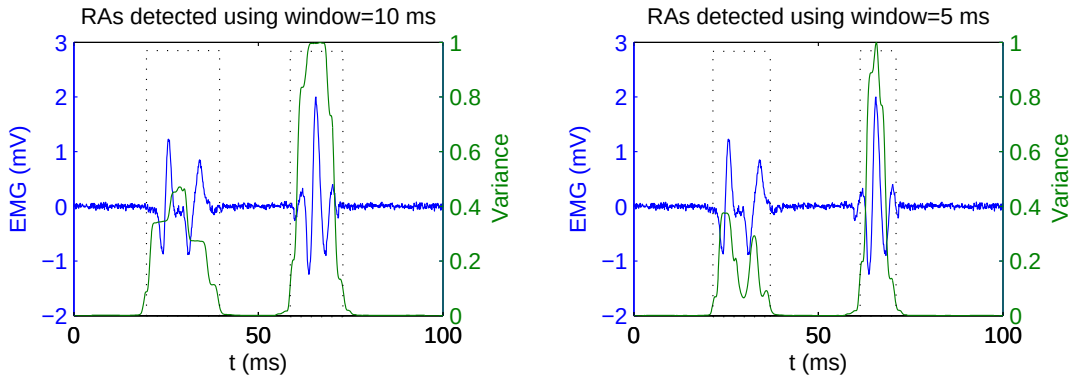

Figure 3.8: Regions of activity detected using variance. The information extracted from the signal is affected by the size of the sliding window.

Both amplitude and slope are used in [90] to detect the RAs. An initial threshold is set as $B1 = \frac{\sum_{i=1}^{n} |V_i|}{n}$ where V_i is a series of extrema in the $[0.5V^{RMS} - V^{RMS}]$ range, being V^{RMS} the root-mean-square value of the entire signal. The slope threshold is represented by a minimum amplitude variation of $B1$ within a 1 ms sliding time window preventing discarding zero crossings where MUAPs show rapid transitions. Waveforms

representing MUAPs are removed from the signal and after this first step, if the average magnitude of the remaining local extrema exceeds the ensuing RMS value by a factor 2, the residual signal is segmented again with threshold $B2 = 2V^{RMS}$. A two-threshold approach optimizes segmentation results for complex signals, focusing on separating large MUAPs that only interfere at their extremities while detecting small MUAPs that would otherwise be overlooked. Again, only the sliding window must bet set. In Fig. 3.9 RAs are detected correctly as during depolarization and repolarization, small amplitude samples are considered as part of the MUAPs because of the slope.

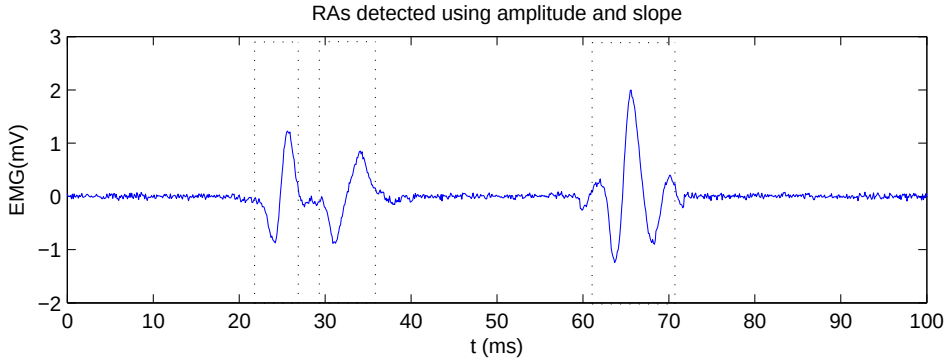

Figure 3.9: Regions of activity detected using amplitude and slope. During depolarization and repolarization, small amplitude are considered as part of the MUAPs because of the slope.

Finally, it is possible to use the amplitude of the raw signal to detect the RAs, as it is done in [87] and [88]. The absolute value of every sample above a threshold is considered as part of a MUAP. After samples are evaluated a post-processor is needed to fill gaps and to refuse noise represented by short MUAPs candidates. In Fig. 3.10 RAs are detected considering only the signal amplitude, but undesirable gaps must be corrected using a postprocessor to eliminate gaps smaller than a threshold, e.g. 2 ms.

MUAP detection tools are to be evaluated in two ways. The first is to use a qualified professional to analyze the signal and compare it to the output given by the automated system. The second option is to work with synthetic data, so the intervals, number of

MUs and MUAPs are known a priori. The main advantage of the second approach is having nearly infinite data set variations for evaluation and a nearly real-time response. The result of the comparison is shown in Chapter 4.

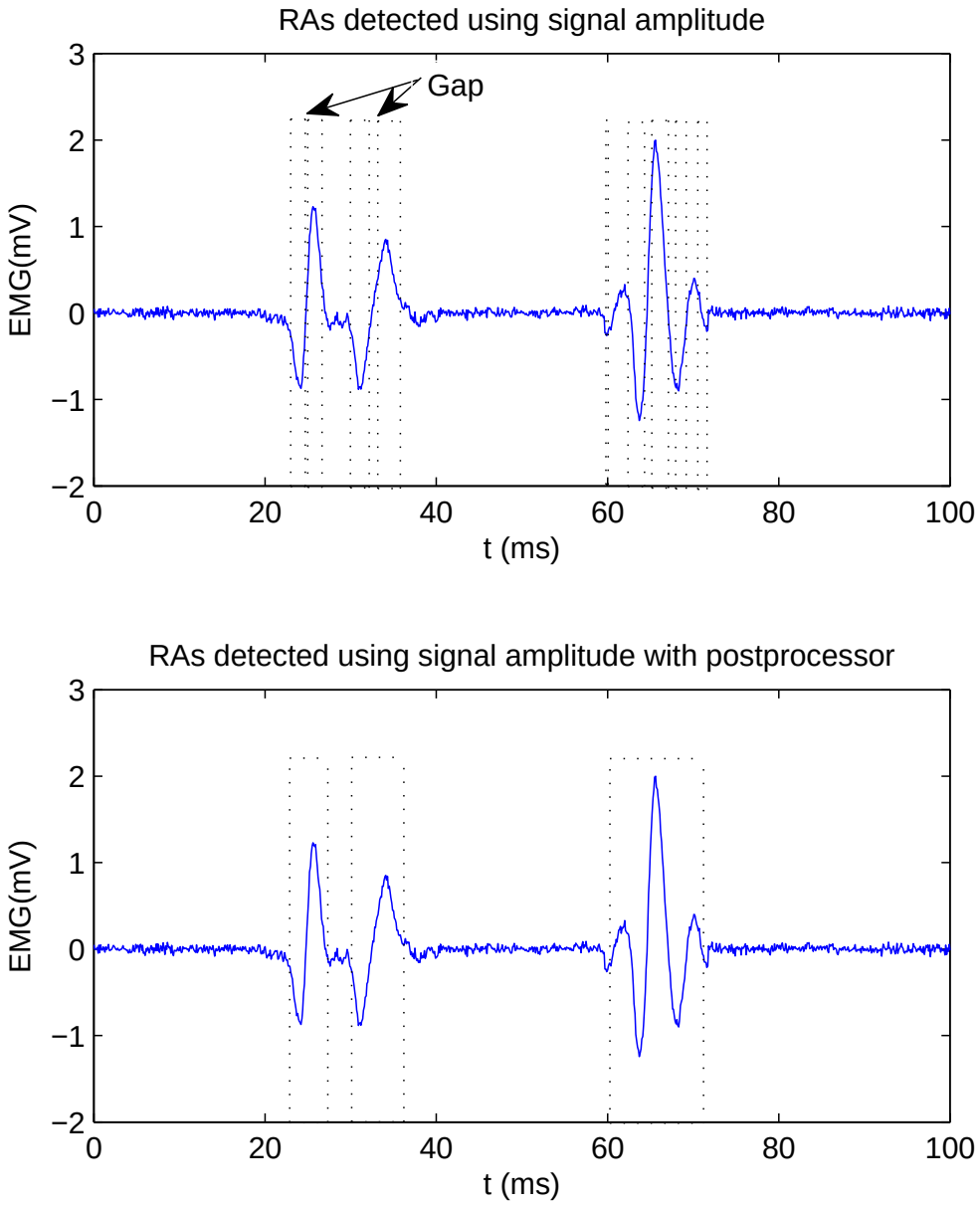

Figure 3.10: Regions of activity detected using amplitude. Gaps are created during MUAPs in cases of small amplitude samples. Those imperfections must be corrected using a postprocessor that will fill gaps smaller than a threshold, e.g. 2 ms.

3.7 Using MUAP as source of information

Before resolving the kind of command it is possible to generate from MUAP detection, it is necessary to remember what the acquired signal represents.

The MUAPs registered in the skin surface change as they propagate through the conductor volume, which acts as a filter. During contraction, activity from deep muscle fibers is not registered and, if the objective is to decode the neural drive (neuronal output) to muscles, the information will be incomplete. In fact, this lack of information is not exclusive to surface electrodes. Single channel intramuscular EMG measurement does not offer representative information on the MU population behaviour due to the electrodes high selectivity [91].

Binary control signals are easily obtained, as a single MUAP detected is enough to classify one epoch as containing EMG activity. As discussed earlier, this kind of signal, though simple, is highly useful when used with FSM. This class of applications demands only one channel.

Progressive signals are more complex to obtain and demand high-density surface electrodes so the EMG signal can be decomposed, and so that posterior activity from MUs can be used to infer the neural drive to the muscle. Complete information is not necessary, as the spread of common synaptic input to motor neurons is observed from the analysis of multiple muscles in complex tasks [92].

Chapter 4

Experiment and Results

This study was designed, though not exclusively, to provide solutions in the AAC field. For this reason, it was natural to employ the cursor control task to evaluate the proposed method of EMG signal-processing and interpretation. This task is a common target for several studies in the last 20 years, as the mouse has become the major device operating human computer interfaces. At this point, it must be highlighted that traditional computer interfaces found in commercial and public OS were not designed for impaired users, and in cases of severe motor limitations, a more suitable interface should be considered. Yet, even for those personalized solutions, the four- directions displacement method offers an interesting tool. Additionally, a previous work developed by our research group provided cursor control using traditional EMG signal processing [81]. For an adequate comparison between the traditional and the novel method on interpreting the sEMG signal, the decision was to choose the identical task as performed in [81]. The timeline for both studies is shown in Figure 4.1.

In the following sections, the methodology and materials used in the trials is presented. Later, the end results - the subject's elapsed time of executing the task, error on selecting targets, and target over-shooting - are analyzed. Finally, the results obtained in this study are compared to the results found using a traditional sEMG signal-processing

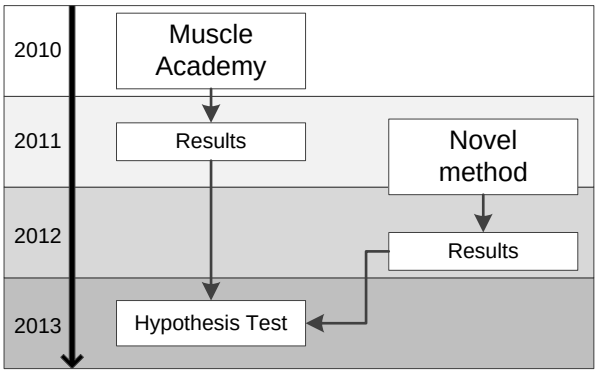

Figure 4.1: Timeline for both studies compared in this document. The first study using traditional sEMG processing and interpretation, resulted in a system called Muscle Academy and it was developed in 2010 with results available in 2011. At the beginning of 2011, the software for the present study was finalized and trials were carried out in 2012. The results from both experiments are compared in 2013.

approach, in order to validate the hypothesis that accessing MUAPs the user is capable of superior performance on a given task.

4.1 The proposed task

The interface designed to evaluate the cursor control task is presented in Figure 4.2 and it was first developed by Andrade [81]. The system was coded in C/C++ language using Visual Studio 2008. Four colored targets were placed 15 cm apart and two perpendicular dashed lines were placed to offer the user some level of assistance.

The degree of difficulty varied according to 3 different values for the square edges: [2, 1 and 0.5 cm], corresponding to what from now on will be referred as protocols 1, 2 and 3 respectively. Evaluating the task design under Fitts' Law (equation 1.2), the index of difficulty increased almost linearly with IDs = 3.19, 4 and 4.95 bits, respectively. Another variable presented by the sequence of targets: clockwise, anti-clockwise and random.

The cursor control is performed by the operator using only one muscle. All subjects operated the system using the *Frontalis* muscle. The four-direction commands are

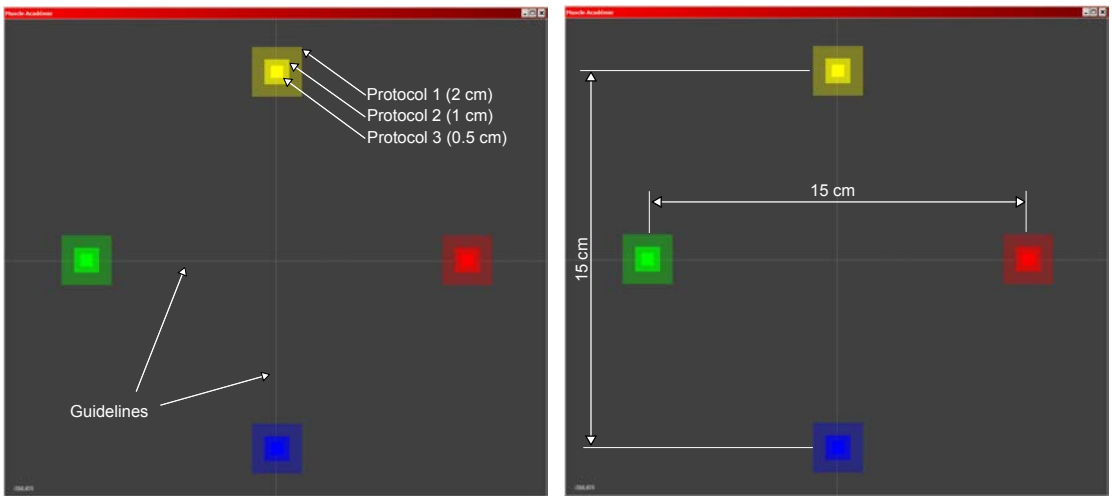

Figure 4.2: Interface screenshot. The image at the left shows the guidelines and targets size using protocols 1, 2 and 3. The image at the right shows the distance between center's targets, which was set to 15 cm.

created using an EFSM, depicted in its simplified form in Figure 4.3.

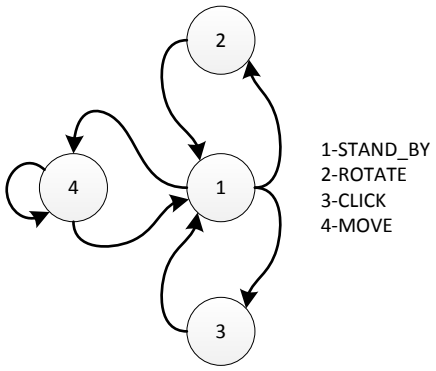

Figure 4.3: Simplified representation of the state machine. At state 1, the cursor stands by. The state 2 evokes the rotation procedure, rotating the cursor icon 90 clockwise. The state 3 evokes the click event and state 4 displace the cursor towards the direction indicated by the cursor.

Contractions smaller than 300 ms rotates the cursor 90 degrees clockwise. If the contraction is longer than 300 ms, the cursor moves towards the direction pointed by the cursor. The target acquisition, i.e. the click event over the target, occurs after 1

s of muscle inactivity. This poses a problem known as the Midas touch, also present in gaze-based devices, causing undesired object selection and requiring more attention from the subject to avoid those errors. A simple solution for this problem is the addition of a secondary channel to perform the click event. For the present study, the *Temporalis* was also considered but technical difficulties did not allow the use of this muscle as the SNR was too low and the signal processing did not provide acceptable results. A second alternative considered was to use two fast contractions from the *Frontalis* to represent the click event. Earlier trials using this same muscle proved it could work [93] but it was also observed that too many fast contractions in the *Frontalis* could cause extreme fatigue. The full EFSM, including the threshold times, is found in Figure 4.4 and perform under three different situations:

- Rotation: starting at state '1' the transition to state '1a' happens when the contraction is first detected. The state remains at '1a' while the counter (TC) is smaller than 300 ms (TH1). While in '1a', if the contraction stops, then the rotation occurs, the counter TR is incremented and the state becames '3a';

- Click: after the end of a contraction, the EFSM is at state '3a'. After the counter (TR) is greater than 1 s (TH2), meaning 1 s without contraction, a mouse Click is generated and the EFSM returns to state '1'. If a contraction occurs before 1 s of inactivity, the EFSM performs the action described in the previous item, as if it was starting from state '1'. If the SNR is low small pauses are noticed by the user;

- Cursor movement: if the contraction is longer than or equal to 300 ms the cursor moves towards the direction shown in the cursor and the EFSM goes from '1a' to '4' and it will remain like this while there is a contraction detected. When the contraction stops, the state becames '3a' and the course of action as described in the previous item is taken.

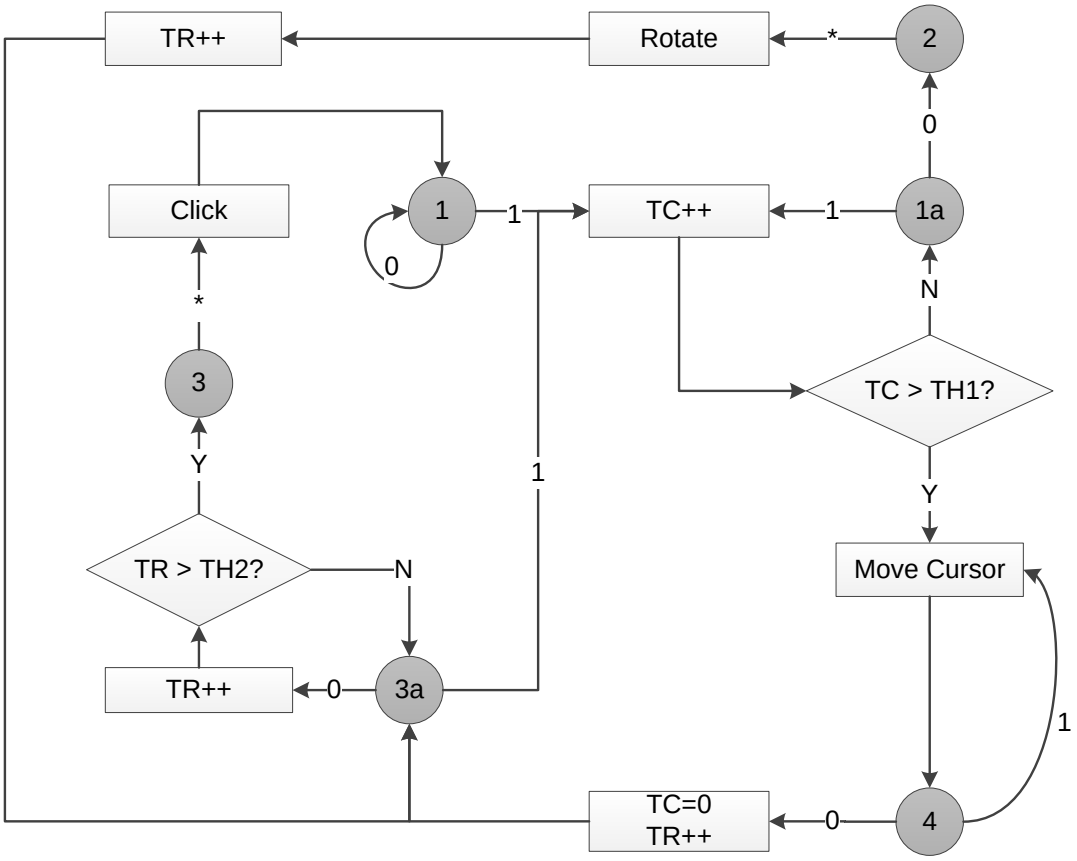

Figure 4.4: The EFSM above controls the emulated mouse events. Two counters are employed: TC and TR referring to contraction and relaxing, respectively. Those two counters are compared to two preset thresholds: THC and THR with values of 300 ms and 1 s. This EFSM is fed by the output of the sEMG signal processing, where input 0 refers to no activity and 1 to muscle contraction.

An example of the state-transition during two contractions is shown in Fig. 4.5. It should be clear now that both states 2 and 3 are transitory and represent the rotate and click events, respectively. The EFSM would move the cursor (state 4), rotate the cursor (transition from state 1a to 3a) and create the click event (transition from state 3a to 1).

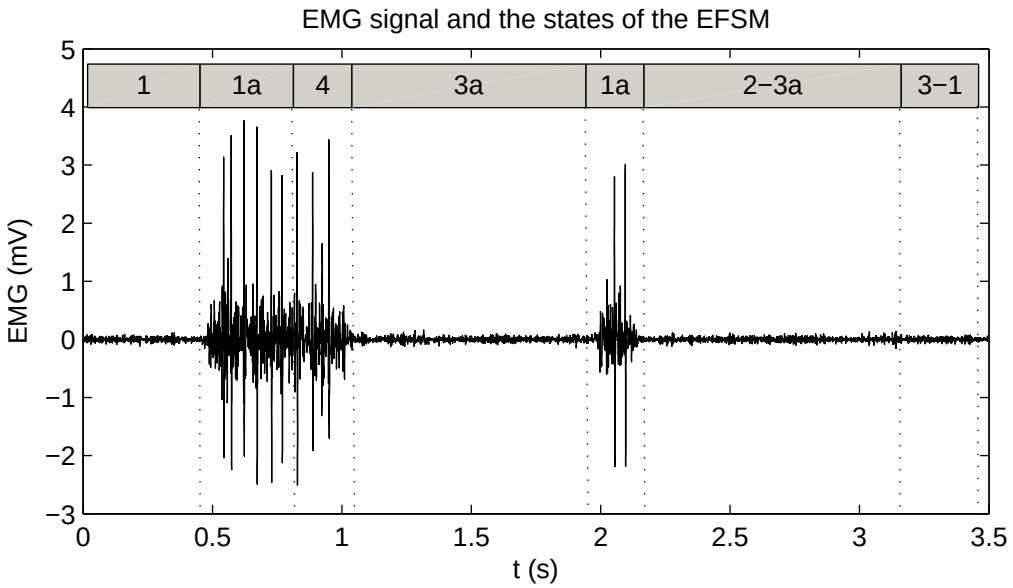

Figure 4.5: A signal with a long (approximately 1 s) and a short contraction (approximately 200 ms). Above the graph, the numbers represent the state of the EFSM. The signal is interpreted as a cursor movement and a rotation. The click occurs only after the short contraction as the interval between both contractions is shorter than 1 s. States 2 and 3 are transitory and represent the rotate and click events, respectively.

The system offered the subject two kinds of feedback: visual - as the current target blinks as it waits the mouse click - and auditive - a beep immediately after the target is acquired. A different sound is executed when the final target in one round is clicked.

4.2 Subject recruiting

The results presented here were produced by testing 12 subjects. The subject demographics are shown in Table 4.1. The subject included 10 able-bodied men and one woman with age of (31±9.11) years old. The 12th subjects was a 35 years old tetraplegic unable to operate a traditional mouse. One could argue that the number of motor impaired subjects tested should be higher for this kind of application, but a system using muscle activity as source of control is practical for anyone capable of controlling the target muscle properly, regardless of the subject's overall mobility. In total, 21 subjects

were volunteers for this study: 14 able-bodied and 7 subjects with disability. From the able-bodied group, three of them were not capable of operating the system correctly. In the motor-impaired group, five of them were not able to carry on the task using the *Frontalis* muscle, and one could not take part after the first session for personal reasons. Only the results gathered from the 12 users that went through all sessions were considered.

Able-bodied	
Number of Subjects	11 (10 male ; 1 female)
Age (years)	30±8
Disabled	
Number of Subjects	1 (male)
Age (years)	35
Handicap	Tetraplegia caused by SCI

Table 4.1: Summary statistics of subject demographics.

4.3 EMG acquisition and processing

The *Frontalis* muscle was used to control the cursor. Located in the head, this muscle is still under control, even by severely impaired subjects such as tetraplegic patients. This muscle is not involved in imperative tasks like speech and mastication. Also, it is a muscle composed of many type I, fatigue-resistant muscle fibers. Therefore, it is a muscle suitable for using AAC devices several hours a day.

The *Frontalis* is not attached to any bone, and has proximal and distal attachments at the galea aponeurotica and the skin around the eyebrows, respectively. For most of the subjects, better signals where obtained when the electrode was placed horizontally 3 cm above the eyebrow, corresponding to the muscle belly, as suggested by the SENIAM project [62] [59]. Nevertheless, in the first session, the optimal electrode placement was obtained by trial and error. At this point, the first complication of this proposed

approach was found: this electrode placement is considerably more difficult than that of traditional large electrodes, and small displacements over the skin greatly affect the amplitude of the sEMG signal. The *Frontalis* is a fairly isolated facial muscle, and activities such as chewing, speaking, and blinking did not affect the signal measured. Head movement was not also an issue, as the cable and electrode was always well fixed. The *Corrugator* muscle, which is responsible for frowning, was the only problem.

(a) (b)

Figure 4.6: The electrode was placed over the Frontalis muscle belly, at about 3 cm above the eyebrow (a). The wire was fixed using a elastic band. (b)

Preliminary tests employed three different versions of electrodes. All of them were mounted over rigid surfaces, were made of silver and had small inter-electrode distance. However, the two first versions had prominent tips which inflicted pain specially for muscles such as the *Frontalis*, extremely thin and presenting a hard surface underneath.

The final design is shown in Figure 4.8. Concentric electrodes show higher spatial selectivity with respect to the traditional detection systems and reduce the problem of electrode location since they are invariant to rotations [94]. Other problem solved by this design was the pain inflicted by earlier designs (using tips) as the force used during

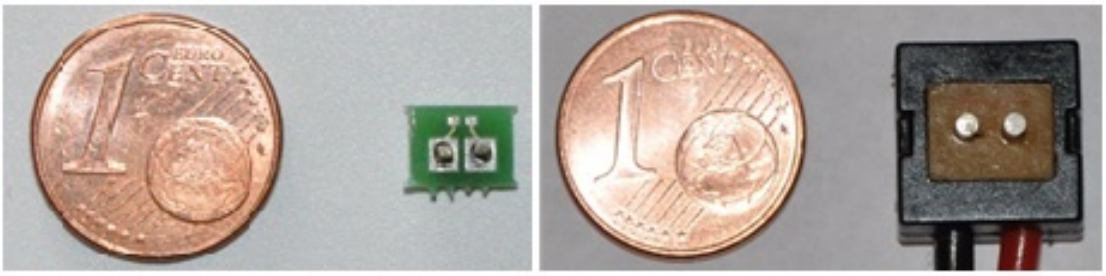

Figure 4.7: Two first designed electrodes, with thin tips.

the electrode placement and throughout the sessions is distributed accordingly over the circular surface formed by the electrode and its base. The detected sEMG signal is amplified by an active preamplifier with gain of 1000.

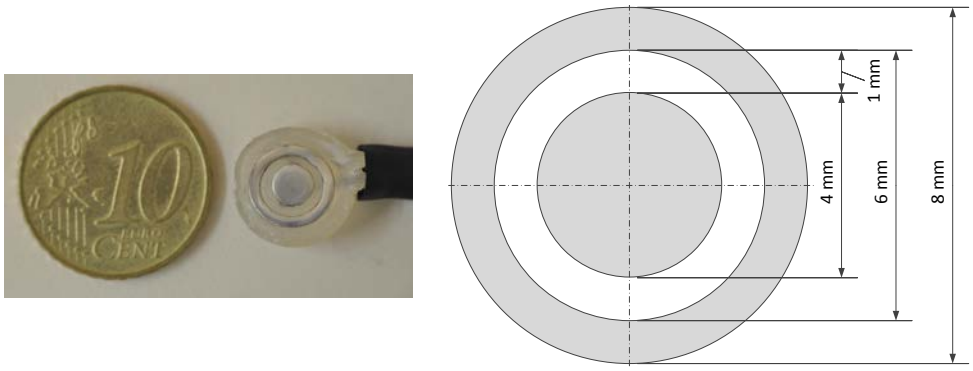

Figure 4.8: Concentric electrode with small inter-electrode distance offering high selectivity.

The signal was acquired and digitized. At first, whether the MUAPs shape and duration would include the features to be extracted was unknown, and the signal was sampled at 10 kHz. Later trials have proven that using an SR of only 5 kHz would suffice for the adequate detection of MUAPs. The 10 kHz value was chosen in the end, and the EMG signal was stored for possible use in future studies, such as EMG signal decomposition.

4.3.1 MUAP detection

Four MUAP detection methods were selected based for comparison were presented in Chapter 3. In [86], the signal envelope is obtained by Hilbert transform, which avoids the necessity to set the low-pass filter usually needed for finding the signal envelope. The envelope amplitude is then compared to a threshold. The default parameter values were chosen.

In [87], the absolute value of each sample's amplitude is compared with a threshold. A post-processor is used to avoid fast transitions between intervals of EMG activity and background noise.

In [89], the variance from signal epochs is extracted to detect EMG activity. After one epoch is considered to contain MUAPs, the original window slides sample by sample to detect onset and offset intervals of activity. The approach to estimate the threshold was not designed for online analysis as it is the case for the proposed task in this study. Thus, a different method to estimate $thrd$ was chosen: $thrd = k \times blmv$ but this time $blmv$ representing the mean variance extracted from the sEMG signal without contraction. The value of k for this method had the best results when set at 20 and the following results were obtained with this value. The sliding window length was set to 10 ms.

In [90], the amplitude and interval's slope are compared to thresholds to detect MUAPs in the signal. Two modifications were made. First, as in [89] the threshold estimation was not suitable for online analysis as information from the whole signal was necessary. Therefore, the threshold was estimated as in [95]. Second, only the first step was performed. However, the essence of using both amplitude and slope information remain.

The method using the raw signal information depends mainly on the choice of the threshold. Again the choice was done as in [95]. Secondly, the acceptable gap was $2ms$, i.e. intervals smaller than this value are interpreted as a flaw and the intervals are united

to represent one or more MUAPs.

The four methods were evaluated using synthetic EMG data based on [95], a data-driven EMG model using real MUAPs. MU firing rate is not constant and follows a gaussian distribution. Usually, the ratio between the standard deviation and the mean of the distribution ranges from 0.1 to 0.25. The mean firing rate varies, depending on the muscle anatomy, the force exerted, and fatigue, but for the muscle the original MUAPs were extracted (the first *dorsal interosseous*), values from 5 to 20 Hz are to be found during low-level contractions. Each MU firing behaviour was set randomly. The SNR was set to 20 dB. The signal length was set to 15 s, and the SR to 10 kHz. Samples of the synthetic EMG signal obtained using three and five MUs are shown in Figure 4.9. The synthetic data parameters allowed EMG signals composed of 2-10 MUs to be used. For each configuration, a hundred files were created.

Epoching in each data file used adjacent windows of 100 ms and the methods were evaluated according to four criteria:

- specificity, as related to false positives (the number of samples with background noise but reported as EMG activity) and true negatives (the number of samples with silence recognized as such);
- sensitivity, as related to false negatives (the number of samples with EMG activity but reported as background noise) and true positives (the number of samples representing EMG activity and recognized as such);
- the percentage of MUAPs found;
- the time required for processing the epoch compared to its length.

Figure 4.10 shows the results of these experiments. All methods are elective for real-time implementation, although the variance method peaked at 28% of the epoch duration and it was systematically slower than the three other options. As the code was

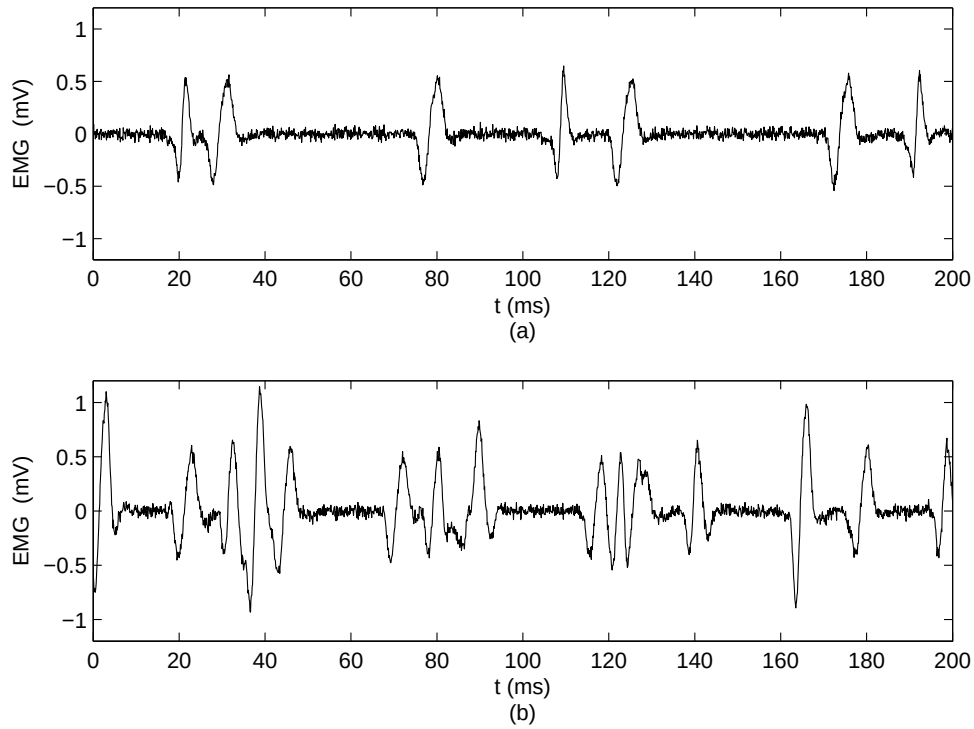

Figure 4.9: Synthetic EMG signal composed by 3 (a) and 5 (b) motor units activity.

executed with a interpreted language in Matlab, it is expected that it runs faster using compiled language.

For some epochs the amplitude and slope method indicated more MUAPs than the actual figure, while envelope and variance methods kept this number low. The latter is expected as MUAPs superposition will cause two or more MUAPs to be detected as one. The advantage of the envelope method over the other three lies in the former's specificity and sensitivity. After this comparison was carried out, a broader analysis of 12 methods [96] also determined that the envelope method obtained by Hilbert transform performed better than the other methods. The envelope estimated using Hilbert transform (as defined in the Matlab documentation) was implemented in C, and the code is presented in the Appendix A. Given the good performance the method created in [86] was chosen

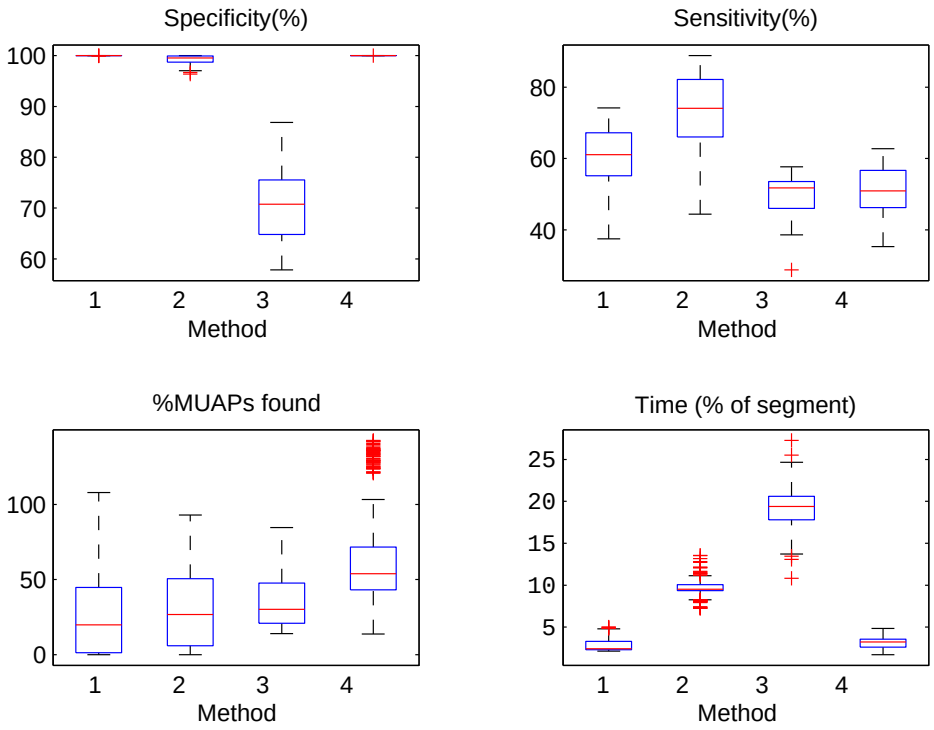

Figure 4.10: MUAP detection methods compared. 1 - Amplitude, 2 - Envelope amplitude, 3 - Variance, 4 - Amplitude and slope

to detect MUAPs. The original algorithm objective was solely to detect areas of activity and to extract candidate MUAPs for further analysis. In the present study, candidate MUAPs less than 4 ms in length were rejected and considered as background noise. Therefore the feature extracted is the signal envelope and its amplitude is compared against a threshold to detect the MUAPs. The MUAP presence or absence is translated into the binary command control, being '1' when a MUAP is detected and '0' otherwise. This command is extracted at 50 ms intervals and is used to feed the EFSM described earlier to emulate mouse events (Figure 4.11). Because skin conditions change over time, and the electrode position over the muscle is not fixed, the threshold was estimated at the beginning of each session. The standard deviation estimated from 5 s without muscle contraction was multiplied by a constant, set at each session for adequate system

operation.

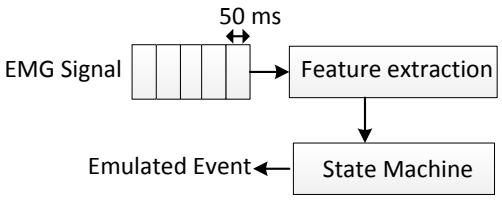

Figure 4.11: The system overview. The sEMG signal is acquired and feature extraction occurs at each 50 ms. The features feed a state machine which in turn emulates mouse events.

In the previous chapter the low-pass differential (LPD) filter was presented as one simple tool to minimize MUAP superposition which could improve the accuracy of the number of MUAPs present in the signal. Unfortunately, at earlier stages in this project, the equipment used had a SNR too low and the LPD did not perform well and its use was discarded. Wavelet de-noise was considered but the final implementation was in the limit for real-time operation. Therefore, no pre-processing was performed prior the signal epoching.

A screenshot from the control module is shown in Figure 4.12 and a 5 s span of the signal recorded is displayed in the left graph. In the center, the last 100 MUAPs are displayed, with the average MUAP highlighted. The right graph demonstrates the binary commands estimated from the signal recorded. In this Figure, three small pulses caused by raising the eyebrow were correctly detected as one 200 ms and two 250 ms EMG activity intervals. For the current system, this would be interpreted as three consecutive rotate commands.

As discussed earlier, the Frontalis is a muscle that activates all available MUs with slow contractions (around 40% MVC). In general, MUAP superposition occurred even for fast contractions and were common for sustained contractions (>300 ms). Despite that behaviour, some subjects provided good quality signal information, as demonstrated in Figure 4.13. Even for circumstances of high MU activity, the MUAPs could be

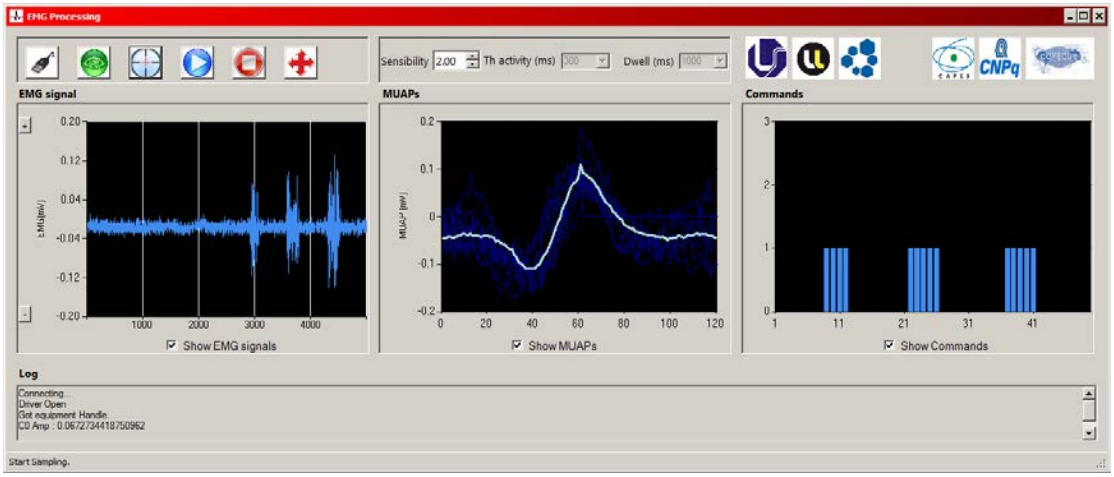

Figure 4.12: The control module composed by graphs of the signal acquired, the MUAPs detected and the binary commands generated.

detected, as shown in Figure 4.12.

Although this study sought higher accuracy control by accessing MUAPs, the second drawback to this approach became apparent: if a single MUAP is capable of stimulating a command, then subjects presenting even the least bit of involuntary muscle activity will not be able to operate the system correctly. This situation occurred among two subjects evaluated, one able-bodied subject, and one tetraplegic patient diagnosed with a neurodegenerative disorder. Unfortunately, the latter presented the best SNR of all of the subjects evaluated, and he was capable of successfully operating the system for about 30 seconds–long enough to acquire the first two targets, but his performance decayed rapidly after this short period of time due to involuntary muscle activity detected by the system. Figure 4.14 shows an epoch of the sEMG signal recorded from that subject, in which two fast contractions had small amplitude MUAPs between them. Several adjustments were made, to no avail, to mask the small amplitude MUAPs without affecting the detection of voluntary contraction.

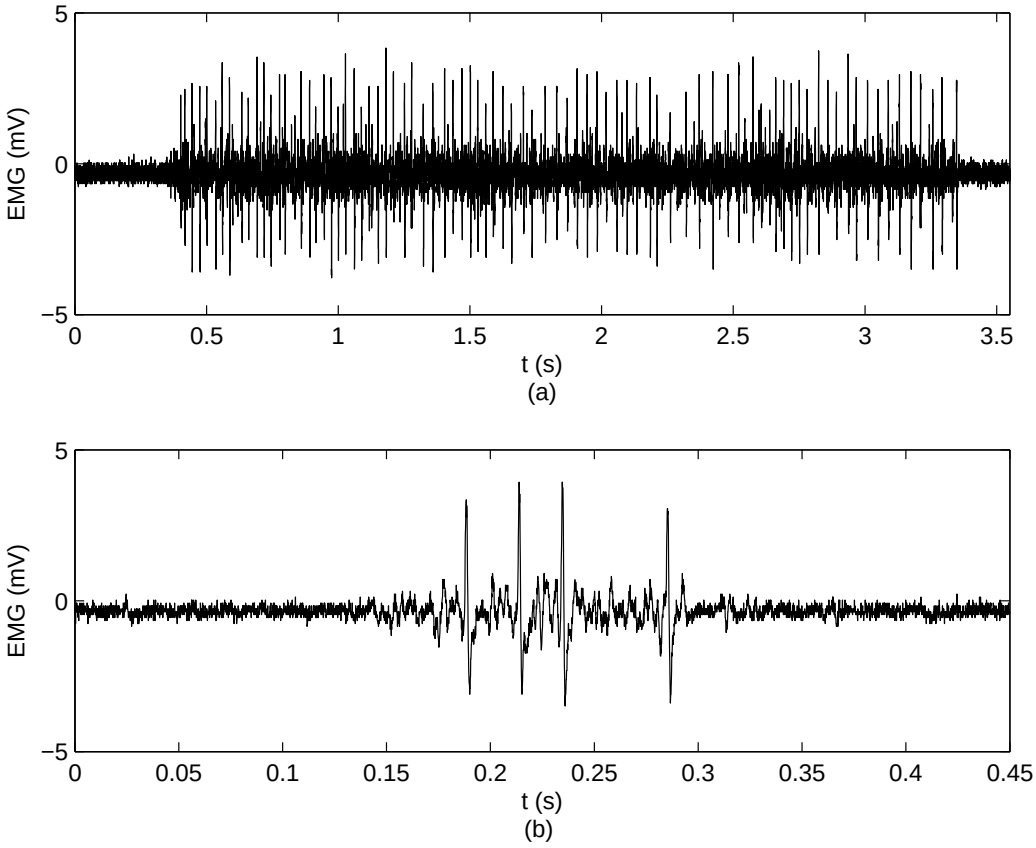

Figure 4.13: Epochs of sEMG signals recorded during trials. A long contraction (a), and a short contraction (b) from the same user.

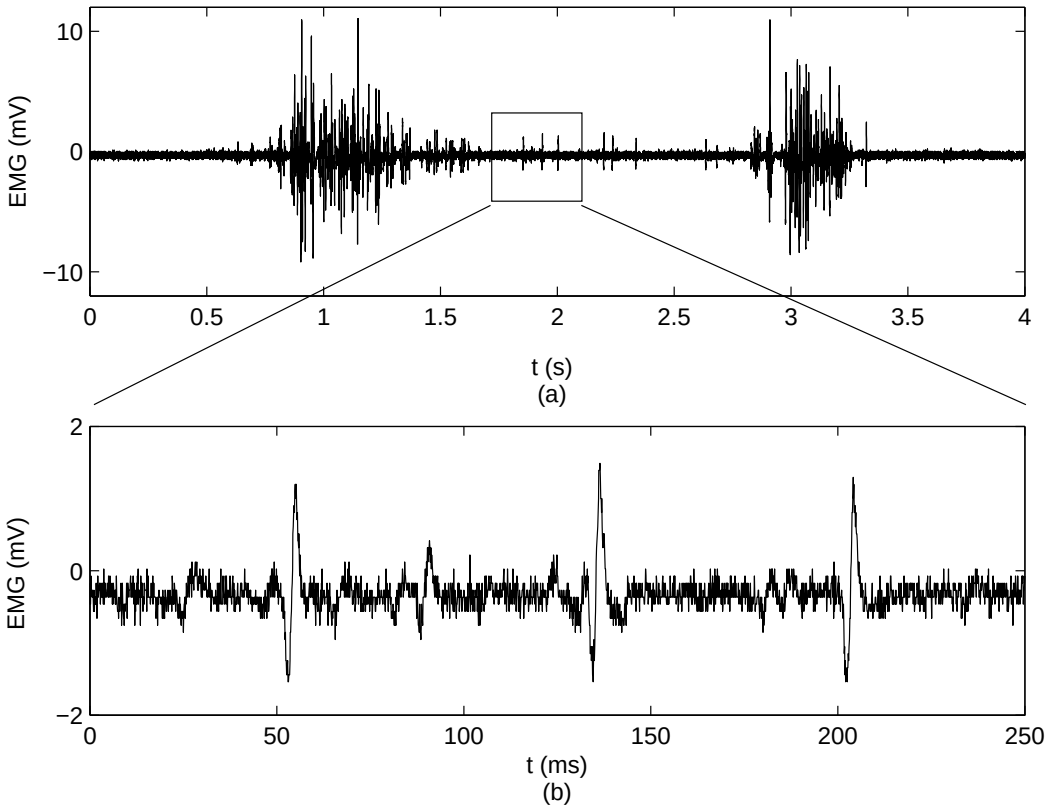

Figure 4.14: Epochs of sEMG signals recorded from a candidate. Between two short contractions (a), several MUAPs caused by involuntary muscle activity were detected (b). The zoomed area has at least three detectable MUAPs.

4.4 Protocol

Each subject was evaluated in five sessions in five different days. At the beginning of each session, the subject's skin was cleaned with an abrasive paste to remove dead skin cells, reducing skin impedance. The same procedure was applied to the wrist where the reference electrode was attached. The bipolar electrode was attached to the skin using adhesive tape and an elastic band. No conductive gel was used in case the low IED would cause a short-circuit.

The subject was required to keep the *Frontalis* muscle still so the background noise could be estimated. After this, a series of long and short contractions was performed, and an appropriate value for the system sensibility was set in the interface control module.

In the first session only, the subject was allowed one round (acquire 5 targets) for understanding the cursor control dynamics. At each session the subject performed a total of 45 rounds determined by following three protocols (square dimensions), three directions (clockwise, counter-clockwise and random) and five repetitions of each combination using the following sequence:

```
for each protocol in {protocol 1, protocol 2, protocol 3}
    for each direction in {clockwise,counter-clockwise,random}
        execute five rounds
```

4.5 Results

The data gathered from the 12 subjects allowed analysis over three aspects off the cursor control task: time taken to move between targets; performance based the number of errors on selecting targets; and the cursor path adopted by the subject.

4.5.1 Time

The main endpoint to be evaluated in this project was the time taken to perform the task. More precisely, the variable chosen was the time between acquiring two consecutive targets. The first target was not considered as the origin point was the center of the screen. For each of the five sessions, there are 60 time values per protocol. The analysis was based on the mean of the time taken between targets and the confidence interval estimated by means of the Bootstrap [97], presented in Table 4.3.

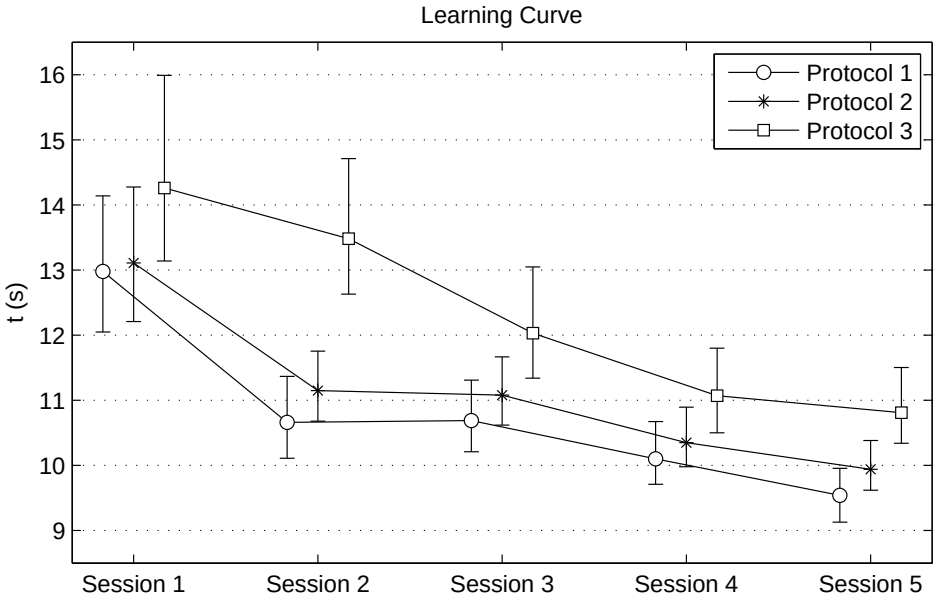

Figure 4.15: Learning curve represented by mean time for each one of the three different protocols using the novel method. Error bars represent the 95% confidence interval. Each point was estimated from the data of the 12 subjects in each session/protocol.

The curve of subject improvement is shown in Figure 4.15. It interesting to notice that the performance for protocol 3 in the last session is, in average, superior to the one registered for the protocol 1 in the first session. Also, from the figure 4.15 is possible to identify that in session 1, the performance for protocol 1 and 2 are quite similar. Actually, the non-parametric MannWhitneyWilcoxon test tells that for each

session, this was the only occasion where no statistically difference was found between the measured time of the three protocols (P1/P2, P2/P3 and P2/P3). The results from this test are shown in 4.2.

Session	Mann–Whitney–Wilcoxon test result (H; p)		
	Protocols 1/2	Protocols 1/3	Protocols 2/3
1	0 ; 0,88125	1; 0,00004	1; 0,00001
2	1; 0,00000	1; 0,00000	1; 0,00000
3	1; 0,00000	1; 0,00000	1; 0,00000
4	1; 0,00406	1; 0,00000	1; 0,00000
5	1; 0,00000	1; 0,00000	1; 0,00000

Table 4.2: In each of the five sessions the protocols 1, 2 and 3 are compared using the Mann–Whitney–Wilcoxon test. If H=1, it means the null hypothesis was rejected.

In each session, it is possible to notice that the task do not follow the linear equation given by Fitts' law. This is clear for the first two sessions. But, using linear regression with the data found in the last session the correlation found was 0.987 with a=7.15 *s* and b=0.73 *s/bit*.

The Principal Component Analysis (PCA) [98] was used in order to visualize clustering in the group of 12 subjects. PCA is mathematically defined as an orthogonal linear transformation that transforms the data to a new coordinate system such that the greatest variance by any projection of the data comes to lie on the first coordinate (called the first principal component), the second greatest variance on the second coordinate, and so on. Using only the first two components allows visualization onto a 2D plane.

For the clustering analysis, each subject was represented by a 3D feature vector given by the mean time for each protocol, found in Table 4.3, e.g. the subject 1 is described by the values (10.05,10.52,11.09) in the overall. PCA was applied to data considering all subjects, and the two most relevant principal components (PCs) were selected based on

the data variability explained by each of them. The scores of each PC were estimated and plotted against each other. The mean time taken to complete the three protocols was measured in three different ways: at the first session only, at the last session, and for the overall performance over the five sessions (Figure 4.16). In Figure 4.16 the lines are the contour plot of the 2D gaussian surface estimated from the scores of PC1 and PC2.

A second approach to visualize clustering of the subjects is represented by dendrograms in Figure 4.17. The distance between subjects was estimated using the Euclidean metric and the linkage used the unweighted average distance method. As using PCA, the users were compared by considering the mean time for the three protocols in three different ways: at the first session only, at the last session, and for the overall performance over the five sessions. For each figure, the subjects were represented by labels (s1,s2,...,s12). Both graphs present similar information, reinforcing the possible groups that could be made from the subjects participating in the trials.

The graphs found in Figure 4.16 should be analyzed together. For instance, in Figure 4.16c subjects 8 and 10 are close to each other, and from Table 4.3 we find the difference of the mean time for protocols 1, 2, and 3 to be 20, 380, and 10 ms, respectively. The similar mean, however, hides the difference of performance verified in the first session, in which subject 8 was, on average, 2 s slower than subject 10 for the three protocols, even in the easiest one. Subject 8 also had inferior performance than subject 10 in protocol three, which was the most difficult. This difference is observed also in Figure 4.16a which represents the performance in the first session. In Figure 4.16b which represents the performance in the final session, when the assumptions are made that all subjects are experienced and minor strategy errors are suppressed, it is possible to see that subjects 8 and 10 are further from each other than in the overall sessions. Therefore, even though these two subjects are positioned closely in the clustering created by the overall mean time, it is invalid to conclude that subjects 8 and 10 demonstrated similar concentration

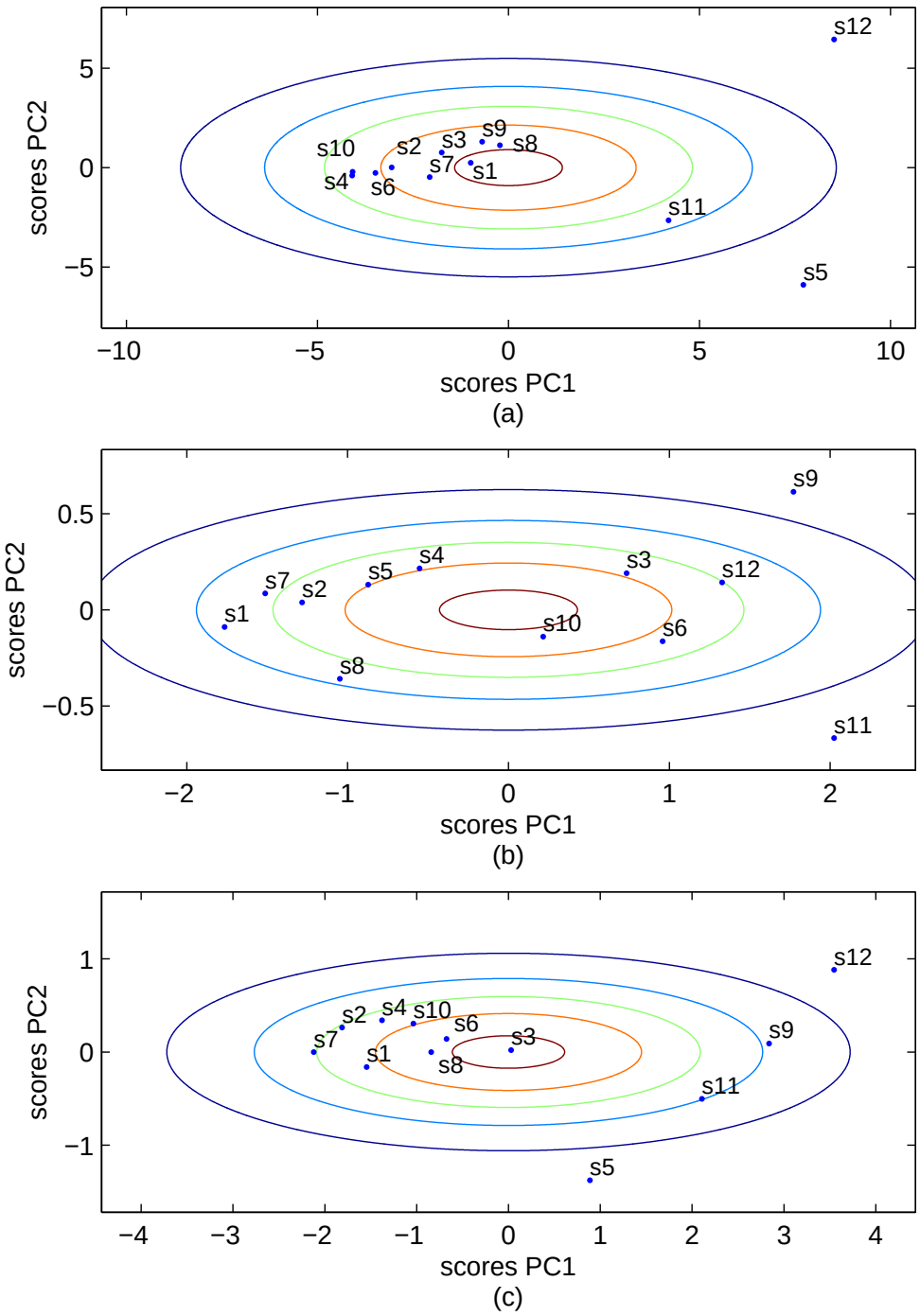

Figure 4.16: PCA analysis for: (a) the first session only, (b) the last session only and (c) the five sessions overall. Subject 12 is tetraplegic and the subject 3 participated in both trials (traditional and novel method).The lines are the contour plot of the 2D gaussian surface estimated from the scores of PC1 and PC2 and the last line represents the 95% interval.

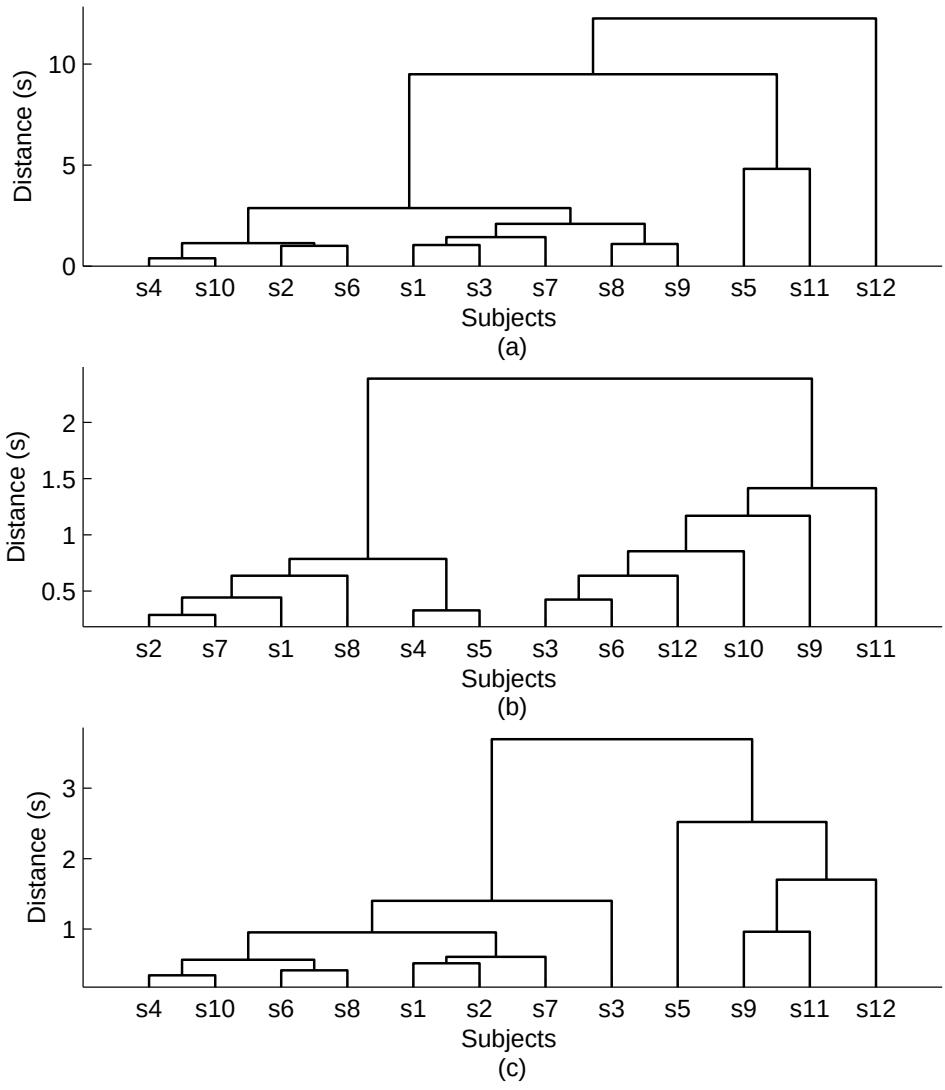

Figure 4.17: Dendrogram for: (a) the first session only, (b) the last session only and (c) the five sessions overall. Subject 12 is tetraplegic and the subject 3 participated in both trials (traditional and novel method).

levels and motor responses. These variations throughout the sessions are also observed between subjects 1 and 9, for example.

It is interesting to observe also the behaviour of subject 12, a tetraplegic patient who is unable to operate a traditional mouse properly. In Figure 4.16a and Figure 4.16c, he is isolated, along with subject 5, and both could be considered as outliers. In fact, considering the mean time for all sessions, subject 12 had the worst performance of all, especially in the first session, and this outlier classification is justified by the fact he, in particular, presented odd strategies for acquiring targets in protocol three. In cases of overshooting, he preferred to take distance from the target before moving the cursor towards it again, instead of trying small displacements. Additionally, instead of using only the *Frontalis* and raise the eyebrow the subject also projected his eyes out causing fatigue and pain. In the last session, however, he was capable of exceeding the performance levels of subjects 9 and 11, and he was able to control the muscles properly, without causing pain. This confusion in muscle control was also observed in an able-bodied subject who was not able to continue trials after the first session. He also overused his eye muscles, and the pain was too great to perform the trial for protocol three. It is important to note that the poor performance of subject 12 was not connected in any way to his disability.

Thus, it is interesting to observe that even though the mean time is important in the overall analysis, the method of learning must be taken into account as well. This is especially true if one assumes that by the last session, small flaws in strategy will be corrected, and the degree of muscular control will represent the main factor in performance differences between subjects.

4.5.2 Path, Overshooting and Errors

The path covered by the cursor is usually analyzed for the cursor control task. Since only vertical and horizontal movements are allowed, the path divides the workspace in box

shapes as seen in Figure 4.18. A 2D matrix was used to represent the interface's pixel and the elements were incremented if the cursor was over the correspondent pixel at a given moment. As the cursor position recording worked at 10 samples per second, the intermediary pixel's position between two consecutive recorded pixels had their elements in the 2D matrix incremented. The raw data did not allow a proper visualization as the lines were too thin, so the images were created by smoothing the path using a 2D 5-span moving average filter.

In the previous section, the strategy adopted by each subject was discussed. The 12 subjects chose a similar strategy, utilizing the guidelines mainly in protocol three. One subject in particular chose a unique strategy, using the guideline whenever possible. Another path was used only when there was a flaw in the commands estimated by the system. The path used by this subject can be seen in Figure 4.18b.

Target overshooting (Figure 4.19) is other way of evaluating cursor control tasks. The data gathered shows that, as expected, overshooting occurs much more frequently in protocol 3.

Finally the number of click evoked with the cursor outside the target is found in Figure 4.20. It is clear that protocol 3 has higher error probability, possibly because of the Midas touch issue that demands attention from the user while he is executing the harder task in the trials. In the end, however, all three protocols have similar behaviour. The peak at session three was caused by one subject in particular, which contaminated the mean.

4.5.3 Improvements over the traditional method

The previous subsections presented the results extracted from the cursor control task using muscle activity, which is not a novelty. In this section, in order to verify the impact of accessing MU activity, the present results are compared to a previous study [81] using traditional sEMG signal acquisition and processing. Both studies share the

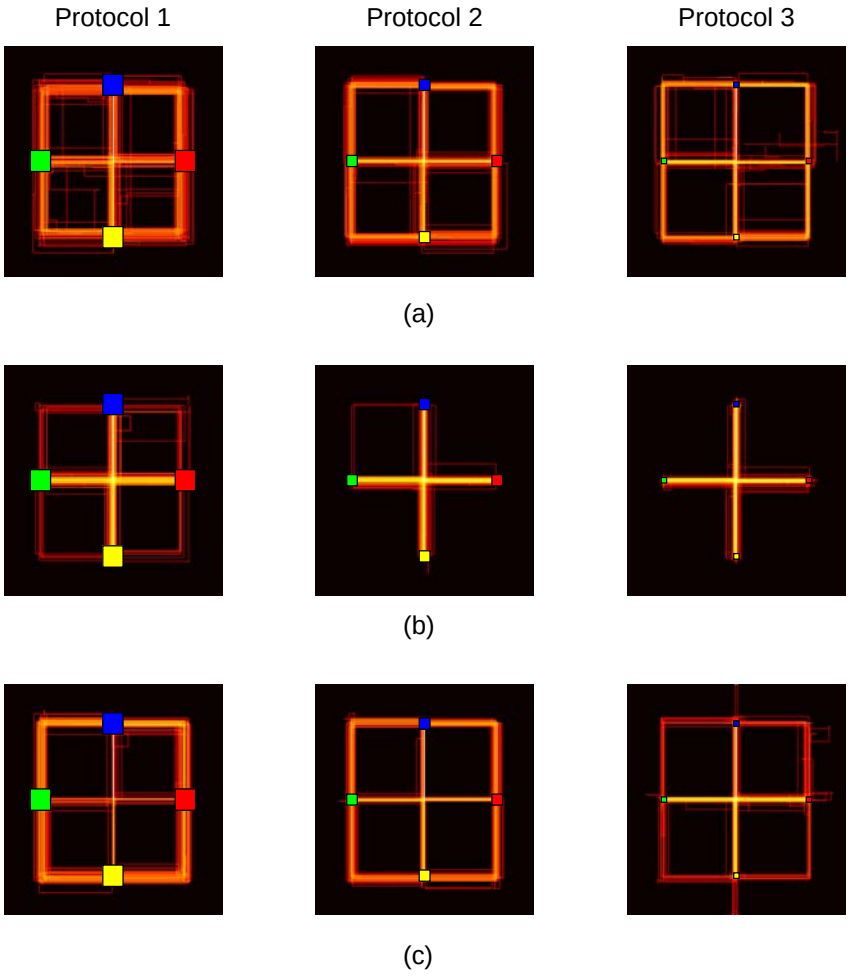

Figure 4.18: Cursor positions during five sessions for (a) the fastest user; (b) a user that even for large targets (Protocols 1 and 2) the guidelines were the preferred path and (c) the slowest user. Lighter points in the image represents positions occupied by the cursor more often.

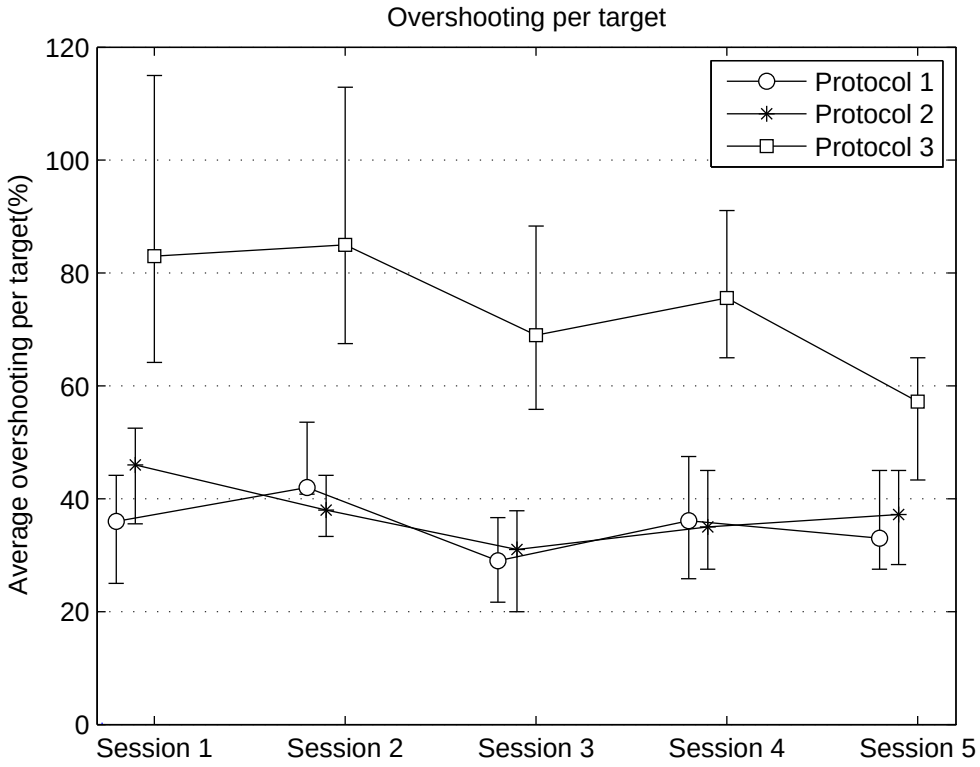

Figure 4.19: Average overshooting per target for each one of the three different protocols using the novel method. Error bars represent the 95% confidence interval. Each point was estimated from the data of the 12 subjects in each session/protocol.

same task, interface and protocols. The previous study, however, uses two facial muscles: the *Frontalis* and the *Temporalis*. The extracted sEMG signal epochs duration was set to 100 ms. For the present study, the *Temporalis* was also considered but technical difficulties did not allow the use of such muscle as the SNR was too low and the signal processing did not provide acceptable results. Preserving the type of muscle used in both experiments allow a direct comparison of results, what would be impossible, if the muscle chosen was one capable of fine movements, such as those found in the hand.

Each epoch is represented by a 3D array, estimated by means of equations 4.1, 4.2 and 4.3

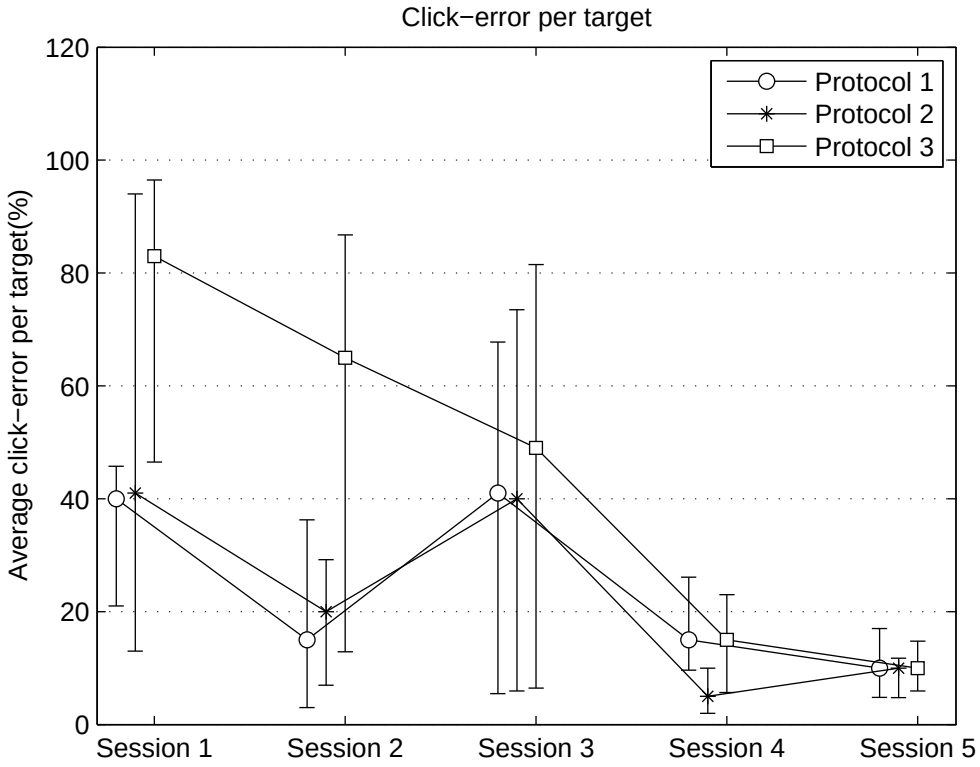

Figure 4.20: Average incorrect click events per target for each one of the three different protocols using the novel method. Error bars represent the 95% confidence interval. Each point was estimated from the data of the 12 subjects in each session/protocol.

$$MAV = \frac{1}{N}\sum_{i=0}^{N-1}|s_i| \tag{4.1}$$

$$AutoCorrAbs = \sum_{i=0}^{N-m-1}|s_i||s_{i+m}| \tag{4.2}$$

$$StdAbs = \sqrt{\frac{1}{N}\sum_{i=0}^{N-1}(|s_i| - |\overline{s}|)^2} \tag{4.3}$$

where MAV is the Mean Absolute Value, which is a feature that captures the overall trend of the signal amplitude; $AutoCorrAbs$ is the non-normalized autocorrelation

function of the signal. If m in Eq. 4.2 is a small value (e.g., 2 as employed) then Eq. 4.2 provides us with a manner to capture changes in the signal amplitude with simultaneous attenuation of noise activity because of the effect of the multiplying factor $|s_i||s_{i+m}|$ which yields a smaller amplitude value when both $|s_i|$ and $|s_{i+m}|$ are less than 1. *StdAbs* is a statistical measure (i.e., the standard deviation) of the absolute value of s, which is also related to changes in the signal amplitude.

No facial movement generate a STANDBY event, which emulates a still mouse cursor. A continuous teeth clenching generates one of the following events: DOWN, LEFT or RIGHT. Each of these events corresponds to the emulation of the continuous movement of the mouse cursor respectively downwards, to the left or right. The generation of one of these events is dependent on the current direction of a cursor which is in the shape of an arrow. A teeth clenching followed by muscle relaxation yields the event SINGLE-CLICK, which emulates the single click event sent by a mouse. A continuous eyebrow raise will generate an UP event, which emulates the continuous upward movement of the mouse cursor. An eyebrow lift followed by muscle relaxation will generate a ROTATE event, which rotates the arrow shaped cursor to one of the following directions: right, left or down. A general side-by-side comparison for both experiments is presented in Table 4.4.

In the previous study [81], 11 subjects were involved, being one suffering from Duchenne muscular dystrophy who had no movement of the lower and upper limbs and could barely support his back. In the present study, a similar proportion was obtained as there was one tetraplegic caused by SCI and 11 able-bodied subjects. The subject 3 was the only that participated in both studies.

The mean time using the traditional approach is shown in Figure 4.21, and can be compared to the data in Figure 4.15 for the novel method. The figures from both graphs is shown in Figure 4.22.

For protocols 1 (target edge = 2 cm) and 2 (target edge = 1 cm), the system using

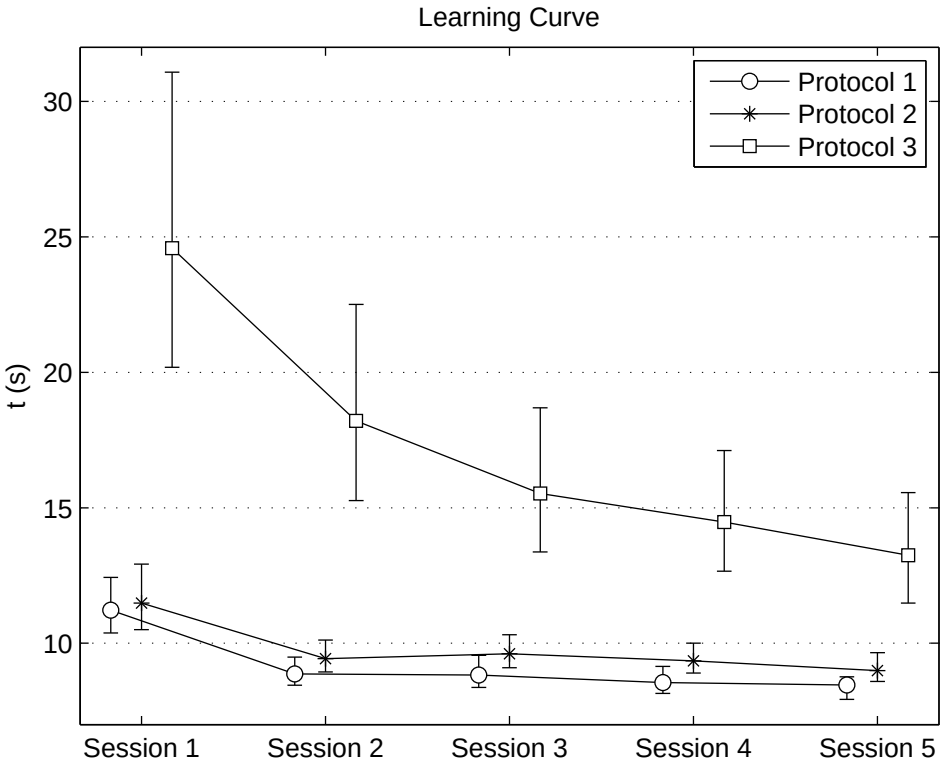

Figure 4.21: Learning curve represented by mean time for each one of the three different protocols using traditional sEMG signal processing. Error bars represent the 95% confidence interval.

the traditional approach outperformed the system using the novel method, as the former uses muscle activity, while the latter uses a dwell time of 1 s for emulating the mouse click. The important data here, however, is at protocol 3 (target edge = 0.5 cm), which presents the highest ID according to Fitts' Law. With this level of difficulty, it is clear that using information extracted from MU provided much more precise control.

Also, Figure 4.23 shows, for both approaches, just how much the subject performance deteriorates when ID increases. The mean time from protocol 2 and 3 are compared to the mean time values found for protocols with ID immediately below, e.g. protocol 2 is compared to protocol 1 and protocol 3 to protocol 2.

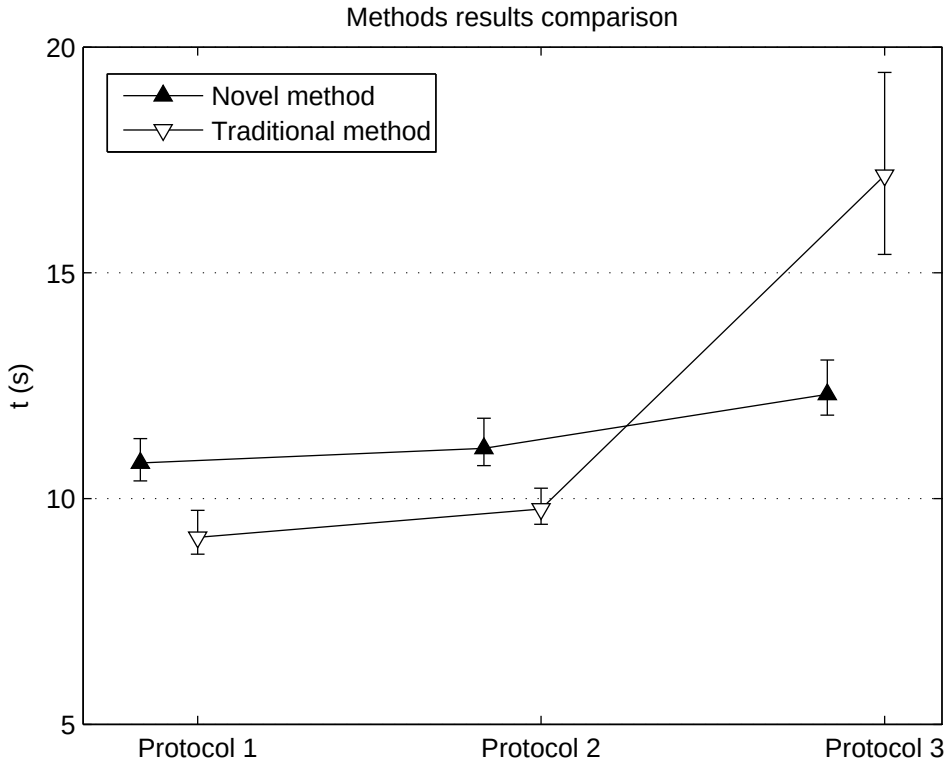

Figure 4.22: Mean time compared for the traditional and novel method on each one of the three different protocols. Error bars represent the 95% confidence interval.

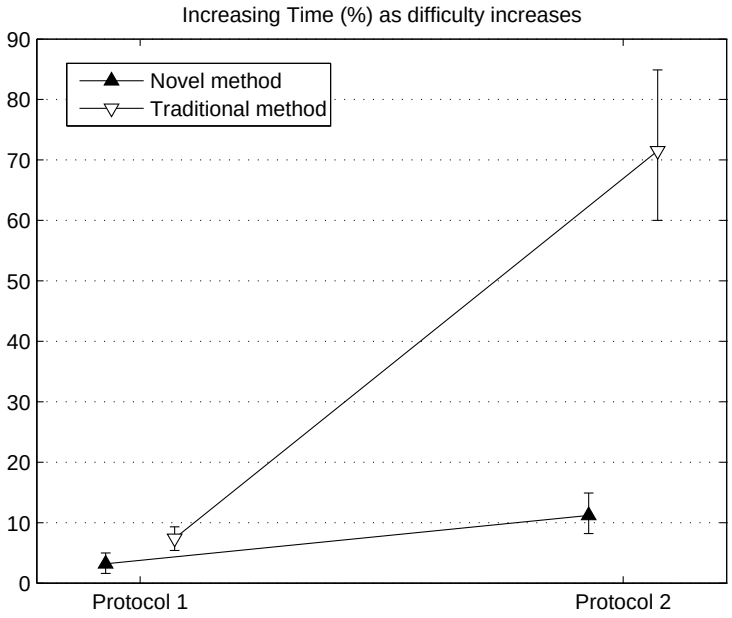

Figure 4.23: Mean time increasing for protocol 2 compared to protocol 1 and protocol 3 compared to protocol 2. Error bars represent the 95% confidence interval.

In Figure 4.24, the improvement on the mean time between the first and last sessions is shown for both methods. The novel method shows almost identical learning for the three protocols, reinforcing the observation that no significant difference exists between protocols when the task is performed with the novel method (Figure 4.15). The traditional method, on the other hand, required more of the subjects' capabilities of learning motor control for protocol 3, as the mean improvement was 46.1%.

The original experiment [81] focused on designing a system capable of operating a cursor and analyzing learning, so the only data collected was the time taken to acquire the targets. Therefore, with the current available data, no comparison is possible regarding selection errors and overshooting.

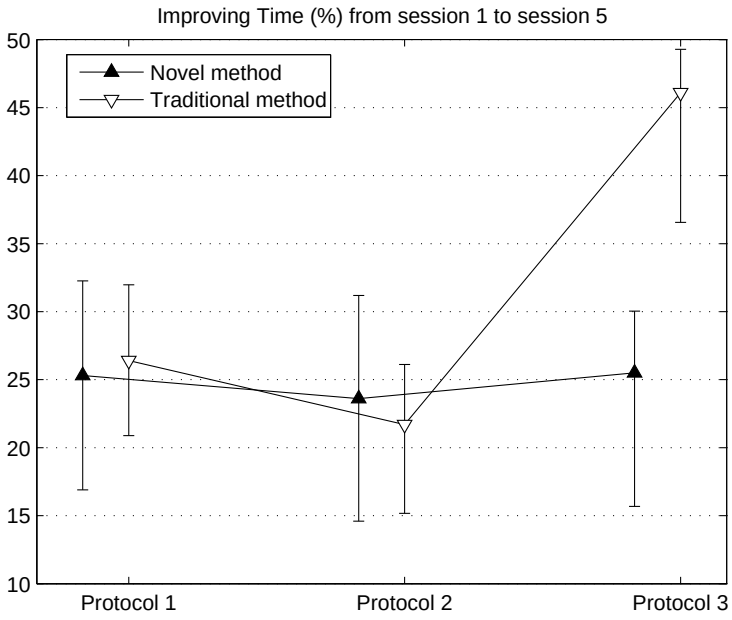

Figure 4.24: Learning for each protocol between the first and the last session. Error bars represent the 95% confidence interval.

Session	Subject 1			Subject 2			Subject 3*		
	Protocol 1	*Protocol 2*	*Protocol 3*	*Protocol 1*	*Protocol 2*	*Protocol 3*	*Protocol 1*	*Protocol 2*	*Protocol 3*
1	12.99 [12.03 14.18]	12.03 [11.39 12.77]	13.74 [12.41 16.31]	11.24 [10.58 12.01]	11.26 [10.85 11.79]	12.53 [11.77 13.41]	12.12 [11.22 13.34]	11.46 [10.91 12.35]	13.80 [12.89 15.18]
2	9.56 [9.26 10.01]	9.99 [9.63 10.51]	11.08 [10.6 11.82]	9.45 [8.87 9.84]	10.03 [9.72 10.39]	11.41 [10.89 12.04]	10.78 [10.34 11.4]	12.55 [12.01 13.35]	13.88 [12.74 15.7]
3	10.10 [9.61 10.78]	10.75 [10.23 11.47]	10.36 [9.86 11.13]	10.19 [9.83 10.67]	10.06 [9.75 10.39]	11.36 [10.8 12.15]	10.55 [10.18 10.98]	10.69 [10.42 11.04]	12.66 [11.69 14.43]
4	9.71 [9.31 10.24]	10.52 [10.04 11.38]	10.45 [10 10.95]	9.69 [9.34 10.09]	9.85 [9.54 10.2]	10.36 [9.95 10.83]	10.06 [9.47 10.52]	10.74 [10.35 11.12]	10.54 [9.96 11.11]
5	8.31 [7.76 8.67]	9.33 [9.06 9.75]	9.67 [9.34 10.56]	8.73 [8.27 9.05]	9.26 [9.04 9.47]	10.04 [9.72 10.43]	10.13 [9.75 10.64]	10.33 [9.75 10.67]	11.09 [10.64 11.88]
Mean	10.13 [9.59 10.78]	10.52 [10.07 11.18]	11.06 [10.44 12.15]	9.86 [9.38 10.33]	10.09 [9.78 10.45]	11.14 [10.63 11.77]	10.73 [10.19 11.38]	11.15 [10.69 11.71]	12.39 [11.58 13.66]
Session	Subject 4			Subject 5			Subject 6		
	Protocol 1	*Protocol 2*	*Protocol 3*	*Protocol 1*	*Protocol 2*	*Protocol 3*	*Protocol 1*	*Protocol 2*	*Protocol 3*
1	10.52 [9.88 10.93]	11.00 [10.73 11.39]	11.67 [11.21 12.49]	17.69 [16.21 19.64]	21.60 [18.69 24.38]	14.17 [13.21 15.48]	11.81 [11.15 12.75]	10.75 [10.23 11.73]	11.88 [11.08 12.9]
2	9.73 [9.09 10.18]	10.53 [10.27 10.9]	12.63 [12.08 13.32]	11.54 [10.9 12.63]	11.30 [10.8 11.93]	13.48 [12.6 15.1]	10.69 [10.15 11.86]	11.33 [10.85 11.89]	14.47 [13.6 15.37]
3	9.28 [8.74 9.57]	10.08 [9.84 10.31]	12.37 [11.76 13.18]	10.49 [10.08 11.02]	10.79 [10.36 11.32]	11.62 [10.99 12.54]	10.28 [9.99 10.85]	10.33 [10.05 10.69]	10.95 [10.49 11.64]
4	11.03 [10.52 11.7]	10.06 [9.83 10.35]	10.66 [10.31 11.13]	9.09 [8.92 9.3]	9.66 [9.33 10.11]	11.18 [10.63 12]	9.99 [9.69 10.33]	10.30 [9.97 10.65]	10.63 [9.99 11.39]
5	9.33 [9.14 9.51]	9.61 [9.43 9.77]	10.35 [10 10.75]	9.06 [8.85 9.34]	9.51 [9.26 9.97]	10.19 [9.76 10.69]	10.00 [9.67 10.49]	10.59 [10.27 10.99]	11.40 [10.86 12.08]
Mean	9.98 [9.47 10.38]	10.26 [10.02 10.54]	11.54 [11.07 12.17]	11.57 [10.99 12.39]	12.57 [11.69 13.54]	12.13 [11.44 13.16]	10.55 [10.13 11.26]	10.66 [10.27 11.19]	11.87 [11.2 12.68]
Session	Subject 7			Subject 8			Subject 9		
	Protocol 1	*Protocol 2*	*Protocol 3*	*Protocol 1*	*Protocol 2*	*Protocol 3*	*Protocol 1*	*Protocol 2*	*Protocol 3*
1	12.86 [12.1 13.79]	11.61 [11.09 12.19]	12.47 [11.64 13.6]	12.59 [11.7 14.2]	12.34 [11.76 13.11]	15.04 [13.57 17.41]	11.50 [10.94 12.22]	12.40 [11.77 13.22]	15.11 [14.02 16.54]
2	9.37 [9.06 9.69]	9.37 [9.09 9.71]	10.64 [10.21 11.22]	9.74 [9.42 10.29]	10.52 [10.07 11.18]	11.53 [10.99 12.32]	11.73 [11.17 12.42]	12.95 [12.14 13.86]	16.61 [15.37 18.26]
3	10.56 [10 11.08]	10.32 [9.88 10.95]	10.29 [9.87 10.88]	9.90 [9.49 10.47]	10.81 [10.34 11.39]	10.73 [10.29 11.34]	13.25 [12.52 14.08]	14.99 [14.16 16.23]	16.20 [14.65 18.17]
4	8.95 [8.72 9.28]	9.57 [9.29 9.91]	9.97 [9.56 10.39]	10.11 [9.63 10.88]	10.78 [10.23 11.58]	11.27 [10.55 12.52]	11.46 [11.01 12.09]	11.63 [11.11 12.32]	13.63 [12.67 14.73]
5	8.61 [8.16 8.97]	9.30 [9.02 9.65]	9.78 [9.45 10.15]	8.57 [8.12 8.97]	9.63 [9.31 10.06]	10.33 [9.83 11.34]	11.13 [10.53 12.08]	10.47 [10.06 11.38]	11.61 [11.08 12.38]
Mean	10.07 [9.61 10.56]	10.03 [9.67 10.48]	10.63 [10.15 11.25]	10.18 [9.67 10.96]	10.82 [10.34 11.46]	11.78 [11.05 12.99]	11.81 [11.23 12.58]	12.49 [11.85 13.4]	14.63 [13.56 16.02]
Session	Subject 10			Subject 11			Subject 12**		
	Protocol 1	*Protocol 2*	*Protocol 3*	*Protocol 1*	*Protocol 2*	*Protocol 3*	*Protocol 1*	*Protocol 2*	*Protocol 3*
1	10.79 [10.17 11.36]	10.73 [10.39 11.12]	11.75 [11.25 12.37]	15.19 [13.66 17.11]	17.53 [15.23 21.22]	14.71 [13.62 16.03]	16.42 [14.95 18.14]	14.56 [13.48 16.02]	24.28 [20.97 30.13]
2	10.20 [9.58 11.04]	10.83 [10.53 11.24]	13.68 [13.03 14.52]	11.08 [10.6 11.7]	11.66 [11.07 12.43]	16.13 [14.86 17.91]	14.10 [12.88 15.33]	12.74 [12 13.67]	16.27 [14.55 18.97]
3	9.99 [9.73 10.51]	10.29 [10.01 10.58]	11.69 [11.19 12.44]	11.99 [11.33 12.8]	12.49 [11.7 13.26]	14.14 [13 16.05]	11.71 [11.04 12.89]	11.32 [10.66 12.37]	11.98 [11.49 12.64]
4	10.29 [9.94 10.66]	10.25 [9.96 10.55]	10.74 [10.16 11.38]	9.87 [9.53 10.54]	10.29 [9.83 11.45]	10.84 [10.38 11.47]	11.00 [10.47 12.45]	10.53 [10.23 11.11]	12.56 [11.81 13.69]
5	9.55 [9.32 9.86]	10.10 [9.86 10.44]	11.01 [10.63 11.55]	10.32 [9.88 10.91]	10.86 [10.37 11.51]	12.56 [11.7 13.76]	10.49 [10.15 10.97]	10.33 [9.99 10.9]	11.65 [11.12 12.47]
Mean	10.16 [9.75 10.69]	10.44 [10.15 10.79]	11.77 [11.25 12.45]	11.69 [11 12.61]	12.57 [11.64 13.97]	13.68 [12.71 15.04]	12.74 [11.9 13.96]	11.90 [11.27 12.81]	15.35 [13.99 17.58]

* Subject was tested with traditional and the novel method
** Tetraplegic Subject

Table 4.3: Mean time and its 95% confidence interval based on BootStrap

Criteria	Previous study using traditional EMG signal processing	Present Study
Number of channels	2	1
Muscles	*Frontalis* and *Temporalis*	*Frontalis*
Clicking	Fast teeth clenching	1 second without muscle activity
Features extracted from epoch	Mean absolute value, non-normalized autocorrelation and the standard deviation of the absolute value.	MUAP presence detected from the signal envelope, which amplitude is compared against a threshold.
Signal interpretation	The three dimensional feature array is higher than a threshold, the epoch is considered as muscle activity.	The envelope amplitude is compared to a threshold. An interval longer than 4 ms above the threshold is interpreted as containing a MUAP.
Epoch length	100 ms	50 ms
Sampling rate	1 kHz	10 kHz
Threshold	The threshold is estimated from a 5 s interval of non-contraction.	

Table 4.4: Comparing experiments using traditional sEMG signal-processing and the novel method.

Chapter 5

Conclusions

This chapter focus on discussing the findings of the present work focusing on the pros and cons of the system proposed in this study. Finally, future works based on the current system are discussed.

5.1 Discussion

For over half a century, information extracted from a sEMG signal for the purpose of operating a given device has not considered the information provided by the basic unit of the muscle: the MU. In this study, the activity from a single MU can represent the activity of a muscle to generating commands to control the cursor in a traditional OS. The purpose of this study was to demonstrate that this kind of information would provide better control signal when compared to the traditional approach on EMG signal-processing.

During planning and execution of this thesis, several methods were investigated, to ensure that the signal could be properly acquired and processed. An investigation into the design of a electrode capable of detecting MUAPs led to the concentric ring electrode, designed by Adriano O. Andrade. An investigation on methods for signal

segmentation (MUAPs detection) indicated that the method developed by Andrade *et al.* [99] using envelope of the signal estimated by the Hilbert transform, was superior to other three alternatives. This same conclusion was made in the work by Siqueira [96] comparing another 8 methods found in the literature.

The strategy adopted to verify the hypothesis was to test the novel approach on the cursor control task, which was utilized in a different study using the traditional approach of EMG signal-processing. Comparing these results would be the ultimate test to validate the hypothesis. Furthermore, this same task of cursor control is being tested by our research group more thoroughly with different variations, but with the same essentials, so a base of knowledge can be firmly built. However, the use of cursor control to operate a traditional OS by motor-impaired subjects is not a consensus, and neither is the proposal in this study. Alternative tactics should be considered first, especially scan-based solutions, using virtual keyboards for commands/speech generation or systems based on pictures and symbols [8], which are easy to learn and helpful in cases of standard communication strategy [100].

The comparison, based on the difficulty of the task estimated by Fitts's Law, indicated that the control signal generated by the novel method provided better precision than that generated by the traditional approach. The difference of performance is clear when considering the results for protocol 3, in which traditional EMG signal-processing techniques required the subject to exert much more effort than for protocols 1 and 2. For the novel method, in contrast, the performances followed a nearly linear progression, as expected from the ID by Fitts's Law used in the design of the task. This means that when motor control was needed the most, the novel method was capable of translating efficiently the motor activity into commands.

The proposed method, on the other hand presented some drawbacks. The electrode placement was a sensitive stage of the system setup prior to operation, as small displacements could make the sEMG signal indistinguishable from background noise. On the

other hand, the conductive gel was not used, and the system operated well in sessions nearly one hour in length. Sometimes, for aesthetic reasons, systems exploring bioelectric signals, which are bulky, are not adopted. However, this may change in the years to come, with progress being made in the generation of flexible electrodes [101] less than 40 μmeters thick that could be used for several days. Once this kind of technology reaches the market, it is possible that assistive devices based on sEMG signals will evolve from laboratory prototypes to real commercial products.

Another problem found was the presence of small MUAPs caused by involuntary activities: these could not be ignored, because it was impossible to change the system sensibility without affecting responses to voluntary activity. In these cases, the subject was discarded from the experiment. Finally, similar to involuntary contractions, motion artifacts present after a long contraction were interpreted by the system as a valid small pulse, causing a rotation. This issue was not addressed since it was noticed only after several subjects had already finished the trials and all subjects should be submitted to the same system. This behaviour was present in only some subjects, in different degrees of intensity, but not in all sessions. Later, a simple solution was devised, which was rendering the system insensitive to new inputs for 100 ms after the muscle activity had ended.

In short, the proposed approach succeeded, as it has provided better control by detecting information at the MU level, instead of detecting muscle activity using large groups of MU activity. However, improvements must be made, specially in the electrode design, allowing the novel method to be widely adopted.

5.2 Future works

At the present stage of the system development, the results strongly indicate that accessing muscle activity at the motor unit level provides better control in the cursor control

task. However, the electrode used in the present study does not allow further investigation on physiological aspects of muscle activity during the task. For example: different groups of MUs are used during short and long contractions? This question can only be answered by using an array of electrodes, an approach already under development by our research group.

Array of electrodes present at least two characteristics that the present system could take advantage of. First, the support for spatial filtering combining the signals from several electrodes. For example, in [102] myoelectric prosthesis control was accomplished using the sequential forward searching (SFS) method, an iterative searching procedure that selects the subset of sEMG signals that provides the highest classification accuracy. The use of spatial filter can also be explored to minimize the crosstalk effect [103], that occurred with some subjects when contracting the *Corrugator* muscle. Finally, surface EMG decomposition [104][105] uses spatial filtering techniques to decreasing the number of sources significantly contributing to the interference signal. From the EMG signal decomposition, progressive control signals could be generated. Although the full information from the neural drive will probably not be available, it is not really necessary, as the spread of common synaptic input to motor neurons is observed from the analysis of multiple muscles in complex tasks [92].

Second, array of electrodes allows extraction of some information, such as the conduction velocity (CV), which are not available when using a single channel electrode. According to Schwartz:2010 [106] the CV can be an indication of fatigue and it could be interpreted by an advanced system of fatigue detection capable of decreasing the number of symbols/states necessary for its operation to cope with the user capability. The cursor control system could be operated by discrete commands if the user is not tired and fall back to the binary control mode when fatigue is detected.

Even without using an array of electrodes, the kind of signal generated is also a point of improvement. In this work, binary command control is generated, but a discrete signal

seems feasible. In fact, an intermediate step in this work contemplated this matter, but its development was suspended, as the focus was on comparing the novel approach with the traditional one, which used binary control commands. The solution was based on Henneman's size principle: smaller motor units are recruited first. The peak amplitude of the largest detected MUAP was then used to determine the command control. In the ideal situation, considering three easily distinguished groups of MUAPs, the signal could generate four levels of commands (0,1,2 and 3). If the clustering was not useful, the command control would be estimated by quantizing the MUAP amplitude.

As stated before, using sEMG signals to control a cursor in an usual OS is possible, but it is probably not the best solution for alternative communication. The next step for the method evaluated in this work could be controlling different interfaces for AAC. Further the same approach could be tested in other fields of assistive technology such as prosthesis and house appliances control.

Finally, it must be reinforced that, not only for the task discussed in this text, the key point to allow myoelectric-based control devices to reach the market is the development of electrodes capable of been worn several hours a day or even a few consecutive days without the necessity of replacement and adjustment. Studies such as the one developed by *Kim et al.*[101] are a huge step toward this end.

Bibliography

[1] J. R. Wolpaw, "Brain-computer interfaces as new brain output pathways", *Journal of Physiology*, vol. 579, no. 3, pp. 613–619, 2007.

[2] Z. Lv, X. Wu, M. Li, and C. Zhang, "Implementation of the EOG-based human computer interface system", in *2nd International Conference on Bioinformatics and Biomedical Engineering*, pp. 2188–2191.

[3] C. K. Battye, A. Nightingale, and J. Whillis, "The use of myo-electric currents in the operation of prostheses", *The Journal of bone and joint surgery. British volume*, vol. 37 B, no. 3, pp. 506–510, 1955.

[4] A. Akhtar, L. J. Hargrove, and T. Bretl, "Prediction of distal arm joint angles from EMG and shoulder orientation for prosthesis control", in *Engineering in Medicine and Biology Society (EMBC), 2012 Annual International Conference of the IEEE*, pp. 4160–4163.

[5] R. N. Khushaba, S. Kodagoda, M. Takruri, and G. Dissanayake, "Toward improved control of prosthetic fingers using surface electromyogram (EMG) signals", *Expert Systems with Applications*, vol. 39, no. 12, pp. 10731–10738, 2012.

[6] D. Beukelman and P. Mirenda, *Augmentative and Alternative Communication*, vol. ISBN 1-55766-333-5. Brookes.

[7] A. Wilson, *Augmentative Communication in Practice: An Introduction*. 2nd. edition ed., 1998.

[8] S. Ghedira, P. Pino, and G. Bourhis, "Conception and Experimentation of a Communication Device with Adaptive Scanning", *ACM Trans. Access. Comput.*, vol. 1, no. 3, pp. 1–23, 2009.

[9] E. F. LoPresti, D. M. Brienza, and J. Angelo, "Neck movement patterns and functional performance for computer head controls", vol. 1 of *Proceedings of the 1999 IEEE Engineering in Medicine and Biology 21st Annual Conference and the 1999 Fall Meeting of the Biomedical Engineering Society (1st Joint BMES / EMBS)*, p. 591, IEEE, 1999.

[10] E. F. LoPresti and D. M. Brienza, "Adaptive Software for Head-Operated Computer Controls", *IEEE Transactions on Neural Systems and Rehabilitation Engineering*, vol. 12, no. 1, pp. 102–111, 2004.

[11] M. R. Williams and R. F. Kirsch, "Evaluation of head orientation and neck muscle EMG signals as command inputs to a human-computer interface for individuals with high tetraplegia", *IEEE Transactions on Neural Systems and Rehabilitation Engineering*, vol. 16, no. 5, pp. 485–496, 2008.

[12] B. Denby, T. Schultz, K. Honda, T. Hueber, J. M. Gilbert, and J. S. Brumberg, "Silent speech interfaces", *Speech Communication*, vol. 52, no. 4, pp. 270–287, 2010.

[13] T. A. Bekinschtein, M. R. Coleman, J. N. III, J. D. Pickard, and F. F. Manes, "Can electromyography objectively detect voluntary movement in disorders of consciousness?", *Journal of Neurology, Neurosurgery, and Psychiatry*, vol. 79, no. 7, pp. 826–828, 2008.

[14] P. E. Patterson, "Development of an inexpensive environmental remote control system for a quadriplegic individual", *Biomedical Sciences Instrumentation*, vol. 31, pp. 275–280, 1995.

[15] P. S. Luna, E. Osorio, E. Cardiel, and P. R. Hedz, "Communication aid for speech disabled people using Morse codification", in *Annual International Conference of the IEEE Engineering in Medicine and Biology*, vol. 3, pp. 2434–2435, 2002.

[16] H.-J. Park, S.-H. Kwon, H.-C. Kim, and K.-S. Park, "Adaptive EMG-driven communication for the disabled", in *Annual International Conference of the IEEE Engineering in Medicine and Biology*, vol. 1, pp. 656 vol.1–, 1999.

[17] Ablenet, "EMG Impulse system", 2009.

[18] C. Perez-Maldonado, A. S. Wexler, and S. S. Joshi, "Two-dimensional cursor-to-target control from single muscle site sEMG signals", *IEEE Transactions on Neural Systems and Rehabilitation Engineering*, vol. 18, no. 2, pp. 203–209, 2010.

[19] A. B. Barreto, S. D. Scargle, and M. Adjouadi, "A practical EMG-based human-computer interface for users with motor disabilities", *Journal of Rehabilitation Research and Development*, vol. 37, no. 1, pp. 53–64, 2000.

[20] C. Chin and A. Barreto, "Neural control of the computer cursor based on spectral analysis of the electromyogram", in *2nd International IEEE EMBS Conference on Neural Engineering 2005*, vol. 2005, pp. 446–449, 2005.

[21] C. A. Chin and A. Barreto, "Enhanced hybrid electromyogram / eye gaze tracking cursor control system for hands-free computer interaction", in *Annual International Conference of the IEEE Engineering in Medicine and Biology*, pp. 2296–2299, 2006.

[22] C. A. Chin, A. Barreto, J. G. Cremades, and M. Adjouadi, "Integrated electromyogram and eyegaze tracking cursor control system for computer users with motor disabilities", *Journal of Rehabilitation Research and Development*, vol. 45, p. 161, 2008.

[23] E. C. Lyons, A. B. Barreto, and M. Adjouadi, "Development of a hybrid hands-off human computer interface based on electromyogram signals and eye-gaze tracking", in *Annual International Conference of the IEEE Engineering in Medicine and Biology*, vol. 2, pp. 1423–1426, 2001.

[24] V. Surakka, M. Illi, and P. Isokoski, "Gazing and frowning as a new human-computer interaction technique", *ACM Trans. Appl. Percept.*, vol. 1, no. 1, pp. 40–56, 2004.

[25] P. M. Fitts, "The information capacity of the human motor system in controlling the amplitude of movement", *Journal of Experimental Psychology*, vol. 47, no. 6, pp. 381–391, 1954.

[26] C. N. Huang, C. H. Chen, and H. Y. Chung, "Application of facial electromyography in computer mouse access for people with disabilities", *Disability and Rehabilitation*, vol. 28, no. 4, pp. 231–237, 2006.

[27] Y. L. Chen, T. S. Kuo, W. H. Chang, J. S. Lai, and E. J. D., "A novel position sensors-controlled computer mouse for the disabled", in *Annual International Conference of the IEEE Engineering in Medicine and Biology*, vol. 3, pp. 2263–2266, 2000.

[28] G.-C. Chang, W.-J. Kang, J.-J. Luh, C.-K. Cheng, J.-S. Lai, J.-J. J. Chen, and T.-S. Kuo, "Real-time implementation of electromyogram pattern recognition as a control command of man-machine interface", *Medical Engineering & Physics*, vol. 18, no. 7, pp. 529–537, 1996.

[29] Y.-H. Tarng, G.-C. Chang, J.-S. Lai, and T.-S. Kuo, "Design of the human/computer interface for human with disability - using myoelectric signal controlled", *Annual International Conference of the IEEE Engineering in Medicine and Biology - Proceedings*, vol. 5, pp. 1909–1910, 1997.

[30] I. Moon, K. Kim, J. Ryu, and M. Mun, "Face direction-based human-computer interface using image observation and EMG signal for the disabled", in *IEEE International Conference on Robotics and Automation*, vol. 1, pp. 1515–1520, 2003.

[31] O. Fukuda, J. Arita, and T. Tsuji, "An EMG-controlled omnidirectional pointing device", *Systems and Computers in Japan*, vol. 37, no. 4, pp. 55–63, 2006.

[32] T. S. Saponas, D. S. Tan, D. Morris, R. Balakrishnan, J. Turner, and J. A. Landay, "Enabling always-available input with muscle-computer interfaces", in *UIST '09: 22nd annual ACM symposium on User interface software and technology*, pp. 167–176, ACM, 2009.

[33] C. Choi, Y. Na, B. Rim, Y. Kim, S. Kang, and J. Kim, "An SEMG computer interface using three myoelectric sites for proportional two-dimensional cursor motion control and clicking for individuals with spinal cord injuries", *Medical Engineering and Physics*, no. 0, 2012.

[34] J. R. Wolpaw, N. Birbaumer, D. J. McFarland, G. Pfurtscheller, and T. M. Vaughan, "Brain-computer interfaces for communication and control", *Clinical Neurophysiology*, vol. 113, no. 6, pp. 767–791, 2002.

[35] R. G. Radwin, G. C. Vanderheiden, and M. L. Lin, "A method for evaluating head-controlled computer input devices using Fitts' law", *Human Factors*, vol. 32, no. 4, pp. 423–438, 1990.

[36] S. Card, W. English, and B. Burr, "Evaluation of Mouse, Rate-Controlled Isometric Joystick, Step Keys, and Text Keys for Text Selection on a CRT", *Ergonomics*, vol. 21, no. 8, pp. 601–613, 1978.

[37] C. E. Stepp, J. T. Heaton, R. G. Rolland, and R. E. Hillman, "Neck and face surface electromyography for prosthetic voice control after total laryngectomy", *IEEE Transactions on Neural Systems and Rehabilitation Engineering*, vol. 17, no. 2, pp. 146–155, 2009.

[38] J. D. Hoit, R. B. Banzett, H. L. Lohmeier, T. J. Hixon, and R. Brown, "Clinical Ventilator Adjustments That Improve Speech", *Chest*, vol. 124, no. 4, pp. 1512–1521, 2003.

[39] L. Ki-Seung, "EMG-Based Speech Recognition Using Hidden Markov Models With Global Control Variables", *IEEE Transactions on biomedical engineering*, vol. 55, no. 3, pp. 930–940, 2008.

[40] R. S. Kumaran, K. Narayanan, and J. N. Gowdy, "Myoelectric signals for multimodal speech recognition", in *Proc. INTERPEECH (Eurospeech)*, pp. 1189–1192, 2005.

[41] S. Kumar, D. K. Kumar, M. Alemu, M. Burry, P. M., K. B., S. A., C. S., P. M., K. B., S. A., and C. S., "EMG based voice recognition", in *Proc. IEEE ISSNIP*, pp. 593–597, 2004.

[42] L. Maier-Hein, F. Metze, T. Schultz, and A. Waibel, "Session independent non-audible speech recognition using surface electromyography", in *Proceedings of ASRU 2005: 2005 IEEE Automatic Speech Recognition and Understanding Workshop*, pp. 307–312, 2005.

[43] H. Manabe and Z. Zhang, "Multi-stream HMM for EMG-based speech recognition", in *Annual International Conference of the IEEE Engineering in Medicine and Biology*, vol. 26 VI, pp. 4389–4392, 2004.

[44] A. D. C. Chan, K. Englehart, B. Hudgins, and D. F. Lovely, "Myo-electric signals to augment speech recognition", *Medical and Biological Engineering and Computing*, vol. 39, no. 4, pp. 500–504, 2001.

[45] M. Wand, C. S. Szu-Jou, and T. Schultz, "Wavelet-based front-end for electromyographic speech recognition", in *Proc. 8th Annual Conference of the International Speech Communication Association*, vol. 3, pp. 1773–1776, 2007.

[46] S. C. Jou, T. Schultz, M. Walliczek, F. Kraft, and A. Waibel, "Towards continuous speech recognition using surface electromyography", in *Proceedings of INTERSPEECH 2006 and 9th International Conference on Spoken Language Processing*, vol. 2, pp. 573–576, 2006.

[47] N. Njd, M. Hannula, N. Narra, and J. Hyttinen, "Electrode position optimization for facial EMG measurements for human-computer interface", *Methods of Information in Medicine*, vol. 47, no. 3, pp. 192–197, 2008.

[48] P. Bonato, T. D'Alessio, and M. Knaflitz, "A statistical method for the measurement of muscle activation intervals from surface myoelectric signal during gait", *IEEE Transactions on Biomedical Engineering*, vol. 45, no. 3, pp. 287–299, 1998.

[49] E. Henneman and L. M. Mendell, *Functional Organization of Motoneuron Pool and its Inputs*. John Wiley and Sons, Inc., 2011.

[50] J. A. Stephens and T. P. Usherwood, "The mechanical properties of human motor units with special reference to their fatiguability and recruitment threshold", *Brain Research*, vol. 125, no. 1, pp. 91–97, 1977.

[51] D. A. Jones and J. M. Round, *Skeletal muscle in health and disease*. Manchester University Press, 1990.

[52] R. E. Burke, *Motor Units: Anatomy, Physiology, and Functional Organization*. John Wiley and Sons, Inc., 1981.

[53] W. Happak, J. Liu, G. Burggasser, A. Flowers, H. Gruber, and G. Freilinger, "Human facial muscles: Dimensions, motor endplate distribution, and presence of muscle fibers with multiple motor endplates", *Anatomical Record*, vol. 249, no. 2, pp. 276–284, 1997.

[54] D. Farina and R. Merletti, "Methods for estimating muscle fibre conduction velocity from surface electromyographic signals", *Medical and Biological Engineering and Computing*, vol. 42, no. 4, pp. 432–445, 2004.

[55] E. Henneman and C. B. Olson, "RELATIONS BETWEEN STRUCTURE AND FUNCTION IN THE DESIGN OF SKELETAL MUSCLES", *J Neurophysiol*, vol. 28, no. 3, pp. 581–598, 1965.

[56] K. Seki and M. Narusawa, "Firing rate modulation of human motor units in different muscles during isometric contraction with various forces", *Brain Research*, vol. 719, no. 12, pp. 1–7, 1996.

[57] K. C. McGill, K. L. Cummins, and L. J. Dorfman, "Automatic decomposition of the clinical electromyogram", *IEEE Transactions on biomedical engineering*, vol. 32, no. 7, pp. 470–477, 1985.

[58] F. Zaheer, S. H. Roy, and C. J. De Luca, "Preferred sensor sites for surface EMG signal decomposition", *Physiological Measurement*, vol. 33, no. 2, pp. 195–206, 2012.

[59] R. Merletti, "Surface electromyography: The SENIAM project", *Europa Medicophysica*, vol. 36, no. 4, pp. 167–169, 2000.

[60] L. Mesin, S. Smith, S. Hugo, S. Viljoen, and T. Hanekom, "Effect of spatial filtering on crosstalk reduction in surface EMG recordings", *Medical Engineering and Physics*, vol. 31, no. 3, pp. 374–383, 2009.

[61] A. Holobar, M. A. Minetto, A. Botter, and D. Farina, *Identification of Motor Unit Discharge Patterns from High-Density Surface EMG during High Contraction Levels*, vol. 37 of *IFMBE Proceedings*, ch. 301, pp. 1165–1168. Springer Berlin Heidelberg, 2012.

[62] D. Stegeman and H. Hermens, "Standards for surface electromyography: the European project "Surface EMG for non-invasive assessment of muscles (SENIAM)"", pp. 108–112, 1998.

[63] T. W. Beck, T. J. Housh, G. O. Johnson, J. P. Weir, J. T. Cramer, J. W. Coburn, and M. H. Malek, "The effects of interelectrode distance on electromyographic amplitude and mean power frequency during isokinetic and isometric muscle actions of the biceps brachii", *Journal of Electromyography and Kinesiology*, vol. 15, no. 5, pp. 482–495, 2005.

[64] D. Stashuk, "EMG signal decomposition: How can it be accomplished and used?", *Journal of Electromyography and Kinesiology*, vol. 11, no. 3, pp. 151–173, 2001.

[65] T. Vukova, M. Vydevska-Chichova, and N. Radicheva, "Fatigue-induced changes in muscle fiber action potentials estimated by wavelet analysis", *Journal of Electromyography and Kinesiology*, vol. 18, no. 3, pp. 397–409, 2008.

[66] R. Gut and G. S. Moschytz, "High-precision EMG signal decomposition using communication techniques", *Signal Processing, IEEE Transactions on*, vol. 48, no. 9, pp. 2487–2494, 2000.

[67] B. Gerdle, N. stlund, C. Grnlund, K. Roeleveld, and J. S. Karlsson, "Firing rate and conduction velocity of single motor units in the trapezius muscle in fibromyalgia patients and healthy controls", *Journal of Electromyography and Kinesiology*, vol. 18, no. 5, pp. 707–716, 2008.

[68] H. Kato, M. Taniguchi, and M. Honda, "Statistical analysis for multiplicatively modulated nonlinear autoregressive model and its applications to electrophysiological signal analysis in humans", *Signal Processing, IEEE Transactions on*, vol. 54, no. 9, pp. 3414–3425, 2006.

[69] O. P. Neto and M. Magini, "Electromiographic and kinematic characteristics of Kung Fu Yau-Man palm strike", *Journal of Electromyography and Kinesiology*, vol. 18, no. 6, pp. 1047–1052, 2008.

[70] T. A. Kuiken, G. Li, B. A. Lock, R. D. Lipschutz, L. A. Miller, K. A. Stubblefield, and K. B. Englehart, "Targeted muscle reinnervation for real-time myoelectric control of multifunction artificial arms", *JAMA - Journal of the American Medical Association*, vol. 301, no. 6, pp. 619–628, 2009.

[71] C. S. L. Tsui, P. Jia, J. Q. Gan, O. Hu, and K. Yuan, "EMG–based hands–free wheelchair control with EOG attention shift detection", in *Proc. International Conference on Robotics and Biomimetics*, pp. 1266–1271, 2008.

[72] C. H. Yang, "Adaptive Morse code communication system for severely disabled individuals", *Medical Engineering & Physics*, vol. 22, no. 1, pp. 59–66, 2000.

[73] C. H. Yang, H. C. Huang, L. Y. Chuang, and C. H. Yang, "A mobile communication aid system for persons with physical disabilities", *Mathematical and Computer Modelling*, vol. 47, no. 3-4, pp. 318–327, 2008.

[74] D. J. McFarland, D. J. Krusienski, W. A. Sarnacki, and J. R. Wolpaw, "Emulation of computer mouse control with a noninvasive brain-computer interface", *Journal of Neural Engineering*, vol. 5, no. 2, pp. 101–110, 2008.

[75] S. Usui and I. Amidror, "Digital Low-Pass Differentiation for Biological Signal Processing", *IEEE Transactions on Biomedical Engineering*, vol. BME-29, no. 10, pp. 686–693, 1982.

[76] A. O. Andrade, S. Nasuto, P. Kyberd, C. M. Sweeney-Reed, and F. V. Kanijn, "{EMG} signal filtering based on Empirical Mode Decomposition", *Biomedical Signal Processing and Control*, vol. 1, no. 1, pp. 44 – 55, 2006.

[77] P. Prakash, C. Salini, J. Tranquilli, D. Brown, and E. Clancy, "Adaptive whitening in electromyogram amplitude estimation for epoch-based applications", *Biomedical Engineering, IEEE Transactions on*, vol. 52, no. 2, pp. 331–334, 2005.

[78] L. Liu, P. Liu, E. Clancy, E. Scheme, and K. Englehart, "Electromyogram Whitening for Improved Classification Accuracy in Upper Limb Prosthesis Control", *Neural Systems and Rehabilitation Engineering, IEEE Transactions on*, vol. PP, no. 99, pp. 1–1, 2013.

[79] K. Englehart and B. Hudgins, "A robust, real-time control scheme for multifunction myoelectric control", *Biomedical Engineering, IEEE Transactions on*, vol. 50, no. 7, pp. 848–854, 2003.

[80] E. A. Clancy, E. L. Morin, and R. Merletti, "Sampling, noise-reduction and amplitude estimation issues in surface electromyography", *Journal of Electromyography and Kinesiology*, vol. 12, no. 1, pp. 1–16, 2002.

[81] A. O. Andrade, A. A. Pereira, C. G. P. Jr, and P. J. Kyberd, "Mouse emulation based on facial electromyogram", *Biomedical Signal Processing and Control*, vol. 8, no. 2, pp. 142–152, 2013.

[82] S. Karlsson, J. Y. J. Yu, and M. Akay, "Time-frequency analysis of myoelectric signals during dynamic contractions: a comparative study", *IEEE Transactions on Biomedical Engineering*, vol. 47, no. 2, pp. 228–38, 2000.

[83] D. Farina and R. Merletti, "Comparison of algorithms for estimation of EMG variables during voluntary isometric contractions", *Journal of Electromyography and Kinesiology*, vol. 10, no. 5, pp. 337–349, 2000.

[84] A. Rainoldi, C. Cescon, A. Bottin, R. Casale, and I. Caruso, "Surface {EMG} alterations induced by underwater recording", *Journal of Electromyography and Kinesiology*, vol. 14, no. 3, pp. 325 – 331, 2004.

[85] T. Felzer and B. Freisleben, "HaWCoS: The "Hands-free" Wheelchair Control System", pp. 127–134, 2002.

[86] A. O. Andrade, S. J. Nasuto, and P. Kyberd, "Extraction of motor unit action potentials from electromyographic signals through generative topographic mapping", *Journal of the Franklin Institute*, vol. 344, no. 34, pp. 154–179, 2007.

[87] C. I. Christodoulou and C. S. Pattichis, "Unsupervised pattern recognition for the classification of EMG signals", *Biomedical Engineering, IEEE Transactions on*, vol. 46, no. 2, pp. 169–178, 1999.

[88] M. S., V. G., S. A.M., and D. P., "Improving detection of muscle activation intervals", *IEEE Engineering in Medicine and Biology Magazine*, vol. 20, no. 6, pp. 38–46, 2001.

[89] M. Nikolic, J. A. Sorensen, K. Dahl, and C. Krarup, "Detailed analysis of motor unit activity", in *Engineering in Medicine and Biology Society, 1997. Proceedings of the 19th Annual International Conference of the IEEE*, vol. 3, pp. 1257–1260 vol.3.

[90] J. R. Florestal, P. A. Mathieu, and A. Malanda, "Automated decomposition of intramuscular electromyographic signals", *Biomedical Engineering, IEEE Transactions on*, vol. 53, no. 5, pp. 832–839, 2006.

[91] D. Farina and F. Negro, "Accessing the neural drive to muscle and translation to neurorehabilitation technologies", *IEEE Reviews in Biomedical Engineering*, vol. 5, pp. 3–14, 2012.

[92] E. Bizzi, V. C. K. Cheung, A. d'Avella, P. Saltiel, and M. Tresch, "Combining modules for movement", *Brain Research Reviews*, vol. 57, no. 1, pp. 125–133, 2008.

[93] C. G. Pinheiro and A. O. Andrade, "The simulation of click and double-click through EMG signals", in *Proceedings of the Annual International Conference of the IEEE Engineering in Medicine and Biology Society*, pp. 1984–1987, 2012.

[94] D. Farina and C. Cescon, "Concentric-ring electrode systems for noninvasive detection of single motor unit activity", *Biomedical Engineering, IEEE Transactions on*, vol. 48, no. 11, pp. 1326–1334, 2001.

[95] A. O. Andrade, *Decomposition and Analysis of Electromyographic Signals*. PhD thesis, 2005.

[96] A. L. D. Siqueira, A. B. Soares, and A. O. Andrade, "Avaliação dos métodos de segmentação de sinais EMG usando sinais sintéticos.", in *XXIII Congresso Brasileiro de Engenharia Biomdica*, pp. 2076–2080, 2012.

[97] B. Efron and R. Tibshirani, *An introduction to the Bootstrap*. Chapman and Hall, 1993.

[98] H. Abdi and L. J. Williams, "Principal component analysis", *Wiley Interdisciplinary Reviews: Computational Statistics*, vol. 2, no. 4, pp. 433–459, 2010.

[99] A. O. Andrade, P. Kyberd, and S. J. Nasuto, "The application of the Hilbert spectrum to the analysis of electromyographic signals", *Information Sciences*, vol. 178, no. 9, pp. 2176–2193, 2008.

[100] P. J. Mesko, A. B. Eliades, C. Christ-Libertin, and D. Shelestak, "Use of Picture Communication Aids to Assess Pain Location in Pediatric Postoperative Patients", *Journal of PeriAnesthesia Nursing*, vol. 26, no. 6, pp. 395–404, 2011.

[101] Y. Kim, N. Doh, Y. Youm, and W. K. Chung, "Development of human-mobile communication system using ElectroOculoGram signals", vol. 4, pp. 2160–2165, 2001.

[102] H. Huang, P. Zhou, G. Li, and T. Kuiken, "Spatial filtering improves EMG classification accuracy following targeted muscle reinnervation", *Annals of Biomedical Engineering*, vol. 37, no. 9, pp. 1849–1857, 2009.

[103] J. P. P. Van Vugt and J. G. Van Dijk, "A convenient method to reduce crosstalk in surface EMG", *Clinical Neurophysiology*, vol. 112, no. 4, pp. 583–592, 2001.

[104] R. Merletti, D. Farina, and M. Gazzoni, "The linear electrode array: a useful tool with many applications", *Journal of Electromyography and Kinesiology*, vol. 13, no. 1, pp. 37–47, 2003.

[105] M. Pozzo, A. Bottin, R. Ferrabone, and R. Merletti, "Sixty-four channel wearable acquisition system for long-term surface electromyogram recording with electrode arrays", *Medical and Biological Engineering and Computing*, vol. 42, no. 4, pp. 455–466, 2004.

[106] F. P. Schwartz and F. A. O. Nascimento, "The conduction velocity as a muscular fatigue indicator during isokinetic contractions", in *Health Care Exchange (PAHCE), 2010 Pan American*, pp. 192–192, 2010.

Appendix A - Hilbert transform algorithm

The Hilbert transform returns a complex helical sequence, called the *analytical signal*, from a real data sequence. The imaginary part is a version of the original real sequence with a 90 phase shift.

In detail, Hilbert uses a four-step algorithm:

1. It calculates the FFT of the input sequence, storing the result in a vector x.
2. It creates a vector h whose elements h(i) have the values:
   - 1 for i = 1, (n/2)+1
   - 2 for i = 2, 3, ... , (n/2)
   - 0 for i = (n/2)+2, ... , n
3. It calculates the element-wise product of x and h.
4. It calculates the inverse FFT of the sequence obtained in step 3 and returns the first n elements of the result.

Next, there is the C code created to estimate the signal envelope using Hilbert transform. The FFT was calculated by the Fastest Fourier Transform in the West (FFTW) library.

```
void calc_hilbert_envelope(double buff[],
                           double hil_env[],
                           unsigned long length){
        unsigned long i;
        double *h = new double[length];
        fftw_complex *in;
        fftw_complex *out;
        fftw_plan p;
        in = (fftw_complex*) fftw_malloc(sizeof(fftw_complex) * length);
        out = (fftw_complex*) fftw_malloc(sizeof(fftw_complex) * length);
    for(i=0;i<length;i++)
        in[i][0] = buff[i];
//Step 1: calculates the FFT (FFTW_FORWARD)
//of the input sequence
        p = fftw_plan_dft_1d(length, in, out,
                        FFTW_FORWARD, FFTW_ESTIMATE);
        fftw_execute(p);

//Step 2: set vector h
//1 for i = 0, (n/2)
        h[0]=h[length/2]=1;

//0 for i = (n/2)+1, ... , n-1
        for(i=1+length/2;i<length;i++)
                h[i]=0;

//2 for i = 1, 2, ... , (n/2)-1
```

```
        for(i=1;i<length/2;i++)
                h[i]=2;

//calculates the element-wise product of x and h.
        for(i=0;i<length;i++){
                out[i][0] *=h[i];
                out[i][1] *=h[i];
        }
//calculates the inverse FFT (FFTW_BACKWARD)
        p = fftw_plan_dft_1d(length, out, in,
                        FFTW_BACKWARD, FFTW_ESTIMATE);
        fftw_execute(p);
        fftw_destroy_plan(p);

//calculates the envelope
        for(i=0;i<length;i++)
                hil_env[i] = Math::Sqrt(Math::Pow(in[i][0],2)+
                        Math::Pow(in[i][1],2))/length;
        fftw_free(in);
        fftw_free(out);
        delete [] h;
}
```